THE GEOLOGY AND GEOCHEMISTRY OF THE MADZARINGWE FORMATION IN THE VELE COLLIERY, TULI COALFIELD, LIMPOPO PROVINCE, SOUTH AFRICA

By

ELELWANI DENGE

Dissertation submitted in fulfilment of the requirement for the degree of

MASTER OF SCIENCE
In
GEOLOGY

DEPARTMENT OF GEOLOGY AND MINING
SCHOOL OF PHYSICAL AND MINERAL SCIENCES
FACULTY OF SCIENCE AND AGRICULTURE
UNIVERSITY OF LIMPOPO, SOUTH AFRICA

SUPERVISOR: DR CHRISTOPHER BAIYEGUNHI

2021

GENERAL DECLARATION

I, Elelwani Denge declare that this dissertation titled “The geology and geochemistry of the Madzaringwe Formation in the Vele Colliery, Tuli Coalfield, Limpopo Province, South Africa” to be my own unaided work. The research reported in this dissertation, except where otherwise indicated, contain the original research results and has not been previously accepted or concurrently submitted to any other university for any degree award or examination purposes.

13/09/2021

……. …….

Elelwani Denge Date

University of Limpopo, Mankweng

DECLARATION ON PLAGARISM

I, Elelwani Denge declare that I am fully aware of the University of Limpopo's policy on plagiarism and I have taken every precaution to comply with the regulations. Where other sources of information have been used, they have been acknowledged and appropriately referenced.

13/09/2021

…….. ……..

Elelwani Denge Date

University of Limpopo, Mankweng

DEDICATIONS

The dissertation is dedicated to my husband for the love and support, to my Dad for constantly motivating me to never stop developing myself and to my dearest mom for your constant prayers. My dear siblings for the motivation. Above all, this thesis serves as an educational motivation to my three Daughters (Onewa, Gabriella and Vhutali (Talia), “never forget that I love you, life is filled with hard and good times, learn from everything, that you can be the woman I know you can be”.

ACKNOWLEDGEMENTS

Foremost, I would like to thank God for wisdom and guidance. I would also like to wish profound gratitude to my supervisor, Dr Christopher Baiyegunhi for his valued logical guidance, determination, optimistic criticism and motivation in my MSc study, above all, his patience and the inspiration not to give up. The Coal of Africa (Vele colliery) team, is appreciated for giving me the opportunity access to the boreholes and mine site for sampling. Thank you to John Sparrow (Chief Geologist at Vele colliery) and Mulalo Mashamba former Geologist in Vele colliery for providing me with all the necessary data, MQA (Mining Qualification Authority) for funding this study.

My gratitude to Prof Nikki Wagner of the University of Johannesburg for her assistance with coal petrography analysis. The Council for Geoscience is appreciated for XRF analysis. I would also like to thank the Department of Geology and Mining, University of Limpopo staff members particularly, Professor Millsteed, Professor Dunlevey, Mr Jones and Mr Makulana for their input in my research. My gratitude to two former honours students Grace and Vincent for their assistance in data analysis.

My genuine thanks going to my husband, family and friends and everybody, who contributed in various ways towards the achievement of my Masters research.

ABSTRACT

The Madzaringwe Formation in the Tuli Basin, Limpopo Province of South Africa is one of the coal-bearing late Palaeozoic units of the Karoo Supergroup. The Madzaringwe Formation in the former Vele colliery (now referred to as Vele MC Mining) is the focus of this study and it consists of sandstone and shale with thin coal seams. To date, published data gives an overview of the stratigraphy of the Madzaringwe Formation in the Tuli coalfield. Little is known of the petrographic characteristics, lithofacies and geochemistry of the Madzaringwe Formation. Hence, this research work is undertaken to better define the lithological characteristics, provenance and tectonic setting of the Madzaringwe Formation in the Vele Colliery, Limpopo Province, South Africa.

In the Vele colliery, the Tshidzi Formation forms the base of the Karoo sequence, consisting of diamictite and attains a maximum thickness of about 10 m. The Madzaringwe Formation overlies the Tshidzi Formation and it is made up of shale, mudstone and sandstones with subordinate siltstones and coal seams. Succeeding the Madzaringwe Formation is the Mikambeni Formation, comprising of black carbonaceous shale, mudstone and sandstones with minor coal layers. The Fripp Formation overlies the Mikambeni Formation and it consists of sandstones with subordinate grey mudstones and attains a maximum thickness of about 15 m. The Madzaringwe, Mikambani and Fripp Formations in the Vele colliery can be correlated with the Ecca Group of the main Karoo Basin.

Based on the detailed sedimentological analyses of borehole and open pit data, ten lithofacies were identified and four facies associations (FAs) were recognised. The facies associations are: FA 1: Carbonaceous and pyritic shale and mudstones (Fls + Fss), FA 2: Black coal and shaly coal (C + Cs), FA 3: Dark grey micaceous and

calcareous shale and mudstone, with subordinate siltstones (Fls + Fm, Fc + Fms + Fmb), and FA 4: Siltstone intercalated with fine to coarse grained sandstones (Fms + Fss + Sm + D). Sedimentological characteristics of the identified facies associations indicate shallow lake and floodplain depositional environments.

The petrographic characterization revealed that vitrinite is the dominant maceral group in the coals, making up to 81-92 vol.% (mmf) of the total sample. Collotellinite is the dominant vitrinite maceral, with total count varying between 52.4 vol.% (mmf) and 74.9 vol.% (mmf), followed by corpogelinite, collodetrinite, tellinite and pseudovitrinite with count ranging between 0.8-19.4 vol.% (mmf), 1.5-17.5 vol.% (mmf), 0.8-6.5 vol.% (mmf) and 0.3-5.9 vol.% (mmf), respectively. The dominance of collotellinite gives a clear indication that the coals are derived from the parenchymatous and woody tissues of roots, stems and leaves. The mean random vitrinite reflectance values range between 0.75 and 0.76%, placing the coals in the medium rank category (also known as the high volatile bituminous coal) based on the UN-ECE coal classification scheme. The high amount of inertinite, especially fusinite with empty cells and semifusinite in the coals will pose a threat to coal mining because it aids the formation of dust.

The sandstones of the Madzaringwe Formation are classified as sub-arkoses and sub-litharenites. Petrographic and geochemical analyses of the mudrocks and sandstones show that the rocks are from silicic or felsic igneous rocks. The tectonic setting discrimination diagrams support passive-active continental margin settings of the provenance. The indices of weathering/alteration and the binary plot of the index of compositional variability (ICV) against chemical index of alteration shows that the studied samples have been subjected to moderate to intensive weathering.

Keywords: Geology, geochemistry, Madzaringwe Formation, Tuli Coalfield, South Africa

TABLE OF CONTENTS

LIST OF FIGURES

LIST OF TABLES

LIST OF ABBREVIATIONS AND ACRONYMS

ACM:	Active Continental Margin
BSE:	Back Scattered Electron
CIA:	Chemical Index of Alteration
CIA:	Continental Island Arc
CIW:	Chemical Index of Weathering
GPS:	Global Positioning System
HFSE:	High Field Strength Elements
ICV:	Index of Compositional Variability
ICCP:	International Committee for coal and organic petrology
LILE:	Large Ion Lithophile Elements
LOI:	Loss on ignition
Ma:	Million years
NASC:	North American Shale Composite
PAAS:	Post Archaean Australian Shale
PI:	Production Index
PIA:	Plagioclase Index of Alteration
PM:	Passive Continental Margin
XPL:	Crossed Polarized Light
PPL.	Plane Polarised Light

CHAPTER 1

GENERAL INTRODUCTION

1.1 Background of the study

The Permian stratigraphy of the Tuli Coalfield in the study area, from the base to the top, comprises of the Tshidzi Formation, Madzaringwe Formation, Mikambeni Formation and Fripp Formation (Chidley, 1985). The Madzaringwe Formation in the former Vele Colliery (now referred to as Vele MC Mining) is the focus of this study and it consists of sandstone and shale with thin coal seams. The Madzaringwe Formation in the Tuli Basin in the Limpopo Province of South Africa is a coal-bearing late Palaeozoic units of the Karoo Supergroup. The Tuli Coalfield in the Tuli Basin occurs on both sides of the borders of South Africa, Zimbabwe and Botswana. The Karoo Supergroup sedimentary and igneous rocks filled the coalfield, maximum thickness ranging between 450 m and 500 m (Bordy, 2000). The Karoo Supergroup in the main Karoo Basin as compared to the correlative Late Carboniferous-Middle Jurassic sedimentary rocks is less continuous when (Catuneanu et al., 2005).

The Tuli basin in South Africa is located north-west of Musina, extending from Point Drift in the west to Beit Bridge in the east. Bordy and Catuneanu (2002) documented that the sedimentary rocks in the South African part of the basin occupy an area of about 1000 km^2, with frequent deposits like parabreccial, conglomerate-breccias, conglomerate, sandstone, fine-grained sediments, calcretes and silcretes and terrigenous clastic (Bordy and Catuneanu, 2002). The Madzaringwe Formation, which is the focus of this study has about 120 m coal-bearing unit and it is the lowermost part of the Ecca Group in the Tuli Basin (McCourt and Brandl, 1980). Several authors (i.e.

Bordy and Catuneanu (2000), Malaza et al. (2013) and Hancox and Gotz, (2014)) indicated that the Madzaringwe Formation comprises cyclic accumulations of sporadic sandstone, siltstone, mudstone and coal layers. Hancox and Gotz (2014) further revealed that the Madzaringwe Formation comprises of three well-defined coal seams contained or hosted in a 150 m thick Main Coal Zone. The coal found in all the three seams is laminated with carbonaceous mudstone.

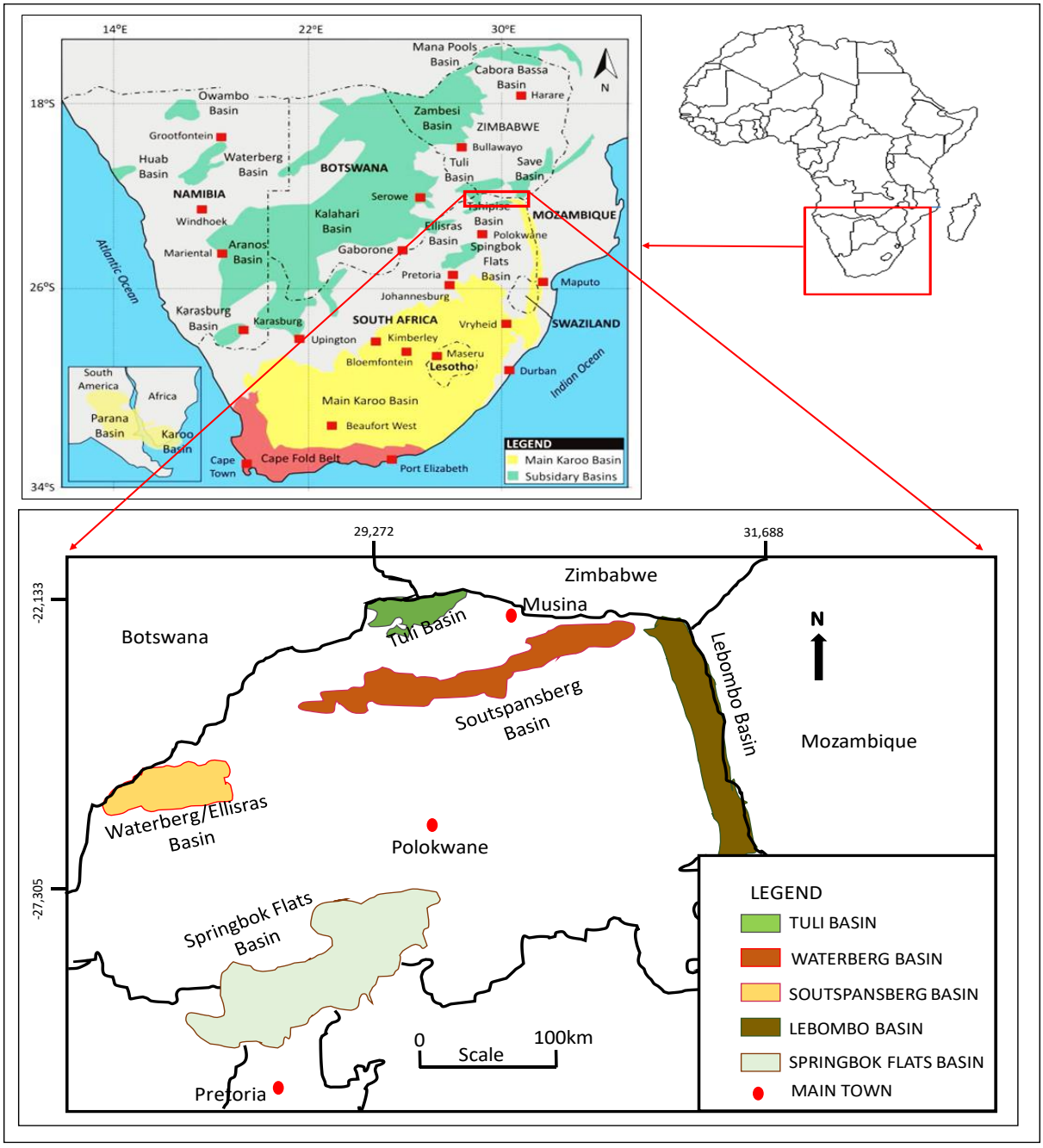

Figure 1.1: Limpopo Karoo basins with the Tuli Basin at the triple junction of Zimbabwe, Botswana and South Africa (after luyt, 2017).

1.2 Location of the study area

The study area is situated in the Vele Colliery core yard and it is located near to the border between South Africa and Zimbabwe in the northern-most extremity of Limpopo Province in South Africa (Figure 1.2).

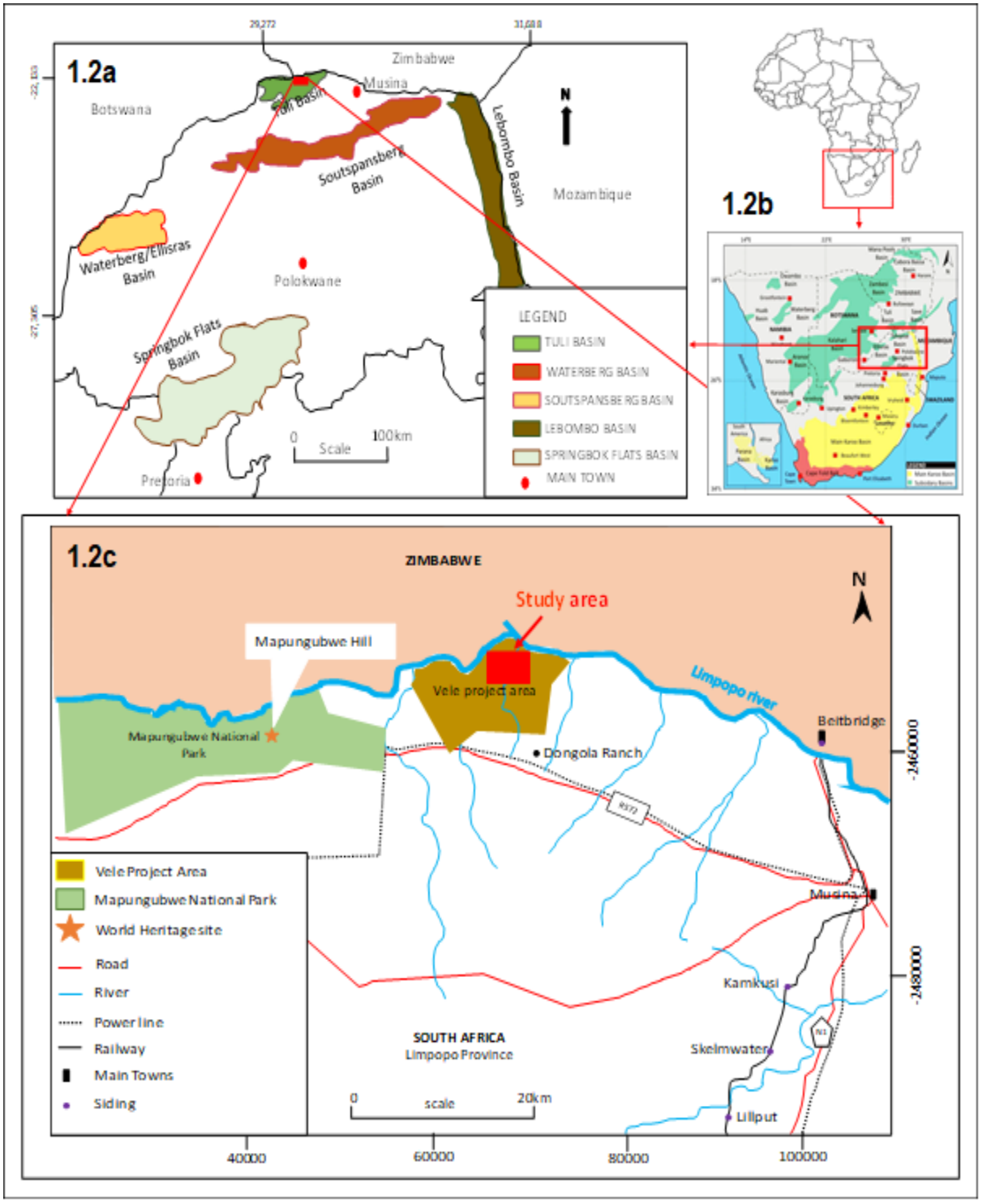

Figure 1.2: (a) Tuli Basin, with neiboring Limpopo Basins waterberg basin, Ellisrus Basin,Soutpansburg Basin and Springbok flats Basin; (b) Locality map of South Africa; (c) Location of the study area within the Vele Colliery (in brown) (after Vele colliery project report 2009).

The Vele Colliery is located approximately 40 km west of the town of Musina and approximately 100 km north of the Alldays town. Also, the eastern border of the Mapungubwe National Park is almost 5 km away to the western boundary of the Vele Colliery. The study area lies geographically between longitudes 29.56º E and 29.66º E and latitude 22.15º S and 22.22º S, with a conserved basin thickness of about 80 km. Furthermore, the area is approximately 10% underlain by economically exploitable coal-bearing strata, containing a valuable proportion of coking coal in South Africa (Snyman et al., 1993).

1.3 Problem statement

Although published data (i.e. Van Der Berg, 1980; Bordy, 2000; Malaza et al., 2013; and Luyt, 2017) gives an overview of the stratigraphy of the Madzaringwe Formation, up to this point, little is known of the petrographic characteristics, lithofacies and geochemistry of the rocks of the Madzaringwe Formation. Hence, the depositional palaeoenvironment, provenance and tectonic setting of the formation is still debatable or not fully established up to now.

1.4 Aim and objectives

The study is undertaken to deliver a piece of more thorough information on the geology and geochemistry of the Madzaringwe Formation to better define the lithological characteristics, provenance and tectonic setting of the Madzaringwe Formation. The specific objectives of this study are to:

i. measure the stratigraphic successions and establish the stratigraphic sequence of the Madzaringwe Formation within the Vele Colliery.
ii. determine the mineral composition.

iii. understand the maceral group in the coal of the Vele Colliery.
iv. determine the elemental compositions of the rocks as well as deduce their paleoweathering conditions, provenance and tectonic setting.

1.5 Significance of the study

The outcome of this study will contribute or improve the body of knowledge because little is known or documented about the sediment maturity, paleoweathering conditions, provenance and tectonic setting of the Madzaringwe Formation. Besides, the results from this study could be used by future or other researchers to tease out an interpretation of the sedimentary history and evolution of the Tuli Basin and it will give improved economic potential of the area/community.

1.6 Delineation and limitations

This research work only covers the Madzaringwe Formation in the Vele colliery. The research study considers field investigation (core logging and obervation of open pit), petrography (coal, mudrock and sandstone petrography) and x-ray fluorescence analysis to unravel the tectonic provenance and paleoweathering conditions of the formation. The petrographic work does not include modal compositional analysis, hence no graphical plot (quartz or microcrystalline quartz - feldspar- lithic fragments) was consider.

CHAPTER 2

LITERATURE REVIEW

2.1 General geology of the Tuli Basin

TheTuli Basin is thought to be a small intracratonic east-west trending fault-controlled basin with a preserved width of approximately 80 km (Chidley,1985). The basin is present in the northernmost part of the Limpopo Province, extending into eastern Botswana and south-eastern Zimbabwe (Figure 2.1). These sediments form part of the Limpopo Karoo Supergroup and they were deposited at the same time with the main Karoo Basin sediments, but they formed as an isolated basin which was fault-controlled from the onset. The Tuli Basin was deposited from approximately Late Carboniferous to Middle Jurassic in a continental tectonic setting (Bordy, 2000). The stratigraphic unit of the Tuli Basin is divided into three units namely; the Basal Unit, Middle Unit and Upper Unit (McCourt and Brandl, 1980; Figure 2.1).

According to Bordy and Catuneanu (2002), two broadly different tectonic settings were involved in the deposition of the Karoo Supergroup. The Tuli Basin forms the Limpopo part of Karoo-age basins. It has been proposed that the Limpopo area forms the western arm of a failed rift triple-junction (Crossey et al., 2006), which later extended in a north-south direction and from the Save Basin in Zimbabwe to the Lebombo Formation in South Africa. Two distinct tectonic regimes that were sourced from the southern and northren margins of Gondwana led to the advancement of the Karoo Supergroup (Baiyegunhi et al., 2017). Brandl (1980) carried out the first detailed work on the Madzaringwe Formation by reporting the sedimentology and stratigraphic succession of the formation. The Madzaringwe Formation was originally named by

Brandl and McCourt (1980). However, only basic lithological and geological periods data of the formation was given.

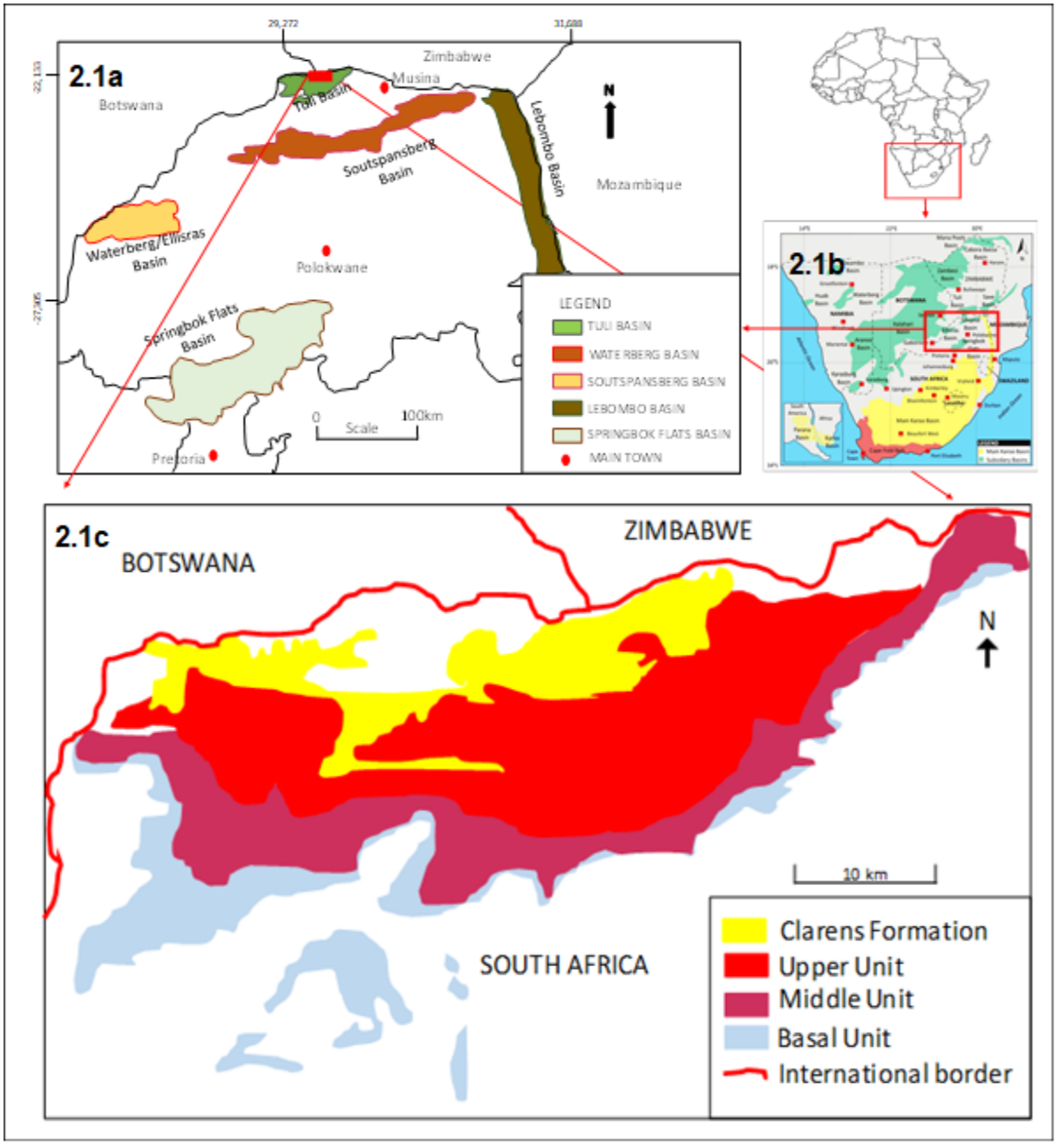

Figure 2.1: (a) Limpopo Karoo Basins(Waterberg Basin,Soutpansberg Basin, Lebombo Basin and Springbok Flats) including the study area in green (Tuli Basin); (b) General map of Africa and South Africa showing locality area (red box); (c) The Karoo Supergroup in southern Africa and the geological map of the southern Tuli Basin (after Reid and Brandl, 1997; Johnson et al., 1996).

Watkeys (1979) reported that the Limpopo area Karoo-age basins are made up of the following basins; Tuli Basin, Tshipise Basin (South Africa, partly Zimbabwe) and Nuanetsi Basin (Zimbabwe). According to the Tuli Basin which trends approximately 1300 km east-west in the shared border region of South Africa, Zimbabwe, and Botswana, preserves an estimated thickness of 450–500 m of strata (Bordy, 2000; Bordy and Catuneanu, 2001, 2002). It has been interpreted as the down-dropped western arm of a failed triple junction related to the break-up of Gondwana (Vail et al., 1969; Burke and Dewey, 1973). However, an episode of mid-Jurassic rifting and associated subsidence fails to accommodate the substantial record of pre-Jurassic strata preserved in the basin. The local geology of the study area is shown in Figure 2.2.

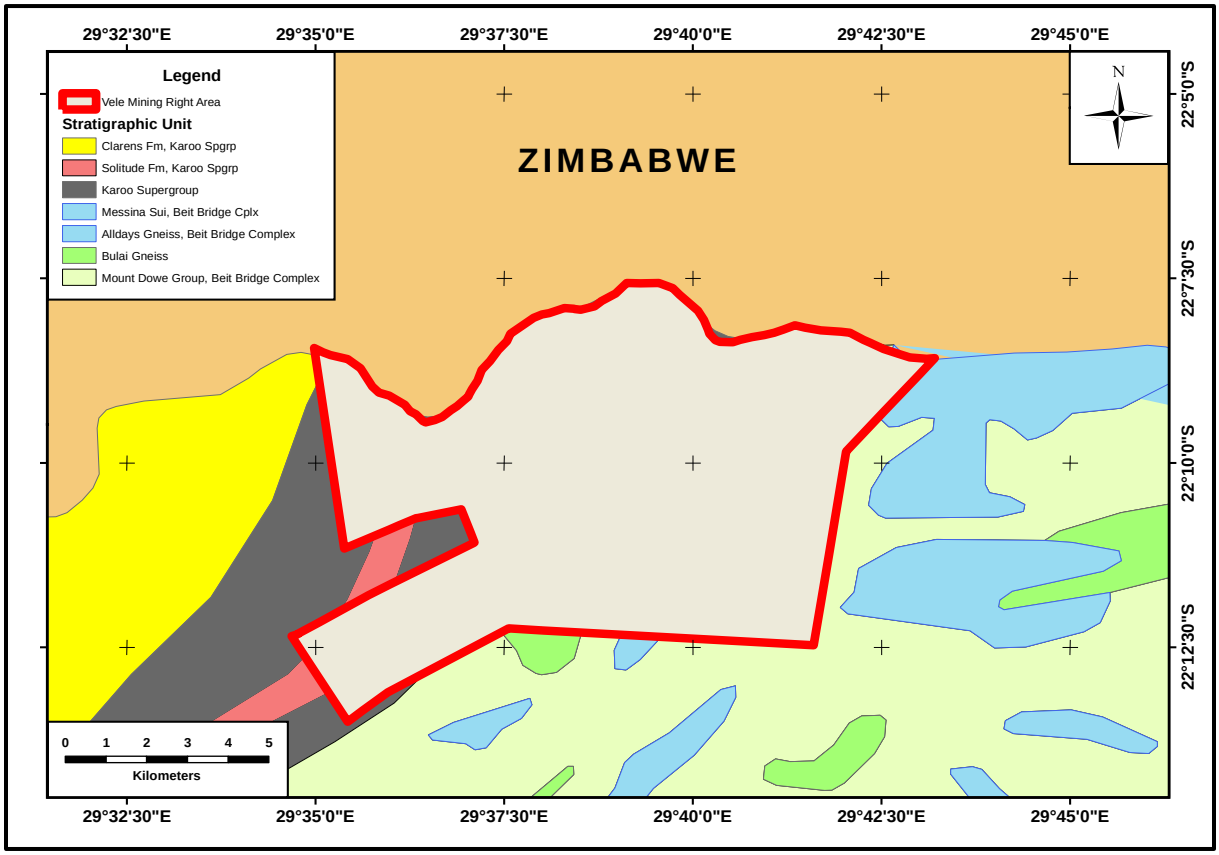

Figure 2.2: The Geology of Vele Mining Right area (after Vele colliery project report 2009).

2.2 Tectonic Setting of the Tuli Basin

The trans-frontier Tuli Basin lies at the triple junction of the Zimbabwean, Botswanan and South African borders (Figure 2.1) and it is generally interpreted that the basin separated from the Tshipise Basin (Bordy, 2000). A major continous ENE trending fault for about 100 km marks the northern boundary of Karoo rocks (Bordy and Catuneanu, 2002). As reported by Bordy and Catuneanu (2002), the Karoo Supergroup deposition occurred in two broadly diverse tectonic settings in southern Africa. The main Karoo Basin comprises of sedimentary rocks that are retro-arc foreland fills. The formations of the Karoo Supergroup are preserved in separate, fault-bounded depositories. In the northern part of the main Karoo Basin, the Karoo sub-

basins (i.e. Tuli Basin) are interpreted either as rift basins or intracratonic thermal sag basins. The Tuli Basin represents the Limpopo area of Karoo-age basins. To date, the tectonic evolution of the Tuli Basin is still debatable, and numerous models were used to unravel the tectonic development of the Tuli Basin. One of the tectonic models which was described by Bordy (2000) may be considered in terms of two right-lateral strike-slip systems as shown by Figure 2.3. The initial one formed an ENE trending divergent wrench zone and this model was responsible for the development of the Tuli Basin, Nuanetsi Basin and Tshipise Basin. The tectonic displacement formed during this tectonic model occurred along pre-existing ENE and NE trending faults during the sedimentation of the lower part of the Karoo Supergroup (Bordy, 2000).

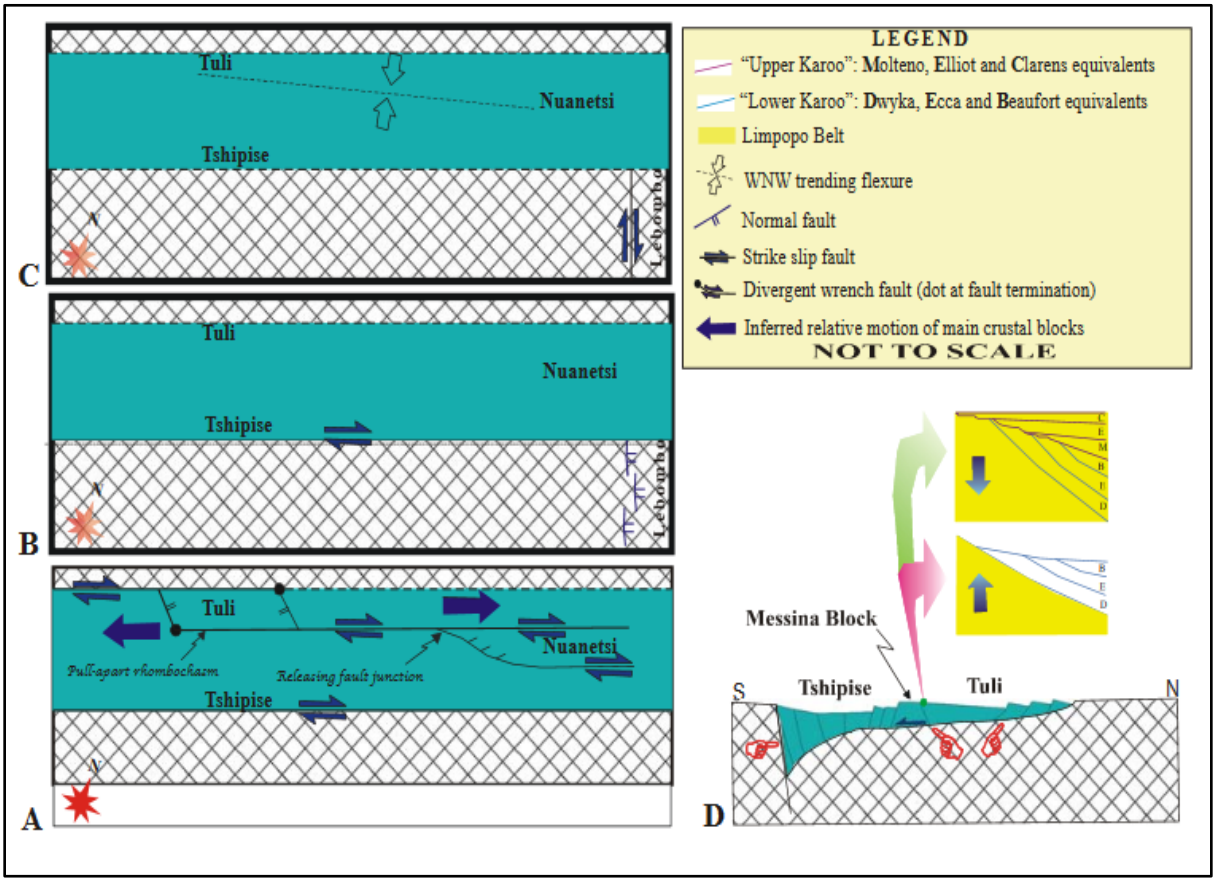

Figure 2.3: Tectonic evolution model of Limpopo Karoo basins (after Bordy, 2000).

Crossey et al. (2006) proposed that the Limpopo area forms the western arm of a failed rift triple-junction, which later extended in a north-south direction and from the Save Basin in Zimbabwe to the Lebombo Formation in South Africa. Likewise, Catuneanu et al. (1999) envisaged that the Tuli Basin reflects, at least in part, tectonic flexure and subsidence in the back-bulge region of the Karoo foreland that commenced in the Late Paleozoic–Early Mesozoic.

The Archean basement can be used as a trace of the Tuli basin, since it is panelled to the axis of the Karoo basin (Barton and Key, 1981). It is supposed that there was a fault zone that was active in post-Karoo times because the Karoo rocks are almost absent on the northern side of the fault (Bordy and Catuneanu, 2001b). A smaller outlier of basalts which appears to be the only the conveyed Karoo Supergroup outcrop – north of the major fault, cover aeolian sandstones of the Tsheung Formation and mostly overlie basement rocks. (Bordy and Catuneanu, 2002). This proposes that the fault was activated just before, and after the deposition of the aeolian sandstones.

The Karoo strata seem to be cut by the fractures of the basin over significant distances, consequently giving the whole structure a graben like character. The late- to post Karoo fracture system faults broadly follows the axis of the Limpopo Belt. This complex, bifurcating fracture system may have functioned until quite recent times (Barton and Key, 1981). Mapping and drilling have not shown any sign of major faulting in the Karoo-age strata south of Limpopo River. The area investigated in this study is located in the Tuli Basin, in the north-eastern part of South Africa near Tshipise-Pafuri Basin. Generally, the Tuli basin trends in the East-West direction and links up with the North-South trending Lebombo Basin, which characterizes the southern end of the East African Rift System (Malaza et al., 2016).

2.3 Stratigraphy of the Tuli Basin

According to Chevallier and Woodford (1999), the main Karoo Basin consists of four major groups which are Dwyka Group (Late Carboniferous-Early Permian), Ecca Group (Permian), Beaufort Group (Late Permian-Triassic) and the Stormberg Group (Late Triassic-Early Jurassic). About 183 Ma, the Karoo sedimentary sequence was intruded by the Early Jurrasic sills and dykes (The Tuli Basin consists of three Formations, namely, the Madzaringwe Formation, Mikambeni Formation and Fripp Formation. The aforementioned formations are the equivalents of the Ecca Group in the main Karoo Basin (Bordy, 2000; Figure 2.4). The sedimentary succession of the Tuli Coalfield consists of Tshidzi Formation at the base and it is mostly composed of diamictite and sandstones. The Tshidzi Formation is equivalent of the Dwyka Group in the main Karoo Basin. The Madzaringwe Formation forms the base of the Ecca Group and overlies the diamictites of the Tshidzi Formation (Mtimkulu, 2009). It consists of sandstone, siltstone and shale with thin coal seams with a maximum stratigraphic thickness of nearly 120 m.

As documented by Malaza et al. (2013), the Madzaringwe Formation in Tuli Basin, which is the focus of this study consists of an alternating succession of feldspathic, cross-bedded conglomerates, sandstone, siltstone, and shale comprising some coal seams. Furthermore, they reported that this formation was deposited on top of the Tshidzi Formation. The coal series found in Madzaringwe Formation are located at the depth of less than 50 m along the southern margin. The coal series can reach a depth of over 300 m close to the Limpopo River (Bordy, 2000). The two major seams which are flat-lying coal have a thickness of about 1.6 m and 1.2 m. These seams are overlain by mudstones and minor sandstones. The economically important coal in

Madzaringwe Formation is interbedded with mudstones (Bordy, 2000). Succeeding the Madzaringwe Formation is the Mikambeni Formation, which is about 60 m thick, consisting of shale, sandstone and coal. The Flipp Formation overlies the Mikambeni Formation and it is composed of about 5-10 m thick successions of sandstone and conglomerates. The Fripp Formation is overlain by the Solitude Formation which is the equivalent of the Beaufort Group in the main Karoo Basin (Table 2.1).

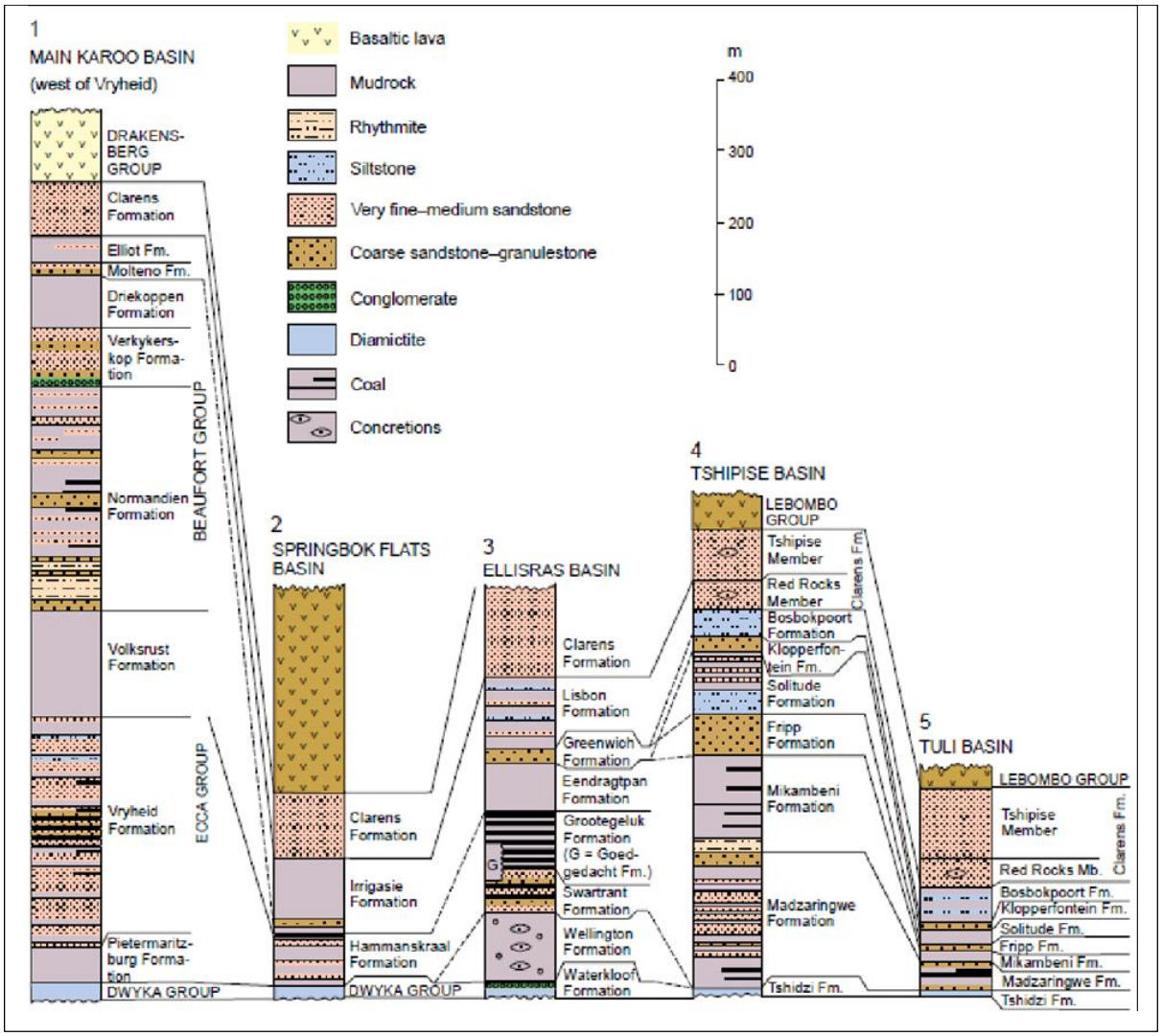

Figure 2.4: Stratigraphy and correlation of the main Karoo Basin and the northern sub-basins (Van der Merwe et al., 2010)

Table 2.1: Summary of the lithostratigraphic nomenclature and correlation of the main Karoo Supergroup strata of the Tuli Basin and main Karoo Basin.

<table>
<tr><th colspan="2">Main Karoo Basin (Johnson,1994)</th><th colspan="2">Tuli Basin (Chidley, 1985)</th></tr>
<tr><td rowspan="3">Stromberg Group</td><td>Clarens Formation</td><td rowspan="2">Clarens Formation</td><td>Tshipise sandstone Member</td></tr>
<tr><td rowspan="2">Elliot Formation</td><td>Red Rocks Member</td></tr>
<tr><td rowspan="2">Molteno Formation</td><td colspan="2">Bosbookspoort Formation</td></tr>
<tr><td colspan="2">Klopperfontein Formation</td></tr>
<tr><td colspan="2">Beaufort Group</td><td colspan="2">Solitude Formation</td></tr>
<tr><td colspan="2" rowspan="2">Ecca Group</td><td colspan="2">Fripp Formation</td></tr>
<tr><td rowspan="3">Basal Beds</td><td>Mikambeni Formation</td></tr>
<tr><td colspan="2">Madzaringwe Formation</td></tr>
<tr><td colspan="2">Dwyka Group</td><td>Tshidzi Formation</td></tr>
</table>

CHAPTER 3

MATERIALS AND METHODS

3.1 Introduction

To achieve the aim and objectives of this research work, desktop study, literature review, field work and laboratory analysis were carried out systematically.

3.2 Desktop studies

Desktop studies are all the research work that was carried out before and after the fieldwork. These studies involve consultation of scientific articles, technical reports, previously unpublished and published thesis on the Tuli coalfield as well as other related areas. The above-mentioned activities were done to have a general idea of the geology and economic potential of the area. Remarkably, the desktop studies provided a better understanding and aided in the selection of the boreholes and research methods.

3.3 Geological fieldwork and sampling

Geological core and pit logging were carried out on the three available boreholes at the Vele Colliery core yard. The instruments used during the logging include a digital camera, measuring tape, core-logging sheets, pencils, grain size charter, sample bags, hand lens, permanent marker, masking tapes, a global positioning system (Garmin eTrex-10) and compass. Diamond core drilling with secondary percussion drilling was used to drill the three existing boreholes, namely, boreholes OV125149, OV125156, and OV125160. These boreholes were drilled down from the surface to the depths of 62 m, 60 m and 42 m, respectively. In addition, there is an abandoned

open-pit within the Vele Colliery yard (Figure 3.1). The depth of the pit is about 30 m from the surface. These boreholes and open-pit were logged by observing and identifying different lithologies, sedimentary structures, vertical packing styles and colour of the rocks. The observed sedimentary structures in the borehole cores were designated, measured with a tape and where necessary, photographs were taken using a digital camera. The thickness of the stratigraphic units was measured perpendicular to the strike of the strata using a measuring tape. Generally, the pit log descriptions give less data on the sedimentary structures and characteristics of the rock sequences. Thus, they were mostly used to determine stratigraphic thickness. The collected stratigraphic data such as lithology, grain sizes, sedimentary structures were used to generate part of the stratigraphy of Madzaringwe Formation in the three existing boreholes. The stratigraphic data was processed using Microsoft Office Excel and PowerPoint and outcomes were conveyed in the form of stratigraphic logs. The samples selection was based on lithological changes. Rock samples were collected in labelled sample bags for further petrographic studies and geochemical investigation.

3.4 Laboratory work

The laboratory work involves preparation of thin sections and polish blocks, petrographic studies and X-ray fluorescence analysis.

3.4.1 Thin section preparation and petrographic studies of mudrocks and sandstones

Thin sections were prepared in the Geology and mining department's thin section laboratory, University of Limpopo, South Africa. The rock samples (hand specimen) were cut into slice-like, small rectangular blocks of approximately 1/8 fraction using

the diamond saw. Thereafter, the rectangular blocks were first grinded on a rough grinding lap. Then, the block is transferred to the finer grinder steel lap to make the surface to be smooth and flat. The rectangular block was heated to be warm and ready to be cemented on the glass slide with the glue. The glue was placed on the smooth and flat surface on the rock. The rock and the glass slide were pressed against each other sensibly in a manner to avoid creating or eliminating air bubbles on the microscope slide. The mounted rock was left for 24 hours so that the samples are firmly stuck to the microscope slide. After the sample had been stuck to the microscope slide, it was trimmed using the 600 silicon powder and subsequently, the 200 silicon powder was used until the thickness of the mounted rock was about 30 µm. The thin sections were made to a thickness of about 30 µm because at this thickness it allows the light from the microscope to pass through the slide. The samples were judiciously cleaned and vertically stored in thin section boxes.

Thirty three representative thin sections (at least 2 thin sections per sample) of the collected samples were studied using the Nikon Eclipse Polarising Microscope to determine their mineral compositions, rock textures, grain shapes and sizes as well as the cement types. The prepared thin sections were photographed and studied under both plane and cross-polarized light. The different mineralogical compositions and textural attributes of the samples were examined. Also, photomicrographs of the studied thin sections were taken with the aid of a built-in camera, equipped to a computer monitor.

3.4.2 Polished blocks preparation and petrographic study of coal

There are various types of petrographic analyses used to characterize coal. Maceral groups give a clear background on the origin of the coals whether, cellular structure, leaves, roots, stems, resins, fats, wax oils and others. In this study, only maceral group analysis was performed on seven coal samples from the Vele colliery in the Tuli Coalfield. The analysis was carried out under the guidance of Prof Wagner at the Coal Petrography laboratory, University of Johannesburg. Sample lumps, approximately 15 mm × 20 mm in size, were cut and placed in 30 mm cups, set in epoxy resin, and placed under vacuum for 24 hours. The hardened block was polished as per the ISO 7404 (part 2) guidelines, with a final stage polish using a 0.05 µm OPS lubricant with a Struers Tegraforce polisher. The polished sample blocks were analysed using a Zeiss AxioImager reflected light petrographic microscope fitted with a Hilgers Diskus-Fossil system for Vitrinite reflectance determination (ISO 7404 part 5). A detailed macerals analysis (in accordance with ISO 7404-4) was conducted at a magnification of ×500 under oil immersion. To precisely determine the organic matter, the samples were viewed under white light (monochromatic and colour cameras), fluorescent mode (to determine the degree of fluorescence), and under ×-polars (to determine the degree of anisotropy). Each sample was photographed at ×100 (air lens) and ×500 (oil immersion lens). The coal petrographic results are reported on a % volume basis, including and excluding mineral matter (mmf) for macerals analysis and micrographs. Thereafter, the vitrinite reflectance analysis results were plotted on the UN-ECE coal classification scheme to classify it in terms of rank.

3.4.3 X-ray fluorescence (XRF) analysis

A total of 38 samples, comprising of 5 coal samples, 20 shale samples and 13 sandstone samples from the Madzaringwe Formation in the Vele Colliery were subjected to X-ray Fluorescence (XRF) analysis at the Council of Geoscience in Pretoria, South Africa. The XRF analysis of the major and trace elements was performed using MagiX Fast spectrometer. Bulk sample preparation consists of drying where necessary, crushing to less than 10 mm, and subsequent milling in a tungsten carbide milling machine to less than 50 µm. The major elements were analysed on fused beads, while trace elements were executed on pressed powder pellets. Several discriminatory plots of the major and trace elements have been used by several researchers (i.e. Taylor and McLennan, 1985; Bhatia and Crook, 1986; McLennan et al., 1993; Armstrong-Altrin et al., 2004; Baiyegunhi et al., 2017) to determine the provenance and tectonic setting. These plots have also been attempted in this study to infer the provenance and tectonic setting of the Madzaringwe Formation. Furthermore, the ternary diagram of Al_2O_3 – (CaO + Na_2O) – K_2O (represented as A-CN-K) was plotted and the chemical index of alteration (CIA), chemical index of weathering (CIW) and plagioclase index of alteration (PIA) were calculated and used to quantify the degree of weathering.

CHAPTER 4

STRATIGRAPHY

4.1 Introduction

Stratigraphy is defined by sedimentologists as descriptive strata science that deals with the form, arrangement, distribution, chronologic succession, lithology and relationship of rock strata. The main purpose of undertaking stratigraphic studies is to generate a stratigraphic section signifying a systematic and chronologic picture of the sequence of events which happened during Earth history (Catuneanu, 2006). Stratigraphic classification encompasses the use of noticeable and measurable properties of rocks and rock sequence and is mostly based on the time of origin. The most commonly used stratigraphic classifications are lithostratigraphy, biostratigraphy and chrono-stratigraphy. Lithostratigraphy covers the description and nomenclature of rocks based on their lithologic and stratigraphic associations. On the other hand, biostratigraphy mainly deals with the correlation and determination of the relative ages of rocks strata based on fossil and fossil assemblages. Chronostratigraphy is a branch of stratigraphy that deals with the studies of rock strata in relation to time. The main purpose of the chronostratigraphic study is to arrange the sequence of deposition for all rock units within geological time.

Within this study, lithostratigraphic investigation of the Madzaringwe Formation within the Vele Colliery was carried out so as to unveil the lateral and vertical variations in the lithological features within the formation. At the Vele colliery, three coal seams horizons are found in the Madzaringwe Formation, these seams are termed Bottom seams, Middle seams and Top seams based on the Coal Africa nomenclature (Hancox

and Götz, 2014). The general description of the lithology was done on three existing boreholes OV125149, OV125156, and OV125160 as well as in the open pit. The three existing boreholes intersect the three coal seams. The Top seam was further differentiated into Top Lower, Top Middle and Top-Bottom, while the Bottom seam was categorized into Bottom Lower and Bottom Upper. It is important to highlight that Top Upper and Top Middle are not of economic interest, due to coal immaturity (Hancox and Götz, 2014). These seams appear not to be consistent in all the boreholes. In fact, some of the seams are absent in other boreholes.

4.2 Stratigraphy of the Madzaringwe Formation

The stratigraphic sequence of the Madzaringwe Formation in the Vele colliery consists of shale, mudstone and sandstones with subordinate siltstones and coal seams (Figure 4.1). In the open pit, the Mikambeni Formation was seen directly overlying the Madzaringwe Formation and it is highly weathered. Although the Madzaringwe Formation is slightly weathered, some geological features like faults and dolerite intrusions (dyke) are visible (Figure 4.1).

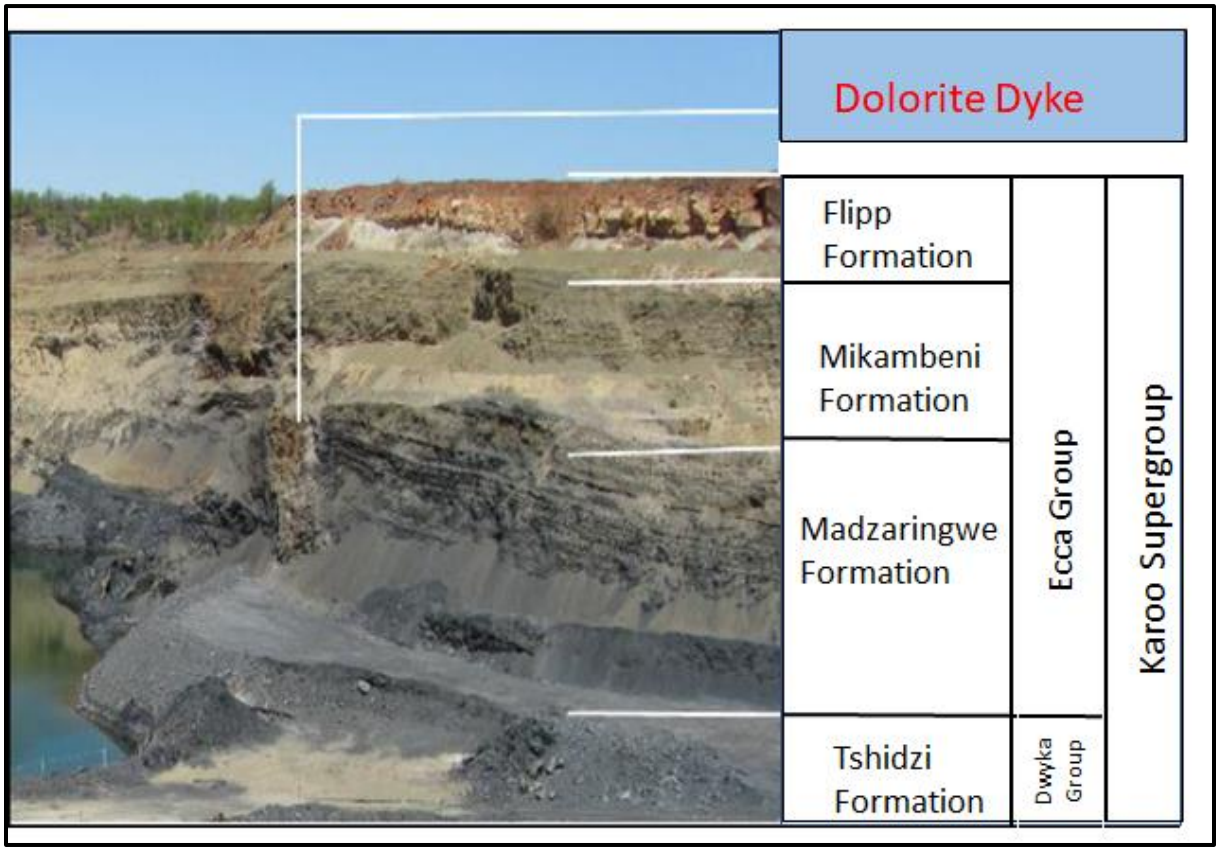

Figure 4.1: Photograph of the open pit within the Vele Colliery showing stratigraphy of the top part of Dwyka and Ecca Groups (the picture has no scale due to safety messures at the mine).

4.2.1 Stratigraphy of the Madzaringwe Formation in borehole OV125149

The stratigraphic sequence of the Madzaringwe Formation in borehole OV125 149 consists of mudstone, shale, and minor coal seams and thin sandstones layers (Figures 4.2 – 4.5). The borehole was drilled down to a depth of 62 m and there is no core recovery from the surface (0 m) down to a depth of about 18 m. From the depth of about 18 m down to a depth of about 34 m, there is a dominant of dark grey massive mudstone. This mudstone covers a thickness of about 16 m before the upper coal seam was intersected at a depth of 34 m. The mudstone is highly weathered up the

depth of 26.43 m and relatively fresh from 26 m to 34 m. From the depth of about 34 m to 50 m, the massive mudstone is occasionally interbedded with coal, mudstones and minor sandstone layers. The upper coal seam is about 1.5 m in thickness. The middle coal seam was intersected at a depth of 43.4 m and it is associated with carbonaceous shales. The bottom seam was intersected at a depth of 48.9 m. An alternating sequence of the black coal and black carbonaceous shale was observed between the depth of 50 m and 61.5 m. The stratigraphy of Madzaringwe in borehole OV125149 is depicted in Figure 4.5.

Figure 4.2: Photograph of borehole OV125149 showing shales with thin layer of sandstones and coal of the Madzaringwe Formation.

Figure 4.3. Photograph of borehole OV125149 showing lighter to darker colour shales and very bright coal of Madzaringwe Formation.

Figure 4.4: Photograph showing the bottom and lower seam, with shaley coal interlaminated with dark grey carbonaceous shale and minor lustrous coal. Note: In the picture, between B4 and B5 is a bottom lower seam with dull lustrous coal for log OV125 149 in Madzaringwe Formation.

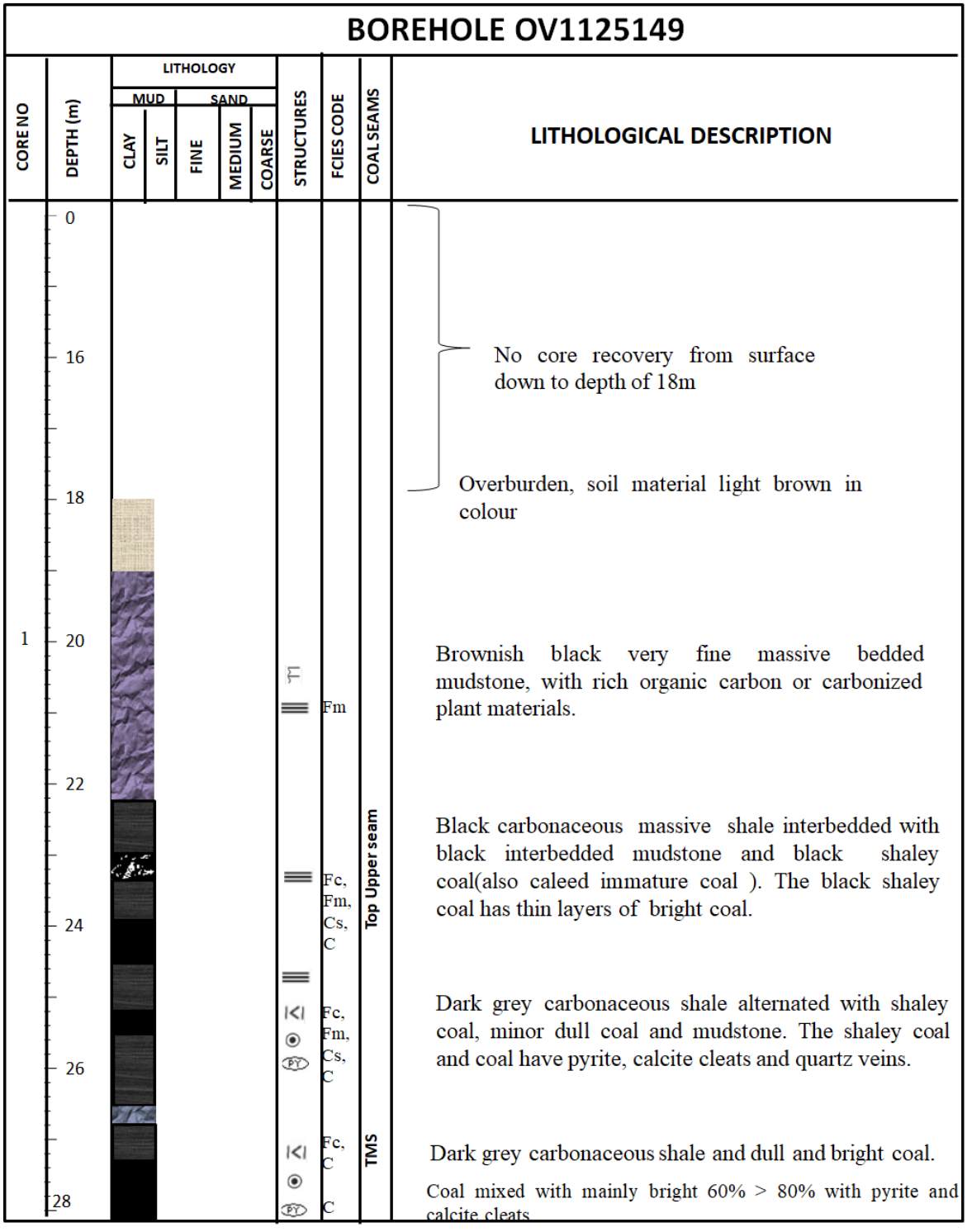
BOREHOLE OV1125149
CORE NO
DEPTH (m)
LITHOLOGY
MUD
SAND
CLAY
SILT
FINE
MEDIUM
COARSE
STRUCTURES
FCIES CODE
COAL SEAMS
LITHOLOGICAL DESCRIPTION
1
0
16
18
20
22
24
26
28
No core recovery from surface down to depth of 18m
Overburden, soil material light brown in colour
Fm
Brownish black very fine massive bedded mudstone, with rich organic carbon or carbonized plant materials.
Fc, Fm, Cs, C
Top Upper seam
Black carbonaceous massive shale interbedded with black interbedded mudstone and black shaley coal(also caleed immature coal). The black shaley coal has thin layers of bright coal.
Fc, Fm, Cs, C
Dark grey carbonaceous shale alternated with shaley coal, minor dull coal and mudstone. The shaley coal and coal have pyrite, calcite cleats and quartz veins.
Fc, C
C
TMS
Dark grey carbonaceous shale and dull and bright coal.
Coal mixed with mainly bright 60% > 80% with pyrite and calcite cleats

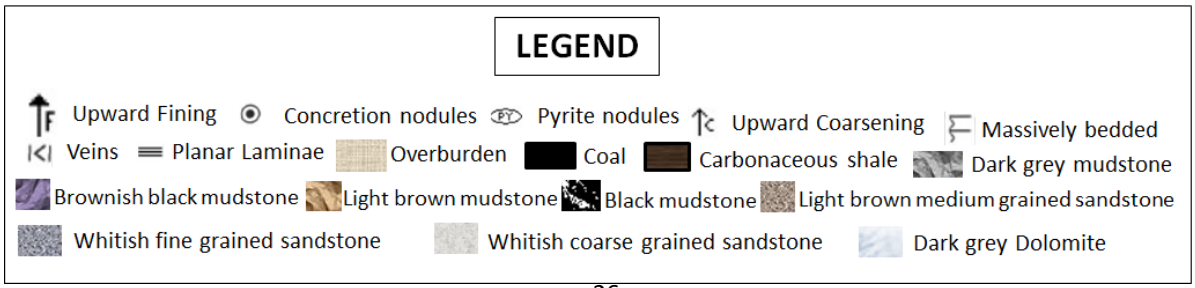
LEGEND
Upward Fining
Concretion nodules
Pyrite nodules
Upward Coarsening
Massively bedded
Veins
Planar Laminae
Overburden
Coal
Carbonaceous shale
Dark grey mudstone
Brownish black mudstone
Light brown mudstone
Black mudstone
Light brown medium grained sandstone
Whitish fine grained sandstone
Whitish coarse grained sandstone
Dark grey Dolomite

BOREHOLE OV1125149

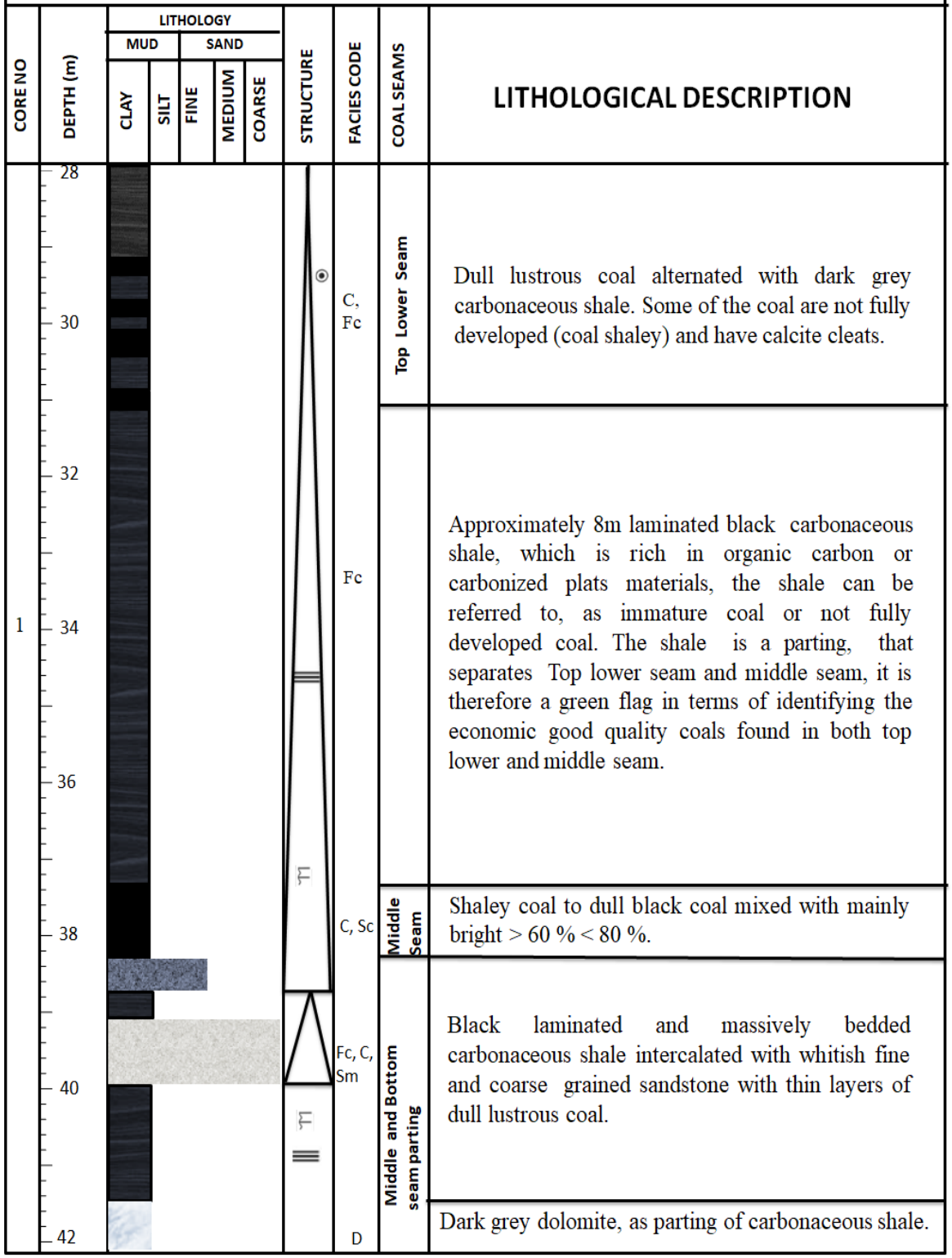

LEGEND

Upward Fining · Concretion nodules · Pyrite nodules · Upward Coarsening · Massively bedded
Veins · Planar Laminae · Overburden · Coal · Carbonaceous shale · Dark grey mudstone
Brownish black mudstone · Light brown mudstone · Black mudstone · Light brown medium grained sandstone
Whitish fine grained sandstone · Whitish coarse grained sandstone · Dark grey Dolomite

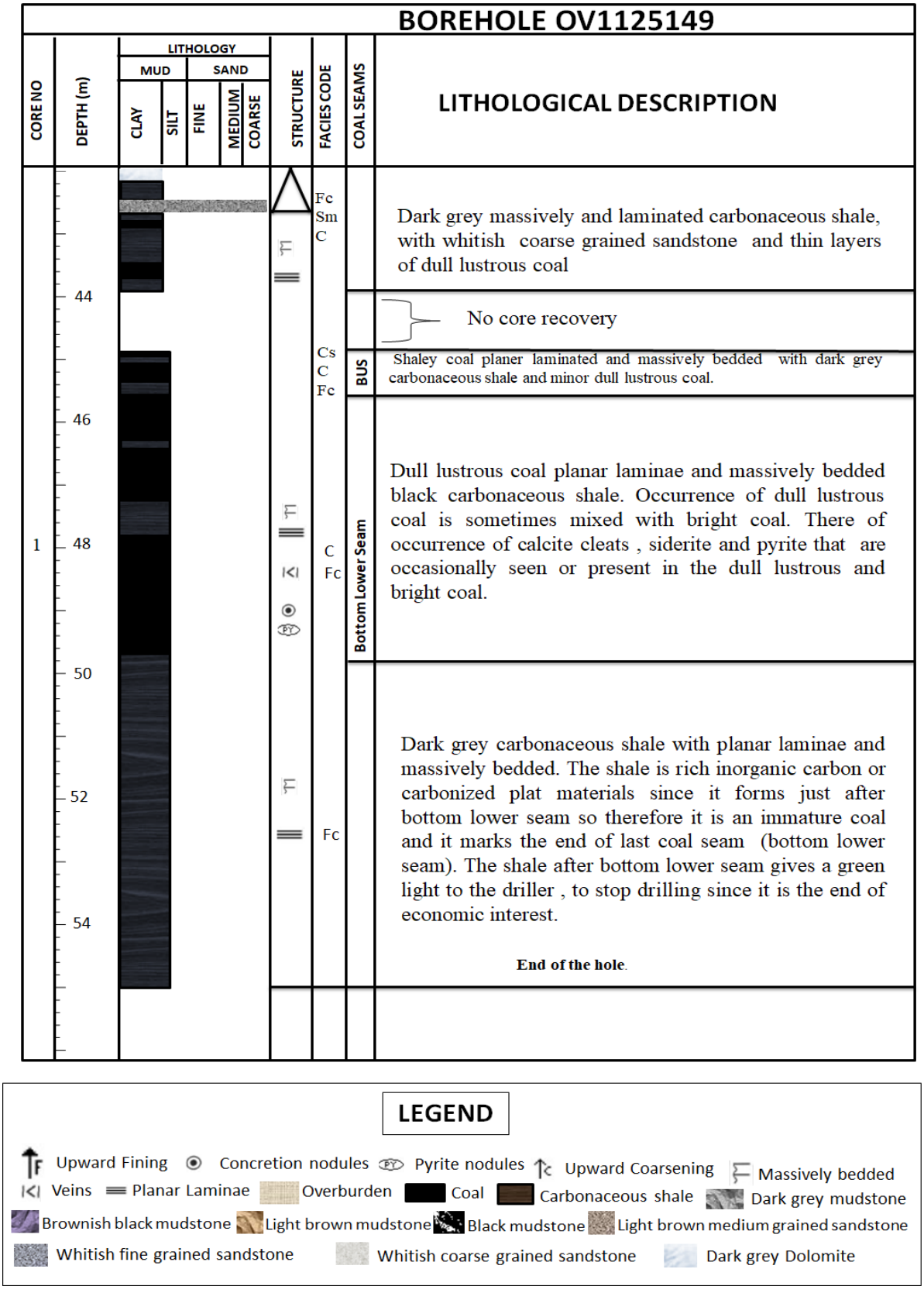

Figure 4.5: Stratigraphy of the Madzaringwe Formation in borehole Ov125149.

4.2.2 Stratigraphy of the Madzaringwe Formation in borehole OV125156

The stratigraphy of Madzaringwe in borehole OV125156 is presented in Figure 4.6. and Figure 4.7.The borehole was drilled down to a depth of 60 m and there is no core recovery from the surface (0 m) down to a depth of about 18 m. From 18 to 43 m there is a dominancy in mudstone but there are also other lithologies such as carbonaceous shame, coal with different characteristic and a layer of clay. From 43 m to 48.8 m there is siltstone, a layer of sandstone and also massive dolomite. An alternating sequence of the black coal and black carbonaceous shale was observed between the depth of 48 m and 53.4 m. The first coal layer was intersected at a depth of 26.4 m within mudstone. The middle coal seam was intersected at 41.2 m to 43 m making a thickness of 1.8 m. The middle coal seam overlies grey siltstone. A 0.6 m thick grey to blue dolomite was intersected at 45.8m depth within a massive grey mudstone. The bottom seam was intersected at 45.6 m depth and it covers a thickness of 3.8 m and comprises of alternating layers of carbonaceous shales and coal. The bottom-most part of this bottom seam overlies the tillites.

Figure 4.6: Photograph showing shale samples of borehole OV125156.

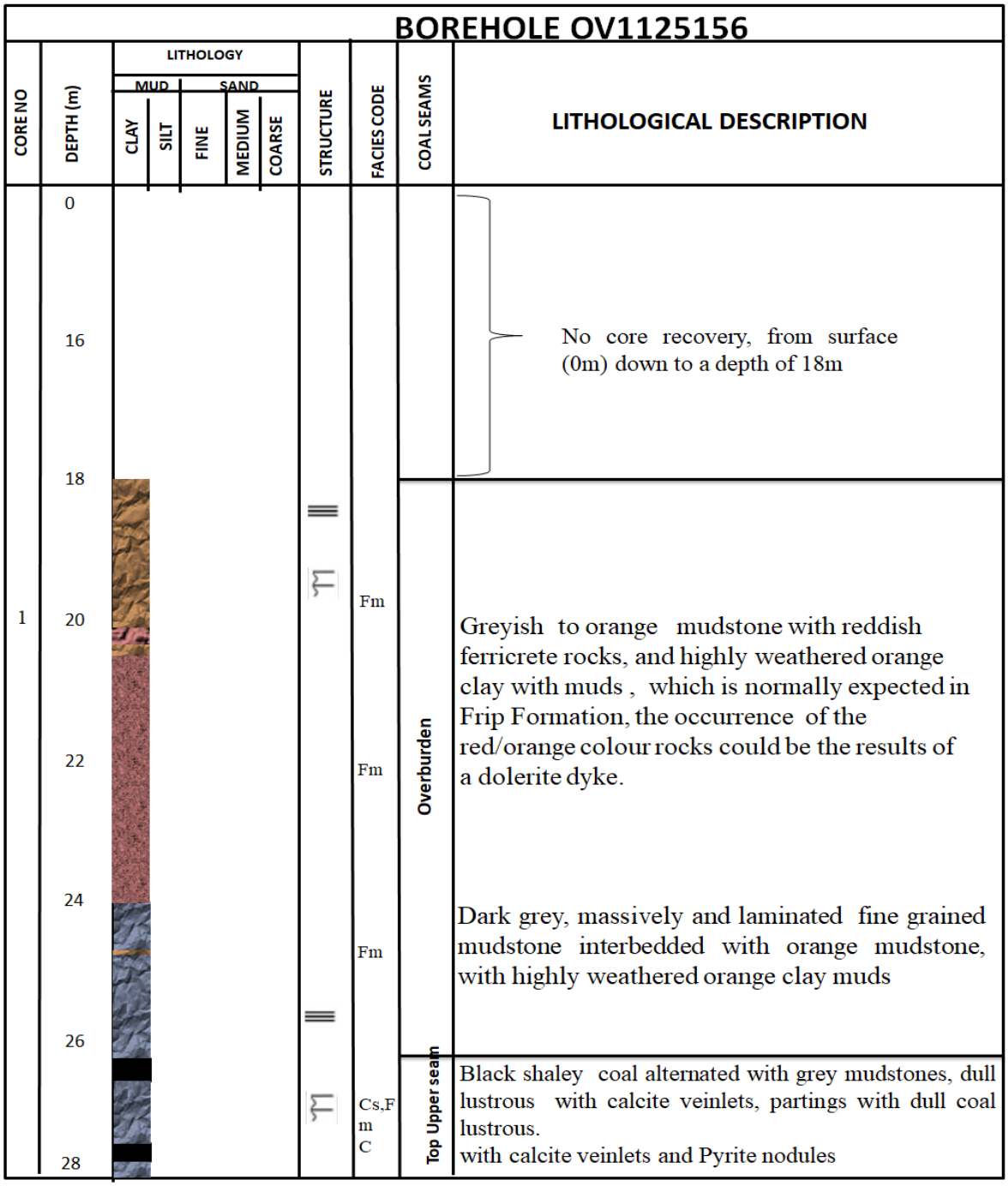
BOREHOLE OV1125156
CORE NO
DEPTH (m)
LITHOLOGY
MUD
SAND
CLAY
SILT
FINE
MEDIUM
COARSE
STRUCTURE
FACIES CODE
COAL SEAMS
LITHOLOGICAL DESCRIPTION
0
16
18
20
22
24
26
28
1
No core recovery, from surface (0m) down to a depth of 18m
Fm
Fm
Fm
Cs,Fm C
Overburden
Top Upper seam
Greyish to orange mudstone with reddish ferricrete rocks, and highly weathered orange clay with muds , which is normally expected in Frip Formation, the occurrence of the red/orange colour rocks could be the results of a dolerite dyke.
Dark grey, massively and laminated fine grained mudstone interbedded with orange mudstone, with highly weathered orange clay muds
Black shaley coal alternated with grey mudstones, dull lustrous with calcite veinlets, partings with dull coal lustrous.
with calcite veinlets and Pyrite nodules

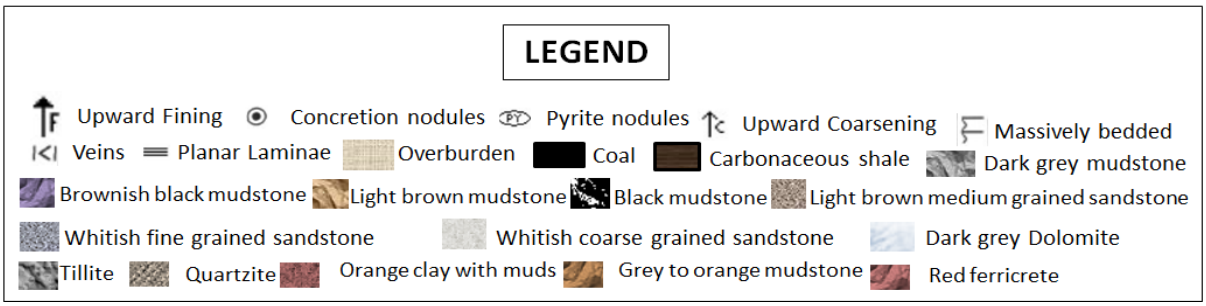
LEGEND
Upward Fining
Concretion nodules
Pyrite nodules
Upward Coarsening
Massively bedded
Veins
Planar Laminae
Overburden
Coal
Carbonaceous shale
Dark grey mudstone
Brownish black mudstone
Light brown mudstone
Black mudstone
Light brown medium grained sandstone
Whitish fine grained sandstone
Whitish coarse grained sandstone
Dark grey Dolomite
Tillite
Quartzite
Orange clay with muds
Grey to orange mudstone
Red ferricrete

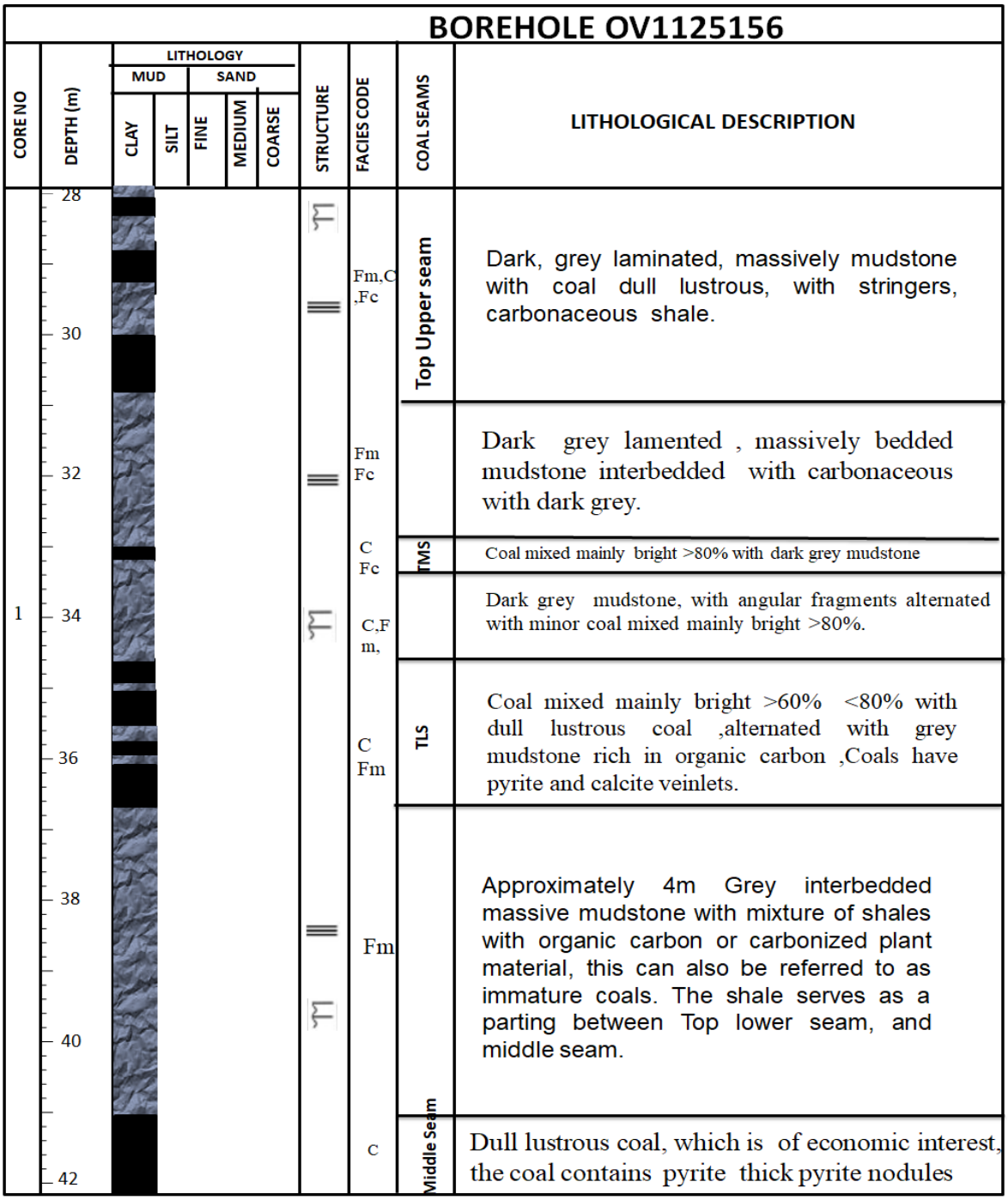
BOREHOLE OV1125156
CORE NO
DEPTH (m)
LITHOLOGY
MUD
SAND
CLAY
SILT
FINE
MEDIUM
COARSE
STRUCTURE
FACIES CODE
COAL SEAMS
LITHOLOGICAL DESCRIPTION
1
28
30
32
34
36
38
40
42
Fm,C ,Fc
Fm Fc
C Fc
C,F m,
C Fm
Fm
C
Top Upper seam
TMS
TLS
Middle Seam
Dark, grey laminated, massively mudstone with coal dull lustrous, with stringers, carbonaceous shale.
Dark grey lamented , massively bedded mudstone interbedded with carbonaceous with dark grey.
Coal mixed mainly bright >80% with dark grey mudstone
Dark grey mudstone, with angular fragments alternated with minor coal mixed mainly bright >80%.
Coal mixed mainly bright >60% <80% with dull lustrous coal ,alternated with grey mudstone rich in organic carbon ,Coals have pyrite and calcite veinlets.
Approximately 4m Grey interbedded massive mudstone with mixture of shales with organic carbon or carbonized plant material, this can also be referred to as immature coals. The shale serves as a parting between Top lower seam, and middle seam.
Dull lustrous coal, which is of economic interest, the coal contains pyrite thick pyrite nodules

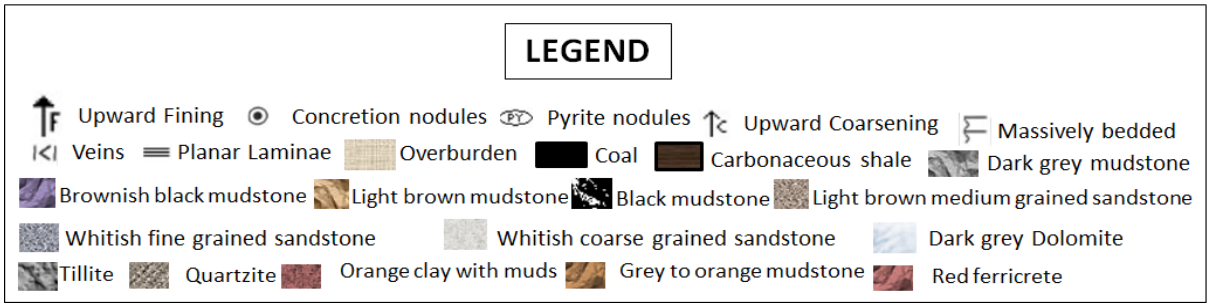
LEGEND
Upward Fining
Concretion nodules
Pyrite nodules
Upward Coarsening
Massively bedded
Veins
Planar Laminae
Overburden
Coal
Carbonaceous shale
Dark grey mudstone
Brownish black mudstone
Light brown mudstone
Black mudstone
Light brown medium grained sandstone
Whitish fine grained sandstone
Whitish coarse grained sandstone
Dark grey Dolomite
Tillite
Quartzite
Orange clay with muds
Grey to orange mudstone
Red ferricrete

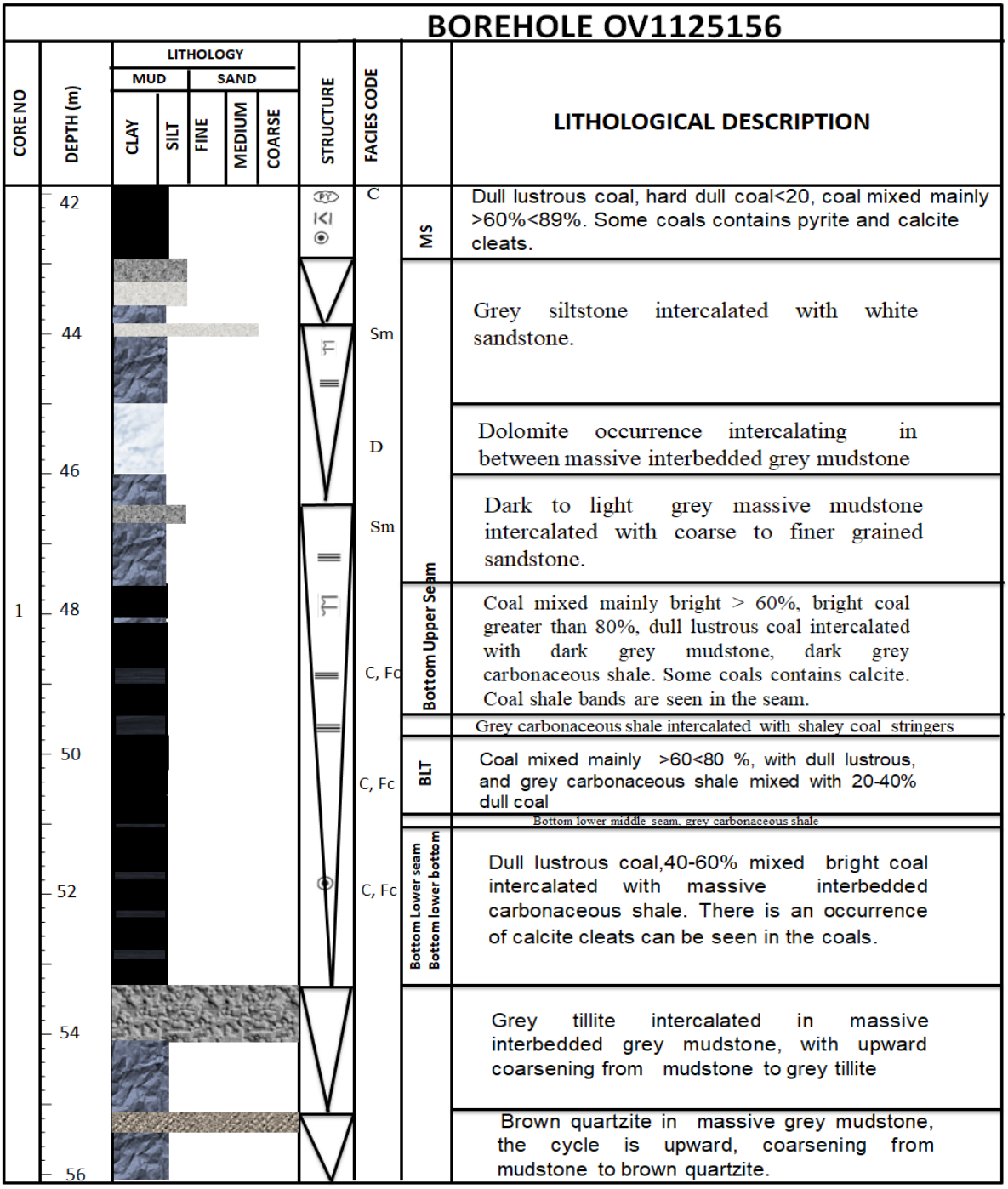
BOREHOLE OV1125156
CORE NO
DEPTH (m)
LITHOLOGY
MUD
SAND
CLAY
SILT
FINE
MEDIUM
COARSE
STRUCTURE
FACIES CODE
LITHOLOGICAL DESCRIPTION
1
42
44
46
48
50
52
54
56
C
Sm
D
Sm
C, Fc
C, Fc
C, Fc
MS
Bottom Upper Seam
BLT
Bottom Lower seam
Bottom lower bottom
Dull lustrous coal, hard dull coal<20, coal mixed mainly >60%<89%. Some coals contains pyrite and calcite cleats.
Grey siltstone intercalated with white sandstone.
Dolomite occurrence intercalating in between massive interbedded grey mudstone
Dark to light grey massive mudstone intercalated with coarse to finer grained sandstone.
Coal mixed mainly bright > 60%, bright coal greater than 80%, dull lustrous coal intercalated with dark grey mudstone, dark grey carbonaceous shale. Some coals contains calcite. Coal shale bands are seen in the seam.
Grey carbonaceous shale intercalated with shaley coal stringers
Coal mixed mainly >60<80 %, with dull lustrous, and grey carbonaceous shale mixed with 20-40% dull coal
Bottom lower middle seam, grey carbonaceous shale
Dull lustrous coal,40-60% mixed bright coal intercalated with massive interbedded carbonaceous shale. There is an occurrence of calcite cleats can be seen in the coals.
Grey tillite intercalated in massive interbedded grey mudstone, with upward coarsening from mudstone to grey tillite
Brown quartzite in massive grey mudstone, the cycle is upward, coarsening from mudstone to brown quartzite.

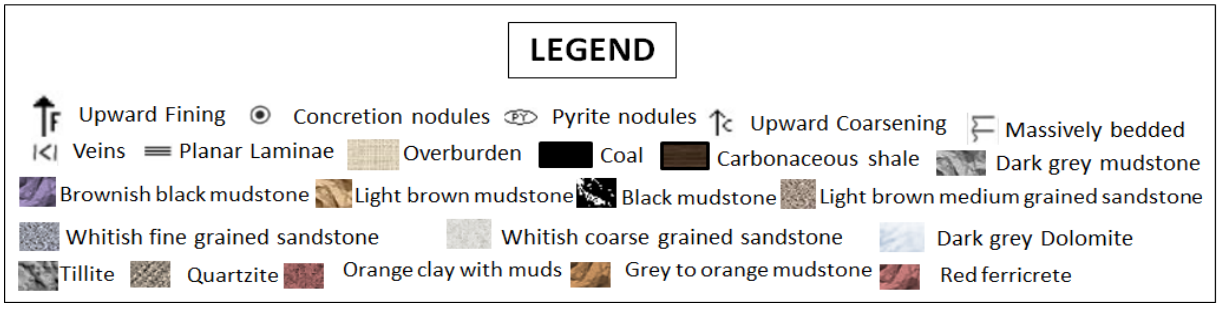
LEGEND
Upward Fining
Concretion nodules
Pyrite nodules
Upward Coarsening
Massively bedded
Veins
Planar Laminae
Overburden
Coal
Carbonaceous shale
Dark grey mudstone
Brownish black mudstone
Light brown mudstone
Black mudstone
Light brown medium grained sandstone
Whitish fine grained sandstone
Whitish coarse grained sandstone
Dark grey Dolomite
Tillite
Quartzite
Orange clay with muds
Grey to orange mudstone
Red ferricrete

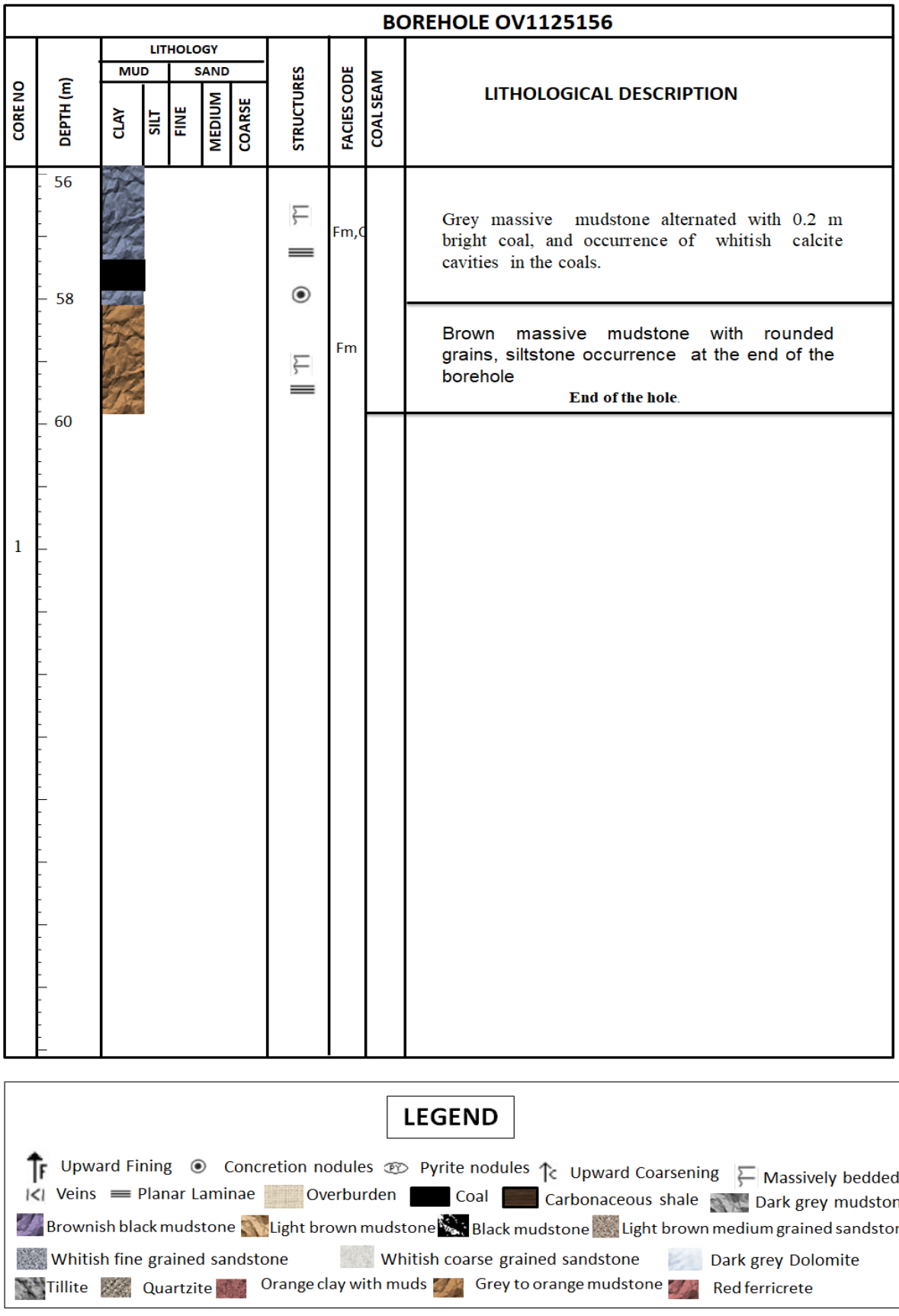

Figure 4.7: Stratigraphy of the Madzaringwe Formation in borehole OV125156.

4.2.3 Stratigraphy of the Madzaringwe Formation in borehole OV125160

Borehole OV125160 was drilled down to a depth of 42 m and there is no core recovery from the surface (0 m) down to a depth of about 18 m. The recovered core starts at a depth of 17 m intersecting a broken coal layers within grey mudstones. The Top lower seam is observed from the depth of 17 down to 23 m and it consists of weathered coal mixed and grey mudstones. From 23 to 30 m, black vitrinite coal, mudstone, fine-grained sandstones, and lenses of siltstone and lenses of gritstone are present. The bottom upper seam occurs between the depth of 30 m and 34 m and it is composed of immature coal and grey carbonaceous shale. The bottom middle seam is seen between the depth of 34m and 36 m and it is made up of coal laminated carbonaceous shale, with pyrite nodules and calcite veinlets. The Bottom lower top seam starts from the depth of 36 m down to 38.6 m and it consists of laminated carbonaceous shaly coal with dull lustrous. From 38.6 to 45.3m is the bottom lower bottom seam and it is made up of coal mixed with manly bright shaley coal and mudstone partings. The stratigraphy of Madzaringwe in borehole OV125160 is portrayed in Figure 4.8.

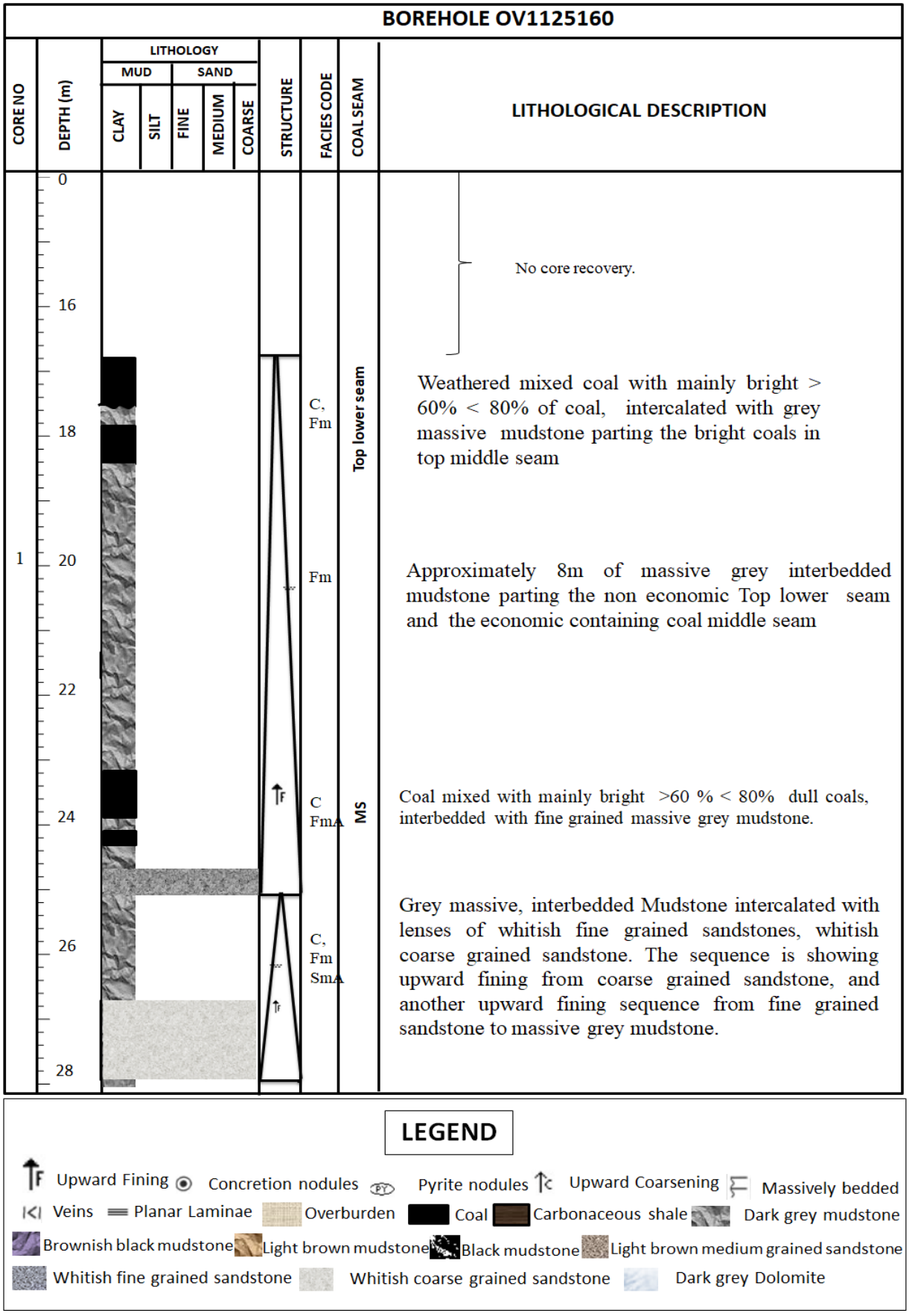
BOREHOLE OV1125160
CORE NO
DEPTH (m)
LITHOLOGY
MUD
SAND
CLAY
SILT
FINE
MEDIUM
COARSE
STRUCTURE
FACIES CODE
COAL SEAM
LITHOLOGICAL DESCRIPTION
0
16
18
20
22
24
26
28
1
No core recovery.
Weathered mixed coal with mainly bright > 60% < 80% of coal, intercalated with grey massive mudstone parting the bright coals in top middle seam
C, Fm
Top lower seam
Approximately 8m of massive grey interbedded mudstone parting the non economic Top lower seam and the economic containing coal middle seam
Fm
Coal mixed with mainly bright >60 % < 80% dull coals, interbedded with fine grained massive grey mudstone.
C FmA
MS
Grey massive, interbedded Mudstone intercalated with lenses of whitish fine grained sandstones, whitish coarse grained sandstone. The sequence is showing upward fining from coarse grained sandstone, and another upward fining sequence from fine grained sandstone to massive grey mudstone.
C, Fm SmA
LEGEND
Upward Fining
Concretion nodules
Pyrite nodules
Upward Coarsening
Massively bedded
Veins
Planar Laminae
Overburden
Coal
Carbonaceous shale
Dark grey mudstone
Brownish black mudstone
Light brown mudstone
Black mudstone
Light brown medium grained sandstone
Whitish fine grained sandstone
Whitish coarse grained sandstone
Dark grey Dolomite

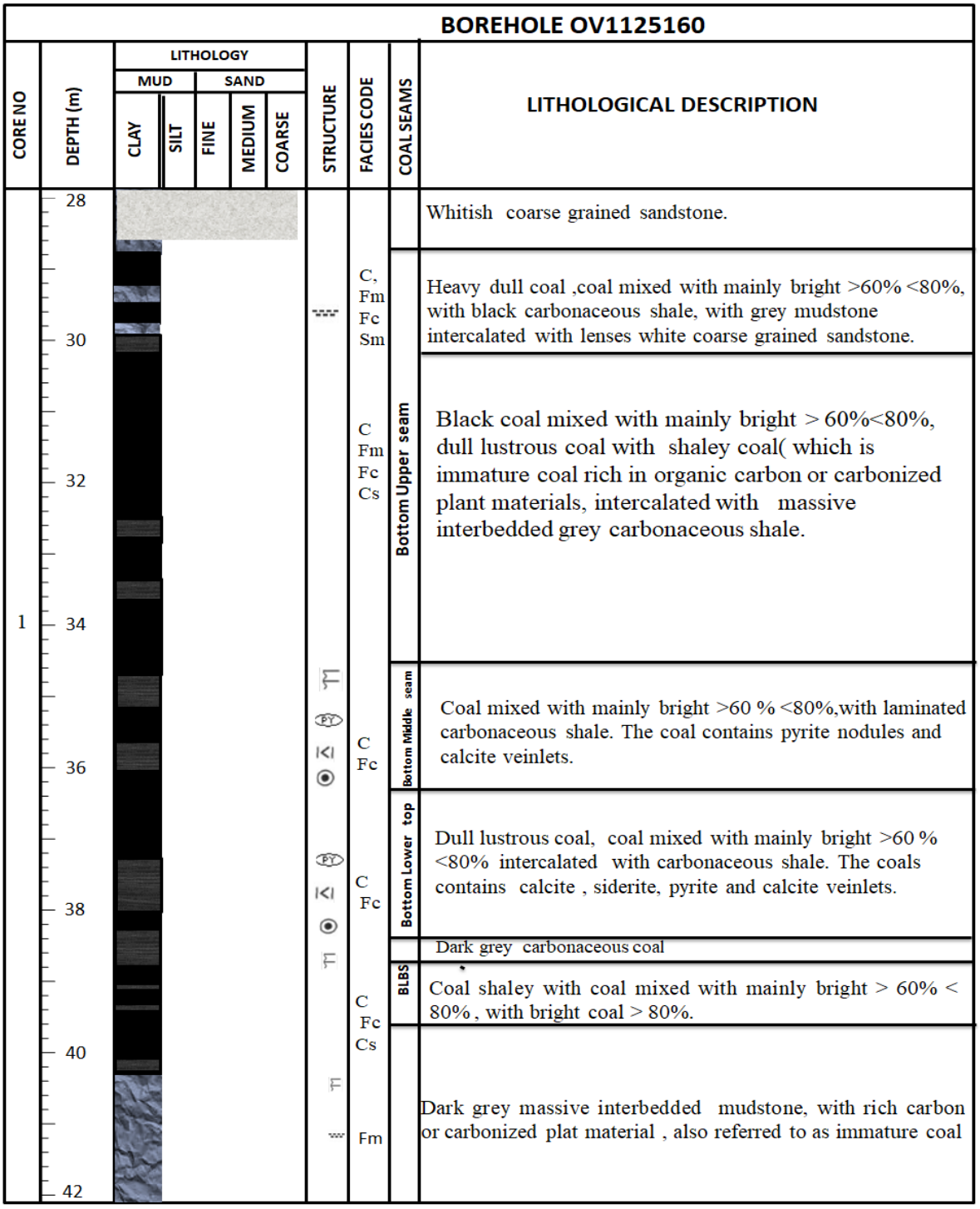
BOREHOLE OV1125160
CORE NO
DEPTH (m)
LITHOLOGY
MUD
SAND
CLAY
SILT
FINE
MEDIUM
COARSE
STRUCTURE
FACIES CODE
COAL SEAMS
LITHOLOGICAL DESCRIPTION
1
28
30
32
34
36
38
40
42
C, Fm Fc Sm
C Fm Fc Cs
C Fc
C Fc
C Fc Cs
Fm
Bottom Upper seam
Bottom Middle seam
Bottom Lower top
BLBS
Whitish coarse grained sandstone.
Heavy dull coal ,coal mixed with mainly bright >60% <80%, with black carbonaceous shale, with grey mudstone intercalated with lenses white coarse grained sandstone.
Black coal mixed with mainly bright > 60%<80%, dull lustrous coal with shaley coal(which is immature coal rich in organic carbon or carbonized plant materials, intercalated with massive interbedded grey carbonaceous shale.
Coal mixed with mainly bright >60 % <80%,with laminated carbonaceous shale. The coal contains pyrite nodules and calcite veinlets.
Dull lustrous coal, coal mixed with mainly bright >60 % <80% intercalated with carbonaceous shale. The coals contains calcite , siderite, pyrite and calcite veinlets.
Dark grey carbonaceous coal
Coal shaley with coal mixed with mainly bright > 60% < 80% , with bright coal > 80%.
Dark grey massive interbedded mudstone, with rich carbon or carbonized plat material , also referred to as immature coal

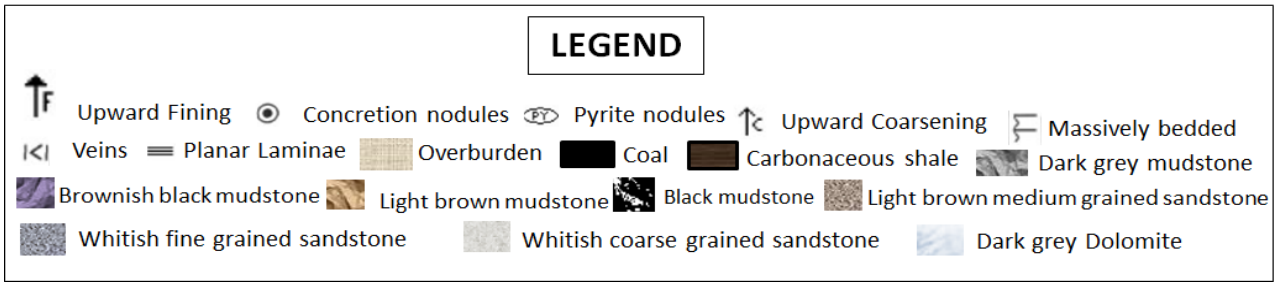
LEGEND
Upward Fining
Concretion nodules
Pyrite nodules
Upward Coarsening
Massively bedded
Veins
Planar Laminae
Overburden
Coal
Carbonaceous shale
Dark grey mudstone
Brownish black mudstone
Light brown mudstone
Black mudstone
Light brown medium grained sandstone
Whitish fine grained sandstone
Whitish coarse grained sandstone
Dark grey Dolomite

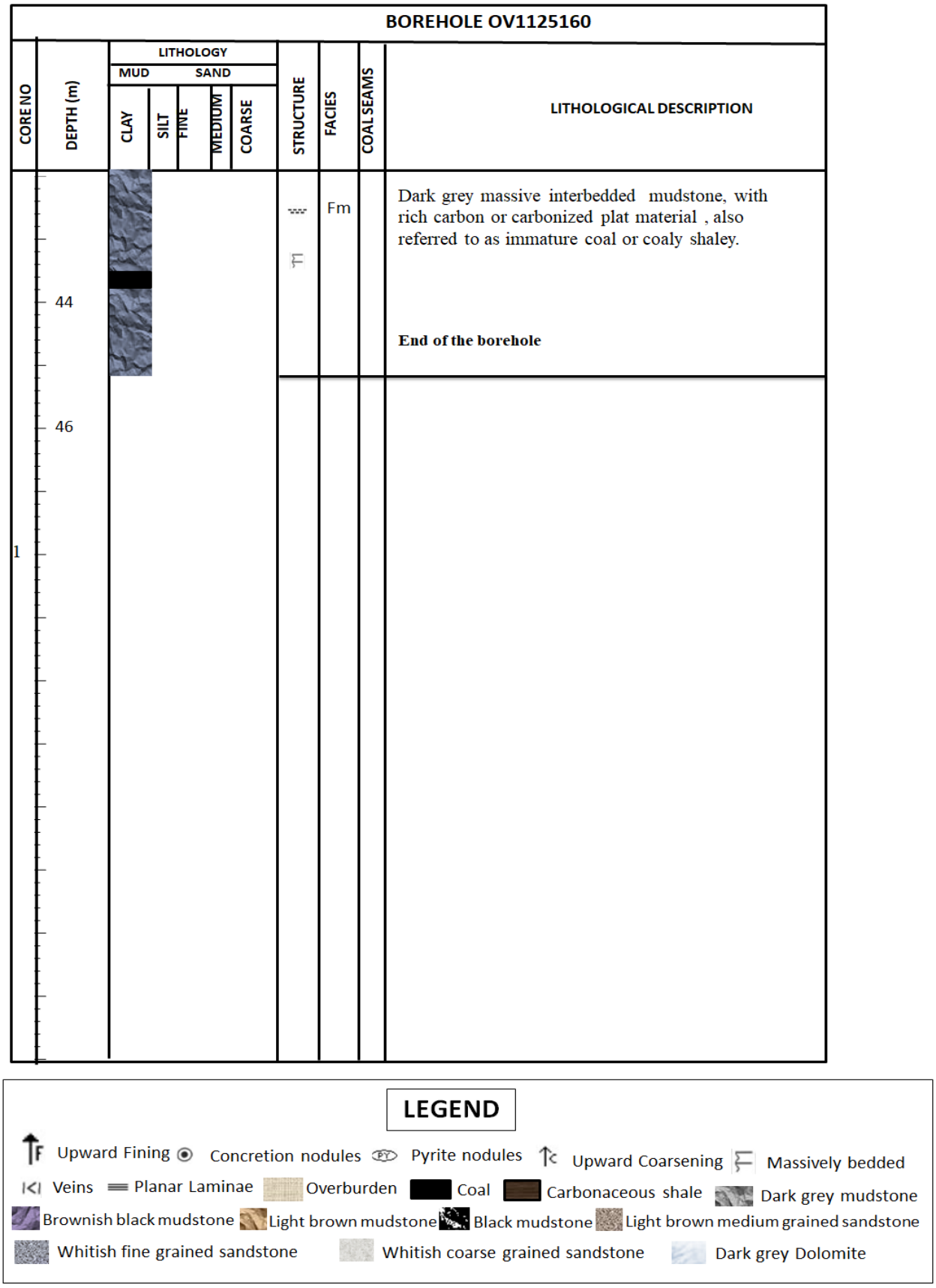

Figure 4.8: Stratigraphy of the Madzaringwe Formation in borehole OV125160.

CHAPTER 5

COAL PETROGRAPHY

5.1 Introduction

Coal is an important organic sedimentary rock because it is used or serves as a source of electricity generation in most countries such as South Africa. Even though coal, in the long run formation the time it takes for coal to form is not practical, because it can take millions of years for coal to be formed. In general, coal is formed under different temperature and pressure over long periods. A progressive increase in pressure and temperature will form different types of coal. Coal type is related to the type of plant material in the peat and the extent of its biochemical and chemical alteration. When organic material goes throgh degrdation to form peat. As more sediments accumulates over the peat and causes the peat to burry under greater pressure and higher temperature, lignite is formed. As more pressure is applied to the lignite and the temperature becomes hotter, the earlier formed lignite changes to bituminous coal. Bituminous coal then becomes anthracite coal as its temperature and pressure increases.

Coal petrography deals with the microscopic identification of the different components of coal and measurement of vitrinite reflectance to determine the coal rank or quality. Coal petrography is a very vital tool in the classification of coal deposits as well as coal products (Suárez-Ruiz et al., 2012). The classification and characterization of coal for coke-making is significant because it allows for selection of coals of a definite quality for specific coking operations, and/or for estimating the quality of the coke that will be produced under certain conditions. Most of the sampling, preparation, and analysis

techniques for coal petrography are determined or controlled by the standard methods reported or documented by a research working group within International Organization for Standardization (ISO) Technical Committee TC 27 for Solid Mineral Fuels. This committee was set up to develop test methods that should be generally used for international trade as well as serves as international standards for coal production.

In the coke-making industry, “the strength of metallurgical coke is one of its most essential properties, and possibly one of the most vital uses of applied coal petrography is the ability to predict coke strength (ASTM stability) from single coals and coal blends” (Suárez-Ruiz and Ward, 2008). The rank or quality and maceral constituent of coal affect the strength of the coke produced, the ratio of reactive to inert macerals is of high importance when predicting the stability coke. The reactive macerals are made up of vitrinite, liptinite and semi-fusinite. The semi-fusinite is often used for South African coals to define a low-reflecting form of inertinite alleged to be reactive and which can increase or add to the reactivity of coal during carbonization (Snyman, 1989). As reported by Steyn and Smith (1977), the appraisal of South African coals for their coking characteristics entails a separate evaluation of the quantity of reactive semi-fusinite in the potential coal.

The Madzaringwe Formation in the Tuli Basin, Limpopo Province is one of the coal-bearing late Palaeozoic units of the Karoo Supergroup. Presently, some coal seams of the Madzaringwe Formation in the Vele Colliery is been mined. However, up to date, the petrological aspects of these coal seams have not been taken into consideration. Although, few technical reports have been documented on the geochemical characteristics of Tuli coalfields based on irregular samples. In this study, only maceral group analysis was performed on seven coal samples (Table 5.1) from the Vele

colliery in the Tuli Coalfield. Herein, an effort has been made to carry out a petrographic study on some selected coal samples from the exploitable coal seams phase (mature and economic) in the Vele Colliery to determine the rank and other intrinsic characteristics of the coal.

Table 5.1: Description of samples analysed for maceral group.

Lab. No	Identification	Borehole	Depth (m)	Description
1675 (1)	B1	OV125156	32.0 - 34.0	Upper middle coal seam
1676 (2)	B1	OV125156	32.0 - 34.0	
1677 (3)	B2	OV125156	32.0 - 34.0	
1678 (4)	B2	OV125146	36.0 - 41.0	Middle middle coal seam
1679 (5)	B3	OV125146	36.0 - 41.0	
1680 (6)	B3	OV125160	23.0 - 24.5	Bottom middle coal seam
1681 (7)	B3	OV125160	23.0 - 24.5	

5.2 Maceral group

Maceral analysis is a technique widely used for providing valuable data on the behaviour of coals during carbonization (Table 5.2). The result of the maceral group is presented in Table 5.2. In this study, the maceral analysis was calculated in terms of total reactive (Vitrinite + exinite + $^1/_3$ semifusinite) and total inerts ($^2/_3$ semi fusinite + other inertinite macerals + mineral matter) (Hower et al., 2012). The organic fragments in coal have been classified into three groups based on the major characteristics pertaining to each group. These are the vitrinite maceral group,

inertinite maceral group and the liptinite maceral group (Table 5.2). Each of the group is further subdivided into macerals and sub-macerals.

Table 5.2: Result of the maceral group analysis.

MACERAL GROUP ANALYSIS (% BY VOLUME)															
THESE RESULTS RELATE ONLY TO THE ANALYSED															
Sample no:		**1675**		**1676**		**1677**		**1678**		**1679**		**1680**		**1681**	
		1		2		3		4		5		6		7	
Maceral Group	**MACERAL(vol%)**	inc.mm vol%	mmf vol%	inc.mm vol%	mmf vol%	inc.mm vol%	mmf vol%	inc.mm vol%	mmf vol%	inc.mm vol%	mmf vol%	inc.mm vol%	mmf vol%	inc.mm vol%	mmf vol%
Vitrinite	Telinite	1.6	2.0	4.7	6.5	1.0	1.3	3.0	3.1	3.9	4.3	2.2	2.3	0.8	0.8
	collotellinite	58.8	74.9	38.5	52.4	48.0	60.6	56.7	60.3	57.7	62.3	51.2	55.5	55.7	58.7
	vitrodetrinite	0.0	0.0	0.0	0.0	0.0	0.0	0.0	0.0	0.0	0.0	0.0	0.0	0.0	0.0
	collodetrinite	1.2	1.5	12.8	17.5	4.1	5.2	4.3	4.6	6.5	7.0	4.9	5.3	8.4	8.9
	corpogelinite	0.8	1.0	3.0	4.0	15.2	19.2	18.3	19.5	15.6	16.8	17.8	19.4	13.1	13.8
	Gelinite	0.4	0.5	0.0	0.0	0.0	0.0	0.0	0.0	0.0	0.0	0.0	0.0	0.0	0.0
	pseudovitrinite	4.6	5.9	0.2	0.3	4.5	5.7	4.5	4.8	1.4	1.5	2.9	3.2	0.8	0.8
Inertinite	Fusinite	5.4	6.9	5.1	7.0	2.7	3.4	1.0	1	2.0	2.1	5.5	6.0	3.5	3.7
	reactive semifusinite	0.6	0.8	0.6	0.8	0.4	0.5	0.8	0.8	0.6	0.6	0.0	0.0	0.6	0.6
	inert semifusinite	1.6	2.0	4.1	5.6	0.6	0.8	1.4	1.5	0.6	0.6	1.6	1.7	0.2	0.2
	Micrinite	0.0	0.0	0.0	0.0	0.0	0.0	0.0	0.0	0.0	0.0	0.0	0.0	0.0	0.0
	Macrinite	0.2	0.3	0.0	0.0	0.2	0.3	0.0	0.0	0.0	0.0	0.4	0.4	0.0	0.0
	Secrinite	0.0	0.0	0.0	0.0	0.0	0.0	0.2	0.2	0.0	0.0	0.0	0.0	0.0	0.0
	Funginite	0.0	0.0	0.0	0.0	0.0	0.0	0.0	0.0	0.0	0.0	0.0	0.0	0.0	0.0
	inertodetrinite R	0.8	0.0	0.0	0.0	0.0	0.0	0.0	0.0	0.0	0.0	0.0	0.0	0.0	0.0
	inertodetrinite I	2.0	0.0	1.8	2.4	0.2	0.3	0.2	0.2	0.6	0.6	0.8	0.9	0.4	0.4
Liptinite	Sporinite	0.4	0.5	2.4	2.4	2.0	2.6	3.3	3.3	3.5	3.8	3.1	3.4	5.3	5.6
	Cutinite	0.0	0.0	0.0	0.0	0.2	0.3	0.6	0.6	0.2	0.2	1.4	1.5	5.7	6.0
	Resinite	0.0	0.0	0.0	0.0	0.0	0.0	0.0	0.0	0.0	0.0	0.0	0.0	0.0	0.0
	Alginite	0.0	0.0	1.1	0.0	0.0	0.0	0.0	0.0	0.0	0.0	0.0	0.0	0.0	0.0
	liptoderinite	0.0	0.0	0.0	0.0	0.0	0.0	0.0	0.0	0.0	0.0	0.0	0.0	0.0	0.0
	Suberinite	0.0	0.0	0.0	0.0	0.0	0.0	0.0	0.0	0.0	0.0	0.0	0.0	0.0	0.0

	exsudatinite	0.0	0.0	0.0	0.0	0.0	0.0	0.0	0.0	0.0	0.0	0.1	0.4	0.4	0.4
mineral matter	silicate (clay/qtz)	7.2		21.7		18.4		2.8		5.7		6.9		3.5	
	Sulfide	5.4		0.8		0.8		0.0		0.2		0.0		0.2	
	carbonate	8.6		3.2		1.6		3.1		1.6		1.0		1.2	
	Other	0.2		1.0		0.0		0.0		0.0		0.0		0.0	
SUMMARY TABLE															
MACERAL GROUP	VITRINITE	67.5	85.9	59.2	80.6	72.8	92.0	86.8	92.3	85.0	91.9	79.0	85.7	78.8	83.1
TOTALS (VOL %)	INERTINITE	10.6	13.6	11.6	15.9	4.1	5.2	3.5	3.8	3.7	4.0	8.2	8.9	4.7	5.0
	LIPTINITE	0.4	0.5	2.6	3.5	2.3	2.8	3.7	4.0	3.7	4.0	4.9	5.3	11.4	12.0
	MINERAL MATTER	21.5		26.6		20.9		7.5		7.5		7.8		4.9	
	TOTAL INERTINITE	10.6	13.6	11.6	15.9	4.1	5.2	3.7	3.8	3.7	4.0	8.2	8.9	4.7	5.0
	TOTAL REACTIVE MACERAL	69.3	88.2	62.3	84.9	75.4	95.3	89.4	97.1	89.4	96.6	83.9	91.1	90.8	95.7

Note: inc mm = mineral matter included in count; mmf = matter free, determined via calculation from total count; Total inertinite= all inertinite macerals; Total reactive macerals= vitrinite + liptinite + reactive semifusinite + reactive inertodetrinite.

5.2.1 Vitrinite

The vitrinite maceral group is grey with a reflectance generally between the range related with the darker liptinites and lighter inertinites. The vitrinite group consists of three subgroups and six macerals. These macerals are derived from different humic materials with varying pathways of transformation within the early peats. The different types of maceral groups, as well as their origin, are presented in Table 5.3. The different molecular components of plants that produce macerals and maceral groups, constitute lithotypes, which later formed the coal. For instance, vitrinite, with or without small amounts of liptinite and inertinites, consists of vitrain, durain and clarain. The durain is made up of three maceral groups in approximately equal proportions. The fusain dominates the inertinite group, whereas the clarain is a blend of vitrain and durain (Hower et al., 2012).

Table 5.3: Maceral groups and their origin (after Hower et al., 2012).

Group	Maceral	Origin	Significance
Vitrinite	Telovitrinite	Humidified stem, root bark and leaf tissue, which has survived intact and displays remnants of cellular structure	High vitrinite content, especially the structured telovitrinite, indicates a permanently water-saturated peatland balanced or high accommodation creation
	Detrovitrinite	Stem, root, bark and leaf tissue deposited as fine-grained attritus before humification	
Liptinite	Sporinite	Resins, fats, waxes and oils	Increased liptinite content indicates loss of biomass associated with poor preservation conditions
	Cutinite	Cuticles of needles, shots, stalks, leaves, roots, and stems	
	Resinite	Raisins, fats waxes and oils	
Inertinite	Micrinite	Product of disproportion reactions, or any other fine-grained oxidised plant material	high inertinite content, especially structured fusinite and semifusinite indicate a low or fluctuation mire water-table and low accommodation relative to peat
	Macrinite	Jellified plant material which has undergone some oxidation	
	Semifusinite	partial oxidation of plant material which has survived intact and shows remnants of cellular structure	
	Fusinite	Plant material which has survived intact following partial combustion in the wilderness. Shows remnants of cellular structure	
	Itertodetrinite	Fragmented semifusinite	

The petrographic characterization revealed that vitrinite is the dominant maceral group in the coals, making up to 81-92 vol% of the total sample. Collotellinite is the dominant vitrinite maceral, followed by corpogelinite, pseudovitrinite and tellinite (Table 5.2). Collotellinite is the dominant vitrinite maceral with 38.5 to 57.7 inc. mm vol.%. The dominance of collotellinite gives a clear indication that the coal in Vele colliery is derived from the parenchymatous and woody tissues of roots, stems, and leaves, composed of cellulose and lignin and originating from herbaceous and arborescent plants (Hower *et al.*, 2012). By geochemical gelification (vitrinitization), the primary structures disappear. The precursor of collotellinite in low-rank coals is ulminite. At higher rank levels, collotelinite is also formed from telinite and its vitrinitic cell fillings. According to the new vitrinite classification (ICCP System, 1994), it is very common in shaly coals and it is part of kerogen Type III.

In the analysed samples, collodetrinite ranges from 1.2 to 8.9 mmf vol.%. According to the new vitrinite classification (ICCP System, 1994), it is derived from parenchymatous and woody tissues of roots, stems and leaves, composed of cellulose and lignin. The original plant tissues are crushed by strong decomposition at the beginning of the peat stage. The small particles are cemented by humic colloids within the peat and successively homogenized by geochemical gelification (vitrinitization). Cellulose derived substances may be the main source of collodetrinite rather than lignin-rich wood precursors of collodetrinite in low-rank coals are attrinite and densinite (ICCP, 2001). The corpogellinite in the samples range from 1.0 to 19.4 maceral mmf vol.%. Corpogellinite belongs to the gelovitrinite subgroup within the vitrinite maceral group and it entails of homogeneous and discrete bodies, signifying cell infillings.

Corpogelinite may be of primary source corresponding to cell contents, derived from the tannin in part; it may also have been derived from secretions of the cell walls. Instead, it may contain secondary infillings of tissue cavities by humic solutions, which consequently precipitate as gels during peatification and early stages of coalification.

All the analysed samples tend to have pseudovitriite, which according to Ward (2016), is a sub maceral of vitrinite. Pseudovitriite is considered to be an alteration product of collotelinite derived by devolatiization and desiccation or oxidation or combination of the processes. Therefore, it is clear that pseudovitriite is known to affect the swelling properties of the coals despite the very high vitrinite content (Suárez-ruiz et al., 2012). The observed vitrinite in coals is formed as an outcome of anaerobic preservation of lingo-cellulosic material in swamps. It also occurs in the shaly coal where organic and mineral matter were deposited rapidly. Vitrinite is the main component of bright coal encompassing the microlithotypes vitrinite, vitrinertite and clarite.

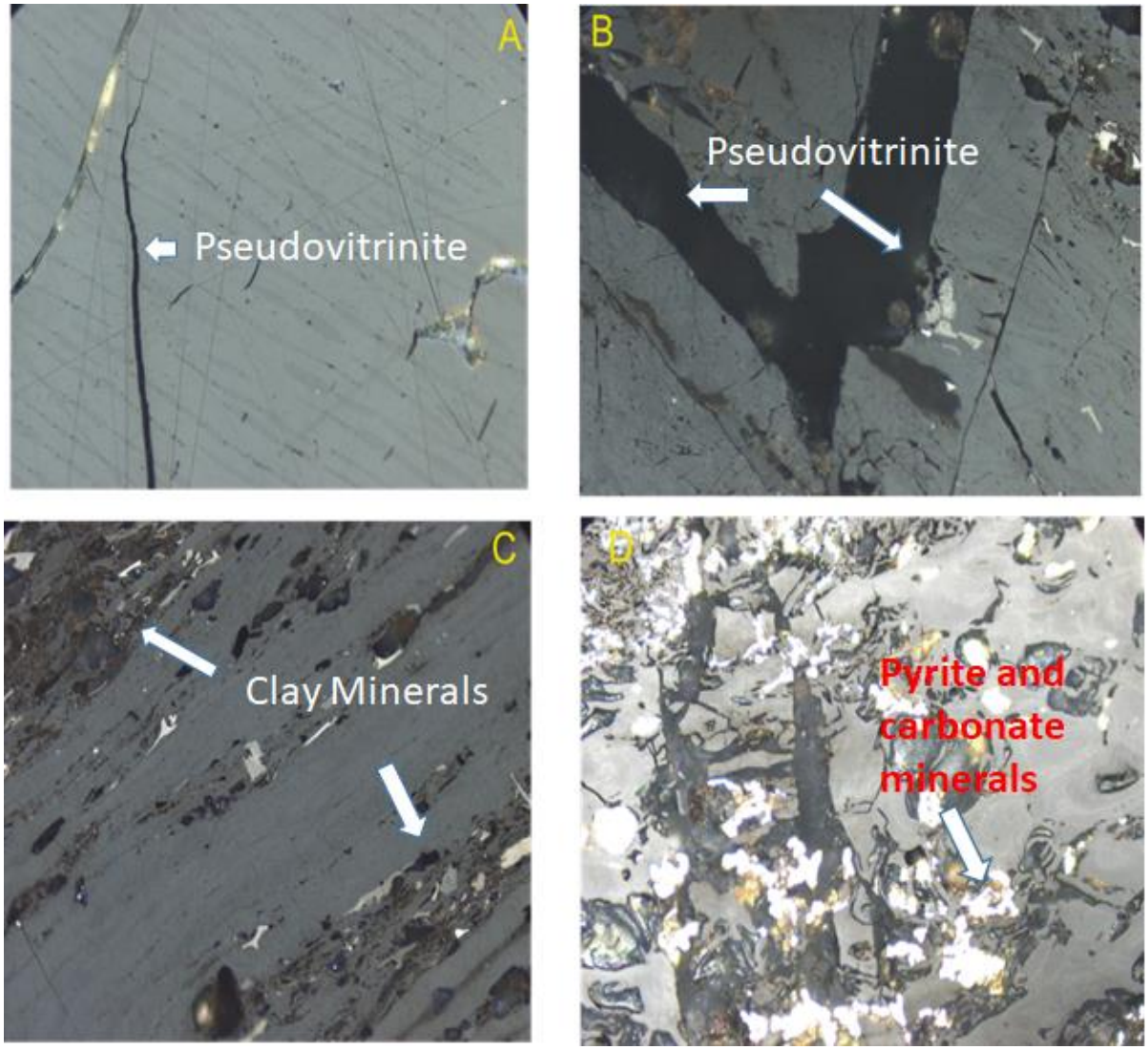

Figure 5.1: Photomicrographs of coal showing vitrinite; (A) Pseudovitriite with pyrite nodules; (B) Pseudovitriite with carbonate minerals; (C) Clay and quartz minerals; (D) Quartz fillings in vitrinite.

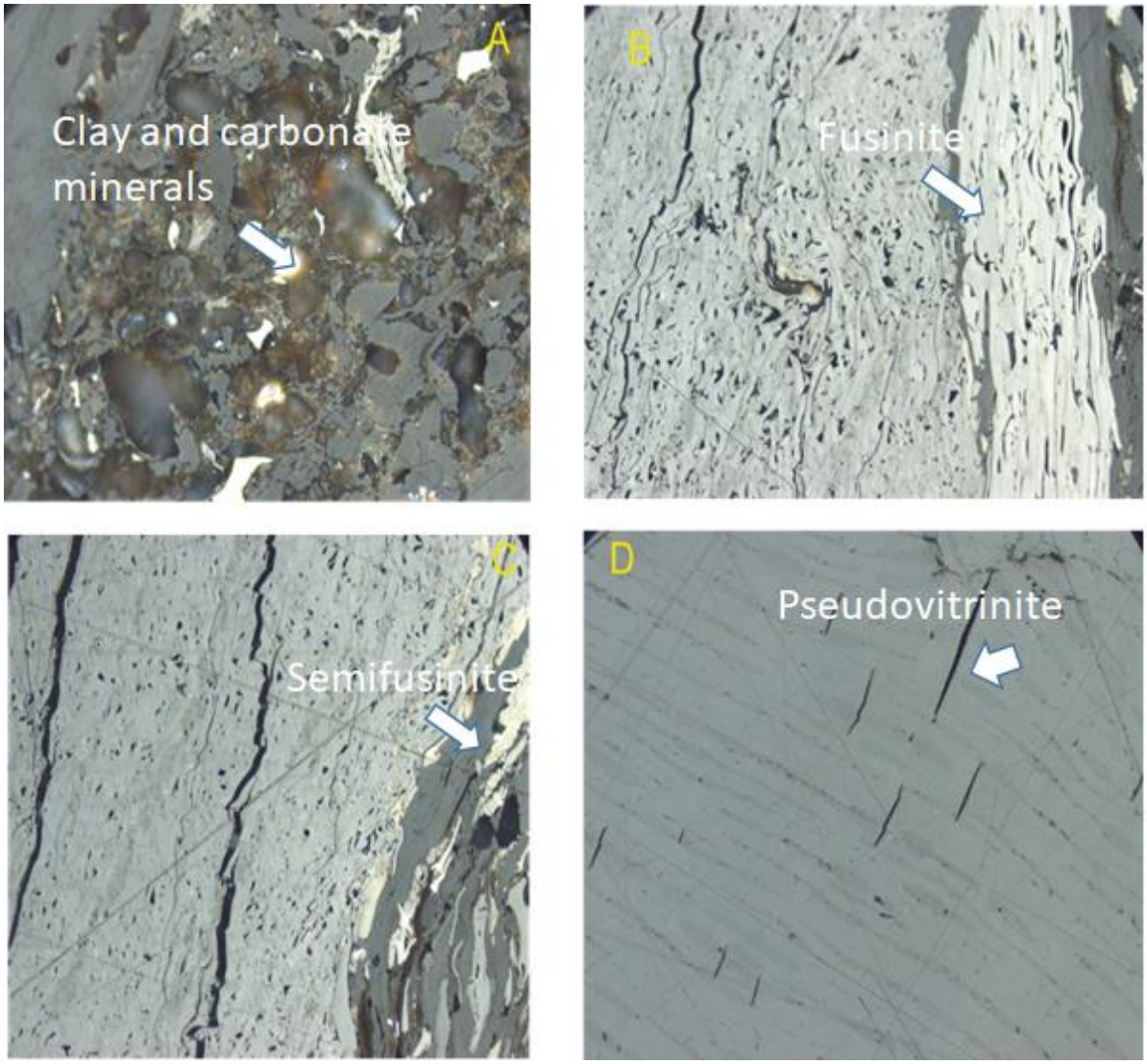

Figure 5.2: Photomicrographs of coal showing: (A) Vitrinite with clay and carbonates; (B) Fusinite and semifusinite with small layers of vitrinite; (C) Semifusinite with dark grey vitrinite and cracks called pseudovitriite; (D) Pseudovitriite in light grey collotellinite.

5.2.2. Inertinite

The Inertinite content is very low in the studied samples, ranging from 4-16 mmf vol.% and it is dominated by fusinite. The higher amount of inertinite, particularly fusinite with empty cells and semifusinite in coals support the formation of dust during mining. It is

also believed that partly fusible and infusible inertinite acts as learning material in coal blends, but improves coke strength when they dispersed. In the case of this study middle coal seam, they appear to be less concentration of inertinite. Fusinite is believed to occur in discrete lenses, thin partings of bands, it may be transported by water or air into the mire sedimentary basin but may also have originated by in situ burning. Fusinite is a characteristic composition of Kerogen IV (dead carbon).

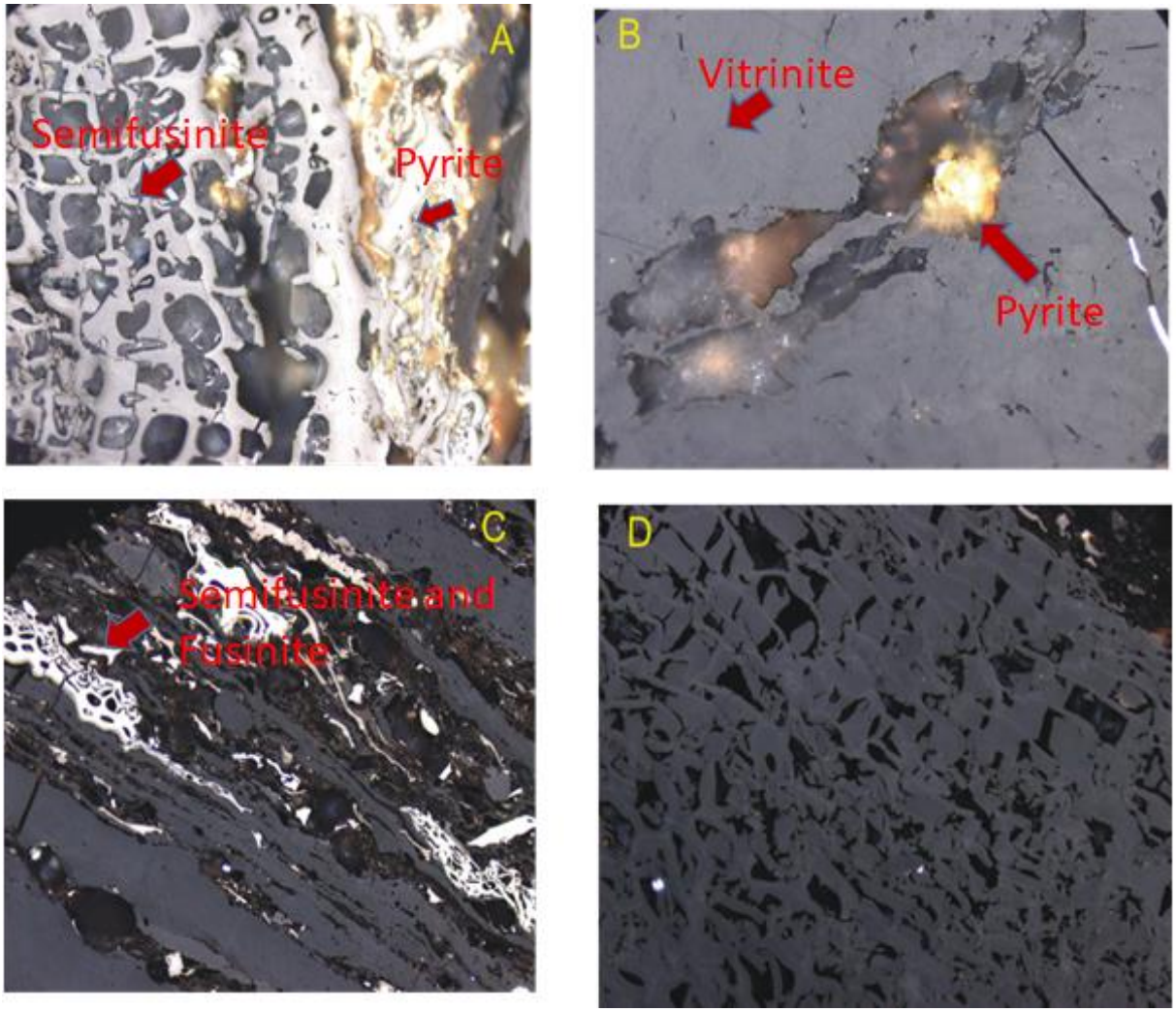

Figure 5.3: Photomicrograph of coal showing: (A) semifusinite with pyrite minerals in yellow ; (B) Vitrinite maceral with pyrite minerals; (C) Semifusinite and fusinite; (D) Fusinite maceral

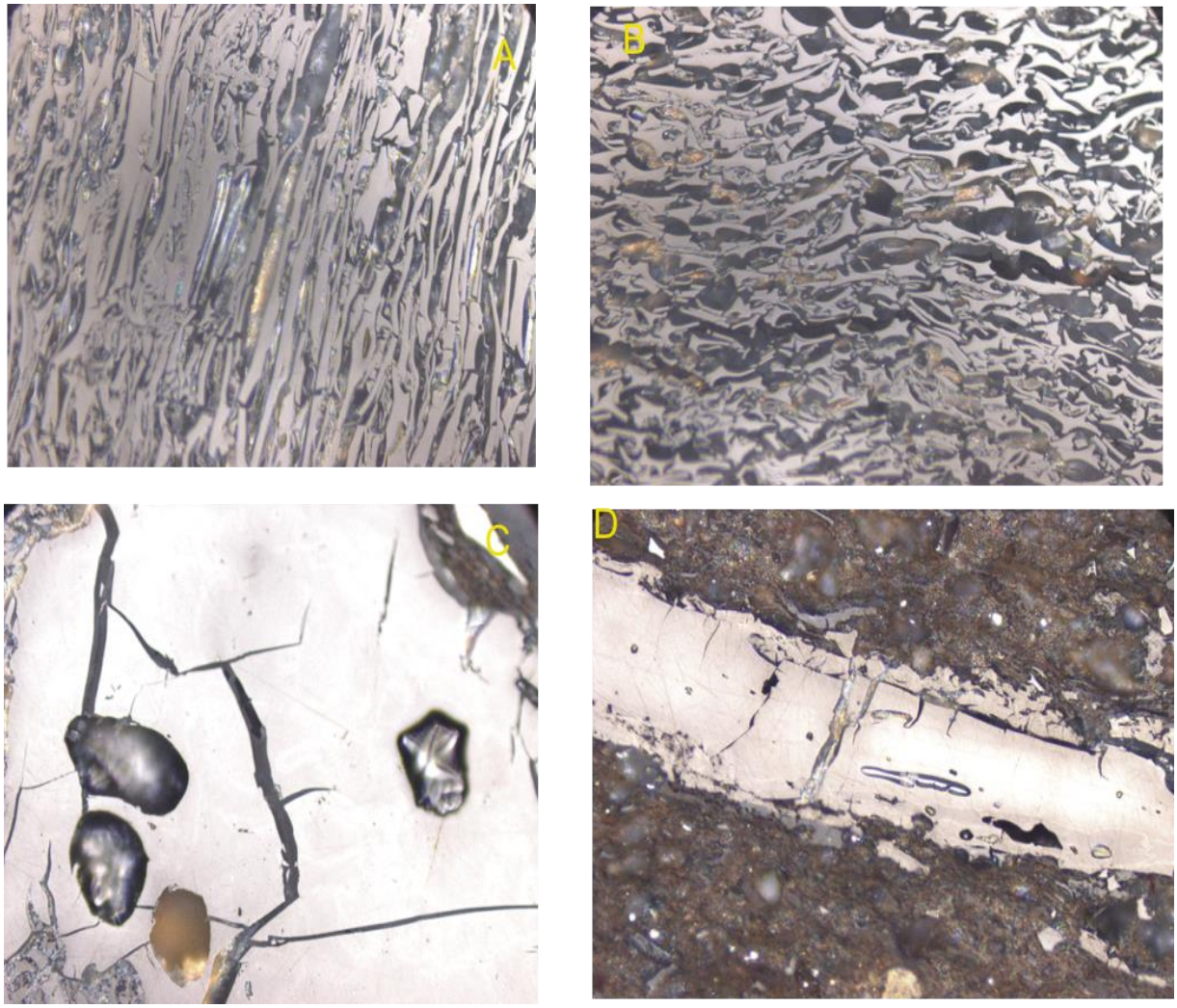

Figure 5.4: Photomicrograph of coal showing: (A) Fusinite with pyrite inclusions; (B) Semifusinite with pyrite inclusions; (C) Pseudovitriite with pyrite nodules on vitrinite and (D) Fusinite maceral surrounded by clay minerals.

5.2.3 Liptinite

Liptinite ranges from extremely low in the top samples (0.5 mmf vol.% in sample 1675), to high in the bottom sample (12 mmf vol.% in sample 1681). Sample number 1681 is dominated by cutinite. Cutinite comprises of fossil cuticles, which forms protective layers of cromophyte epidermal cells. Cuticles arise from leaves and stems. Moreover, endodermal matter and ovular embryo sacs are comprised in the initial materials of

cutinite. Nonetheless, most cuticle fragments are derived from leaves because these are produced and shed in great number (Tyson, 1995).

Cuticle analysis in combination with spore analysis may aid the correlation of coal seams (Stach et al., 1982). Additionally, it plays a significant role in the assessment of facies and stratigraphic questions and the reconstruction of plant communities of brown-coal paleo mires (Schneider, 1969). The occurrence of cutinite in contrast to the very low proportion of liptinite in the top samples indicates different depositional and preservation environments through the sequence.

5.3 Mineral matter in the coal

Common minerals in the coal samples of Vele colliery are calcium-iron minerals such as calcite, ankerite and siderite and pyrite, and also silica in the form of quartz and silicate of clay minerals. The latter minerals are frequently derived from groundwater passing through cracks and fissures in the hardening or hardened coal seams. When saturated, the ions and elements in the groundwater precipitate out, resulting in the formation of mineral, which often takes the shape of the cracks or fissures in which they are precipitated/deposited. The minerals could have formed by water passing through the xylem phloem or cortical cells (supportive and ‘feeding’ cellular tissue) in the ancient tree trunks also led to the precipitation of minerals in those cellular cavities, thereby locking the mineral into those cell structures.

The observable mineral matter ranges from 21-26 vol.% in the top samples (Figure 5.3). The results show that sample 4 from the middle coal seam has the lowest silica mineral percentage of about 2.8 vol.%. Silicate minerals (which can be quartz or clay)

are the most abundant and represent an average of approximately 21.7 vol.% of the total mineral matter associated with coal in the upper-middle seam. Mineral genesis is complex; they may have a detrital origin or maybe a secondary product from aqueous solutions (Hackely and Kolak, 2008). Also, the top samples have a high amount of epigenetic carbonate minerals which are minerals deposited after peat formation at any time, during coalification. Carbonate minerals in the samples appear to have shattered the vitrinites with the lowest effect in sample 7 (lower middle seam) and highest with 8.6 vol.% in sample 1 (upper-middle coal seam). It is supposed that the secondary carbonate minerals precipitate from magma-derived fluids percolating through the coal following the emplacement of the intrusion. The textures and distribution of carbonate minerals suggest that the temperatures and pressures of the fluids may be just as significant in the developing fractures near dykes, particularly those that have multiple phases of geometries (Alexander et al., 2007). The pyrite content is also high in sample 1, with concentration of about 5.4 vol.%, which is a contrast to the other samples where the pyrite content is less than 1 vol.% or completely absent/not observed under the microscope. Sulphur is commonly present in the organic fraction of the coal, whereas inorganic or mineral sulphur is in the form of pyrite. Pyrite may be present as a primary as authegenic minerals in coal and black shale or as secondary pyrite as a result of the reduction of sulphur in fluvial waters.

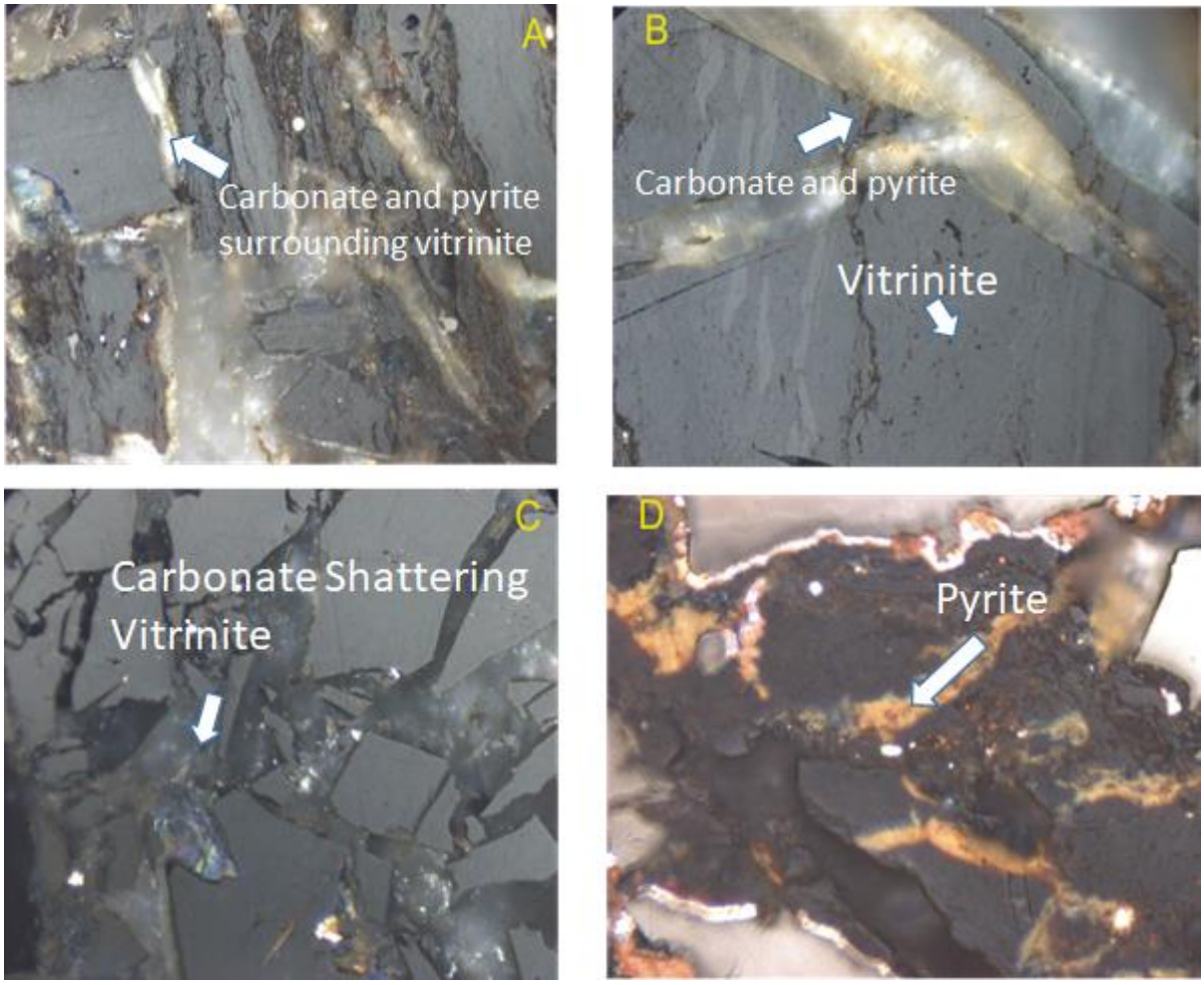

Figure 5.5: Photograph showing: (A) epigenetic carbonate minerals with pyrites shattering vitrinite, with more clay minerals surrounding the shattering: (B) epigenetic carbonate minerals with pyrites shattering vitrinite with specific example to collotelinite in darker grey shades: (C) Carbonate mineral shattering vitrinite: (D) Pyrite mineral in darker yellowish-orange.

5.4 Coal rank determination

As explained at the beginning of this chapter, coal is a complex mixture of organic matter and inorganic mineral matter formed over aeons from successive layers of fallen vegetation. Coals are classified by rank according to their progressive alteration under increasing temperature and pressure, from peat-lignite-bituminous coal-

anthracite. Coal rank depends on the volatile matter, fixed carbon, inherent moisture, and oxygen. The percentage of carbon in coal is used to identify the rank of the coal and its position in the coal series, Although, no single parameter defines the rank. Typically, coal rank increases as the amount of fixed carbon increases and the amount of volatile matter and moisture decreases. Rank is the stage reached by coal in the course of its coalification. The rank depends on the maximum temperature to which the organic matter has been exposed during burial and the time it has been subjected to this temperature. Even though the heat flow from nearby intrusions may have contributed to the coalification, it is in general related to the depth of burial and the geothermal gradient (Smith and Cook, 1980). The rank is determined by various parameters but commonly and most reliably by vitrinite reflectance.

The mean random vitrinite reflectance values obtained for the analysed samples range between 0.75 and 0.76% RoVmr (mean random vitrinite reflectance), placing all samples in the medium rank C category, as per the UN-ECE in seam Classification scheme (Figure 5.6). The medium rank C category is also referred to as the high volatile bituminous coal category. The standard deviation values are low, indicating a single population, with no blending or heat effect determined. The reflectance histograms demonstrate the range of reading. The three values reported in Table 5.4 represent the top, middle and bottom section of the sampling point. The reflectance histogram graphs for top, middle and bottom section of coal seams sampling point are shown in Figure 5.7.

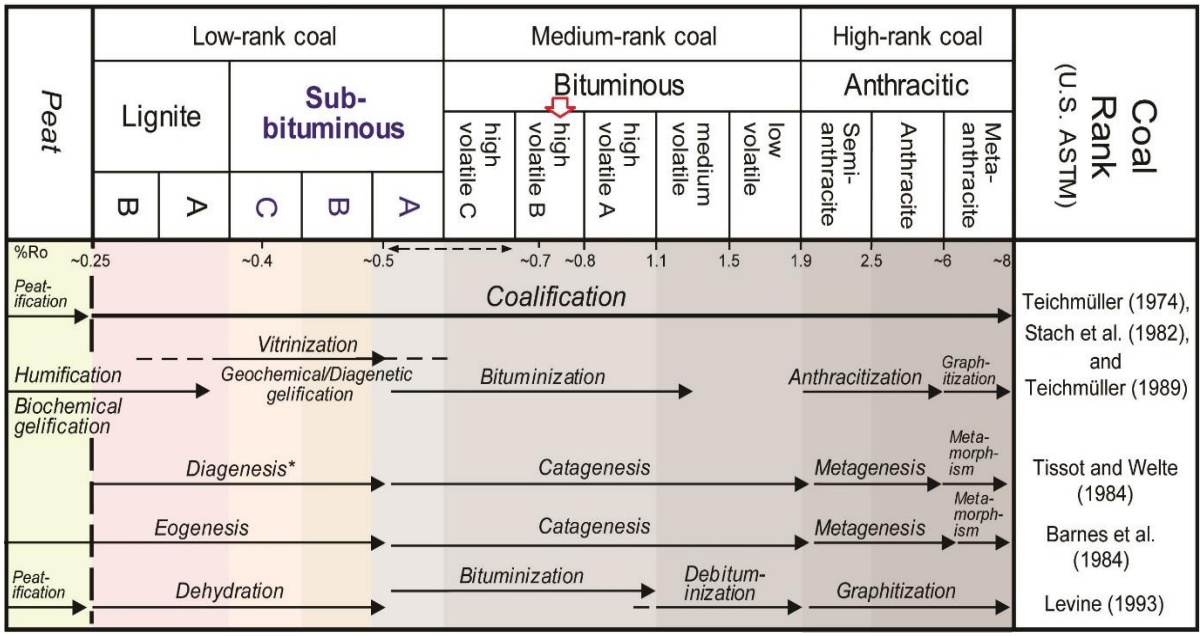

Figure 5.6: Position of the analysed samples in the UN-NCE in seam classification scheme (Bibler, 1998).

Table 5.4: Results of vitrinite reactance analysis (RoV%) of top, middle and bottom section of the sampling point.

VITRINITE REFLECTANCE ANALYSIS (RoV%)								
Sample number		**1675**	**1676**	**1677**	**1678**	**1679**	**1680**	**1681**
Sample Identification		**1**	**2**	**3**	**4**	**5**	**6**	**7**
Sample reflectance Rmax (RoV%)	st.dev							
	Random st.dev	0.76 0.068			0.75 0.048		0.75 0.057	
	max min	0.89 0.57			0.83 0.64		0.88 0.58	
	V classes **RANK CATEGORY**	**Medium rank C**			**Medium rank C**		**Medium rank C**	

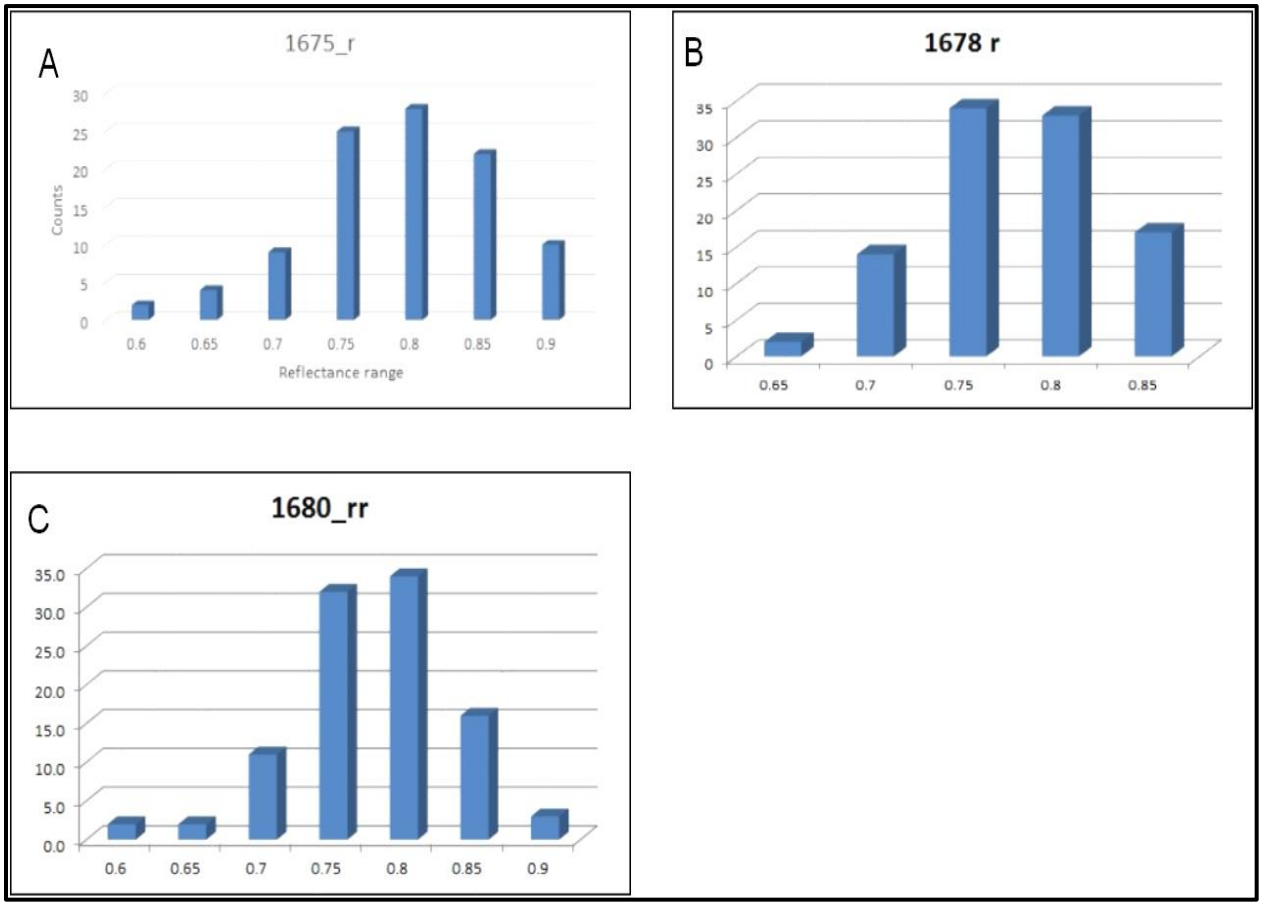

Figure 5.7: Reflectance histogram graphs for top, middle and bottom section of coal seams sampling point.

CHAPTER 6

SEDIMENTARY FACIES AND DEPOSITIONAL ENVIRONMENT

6.1 Introduction

This chapter covers the description of sedimentary facies of the Madzaringwe Formation that were identified in the Vele colliery. The descriptions of the lithofacies were done on the borehole cores and open pit. The observations aided the determination and interpretation of the depositional environments centred on the lithologies, sedimentary structures and their contact relationship. The aforementioned characteristics serve as diagnostic features of depositional processes, hydrodynamic conditions and depositional environments. The Madzaringwe Formation in the Vele colliery is made up of shale, and mudstone with subordinate coal seams, sandstones, siltstones and dolomite. The particular structures/textures in the sediments are generated by the sedimentary processes operating within depositional sedimentary environments. These preserved recognisable characteristics in the rock record on a basis of composition, texture, fossil content, geometry, colour, bedding, lithology, sedimentary structures and paleocurrent patterns are referred to as sedimentary facies (Misiak, 2006).

Sedimentary facies is a concept that is used in a descriptive and interpretative way to deduce the formation processes and depositional environments from which a particular sedimentary rock was sourced or derived. In 1669, Nicholaus Steno inroduced the term “facies” and Gressly (1838) used the word “facies” to define the lithological and paleontological aspects of sratigraphic units in totality. Conversely,

since then, the word has been used by numerous geologists in diverse ways or context. The foremost argument about using the word is whether the word merely relates to a specific set of characteristics as opposed to the stratigraphically unconfined rock bodies as used by Gressly (1838). Contrastingly, whether the word only indicates “aerially limited parts of a designated stratigraphic unit” as used by Moore (1949) or if the term should be used purely for both descriptive (i.e. mudstone facies) and interpretative purposes (i.e. fluvial facies) (Middleton and Hampton, 1976; Reading, 1978).

The term “facies” is defined as a body of sedimentary rock with precise characteristics such as a combination of lithological, physical and biological aspects to differentiate it from neighbouring rock bodies, and it is demarcated based on lithology, colour, bedding, mineral composition, texture, grain size, sedimentary structures, paleocurrent pattern and fossil content. Lithofacies and biofacies are the two major classifications of sedimentary facies. Lithofacies covers the lithological features, such as colour, mineral composition, rock texture and sedimentary structures; whereas the biofacies entails the biological characteristics, such as fossil types, burial and proportion of a specific fossil, fossil assemblage, etc. However, isolated facies is not good enough to indicate depositional history and sedimentary environment. Interpretation of depositional environment is dependent on various factors, including lithological characteristics, biological characteristics, and the vertical and lateral profile of the facies in the field outcrop. It is likely to comprehend the process or set of processes that prevail in the depositional environment by identifying facies associations. The processes that exist or present in the depositional environment

resulted in the characteristics of a depositional environment, consequently, there is a link between the depositional environment and facies associations.

6.2 Facies and facies associations

The lithofacies in the Madzaringwe Formation were recognized mainly based on lithologies and sedimentary structures. Ten lithofacies were recognised in the Madzaringwe Formation (Table 6.1) and they are grouped into 4 distinct facies associations. The characteristics of the facies associations (FA) are presented in Table 6.2.

Table 6.1: Lithofacies identified in the Madzaringwe Formation.

Facies Code	Facies	Sedimentary Structures
Sm	Fine to coarse grain, massive sandstone	Massive to faintly laminated
Fmb	Massive, bioturbated mudstone	Massive and occasionally calcareous
Fc	Black laminated carbonaceous shale and mudstone	Laminated, rich organic carbon or carbonized plant matter
Fls	Laminated to thin-bedded pyritic shale	Laminated to thin-bedded, pencil cleavage
Fms	Greyish thin-bedded mudstone and laminated siltstone	Laminated, thin-bedded
Fm	Massive mudstone	Massive
Fss	Brownish laminated to thin-bedded micaceous and calcareous shale and siltstone	Well laminated to thin-bedded, sometimes with very small ripples

C	Black coal	Coal stringers, 1-7 cm thick; < 2- 3 m long.
Cs	Dark grey shaly coal	Massive
D	Dolomite	Massive and occasionally calcareous

Table 6.2: Facies associations identified in the Madzaringwe Formation.

Facies association	**Facies code**	**Interpretation of depositional environments**
FA 1: Carbonaceous and pyritic shale and mudstones	Fc, Fmb	Flood plain and backswamps
FA 2: Black coal and shaly coal	C, Cs	Thickly vegetated backswamps
FA 3: Dark grey micaceous and calcareous shale and mudstone, with subordinate siltstones	Fls, Fm, Fc, Fms, Fmb	Shallow lake or floodplain deposits
FA 4: Siltstone intercalated with fine to coarse grained sandstones	Fms, Fss, Sm, D	Floodplain, cravasse splay channel deposits

6.2.1 Carbonaceous and pyritic shale and mudstones (FA 1)

FA 1 is made up of the Fc and Fmb facies, and it forms part of the upper part of the Madzaringwe Formation. The Fc facies consists of black laminated carbonaceous and pyritic shale and massive mudstones (Figure 6.1). The Fc facies contain abundant to rare carbonized plant material and form a big part of coal seams (upper, middle and bottom). The Fmb facies overlies the Fc facies and it is made up brownish-black bioturbated mudstones. The contact between Fc and Fmb is sharp but in few areas, it is gradational. FA 1 reaches a maximum thickness of approximately 5.2 m in the borehole, with an average thickness of 3.86 m in the Vele Colliery.

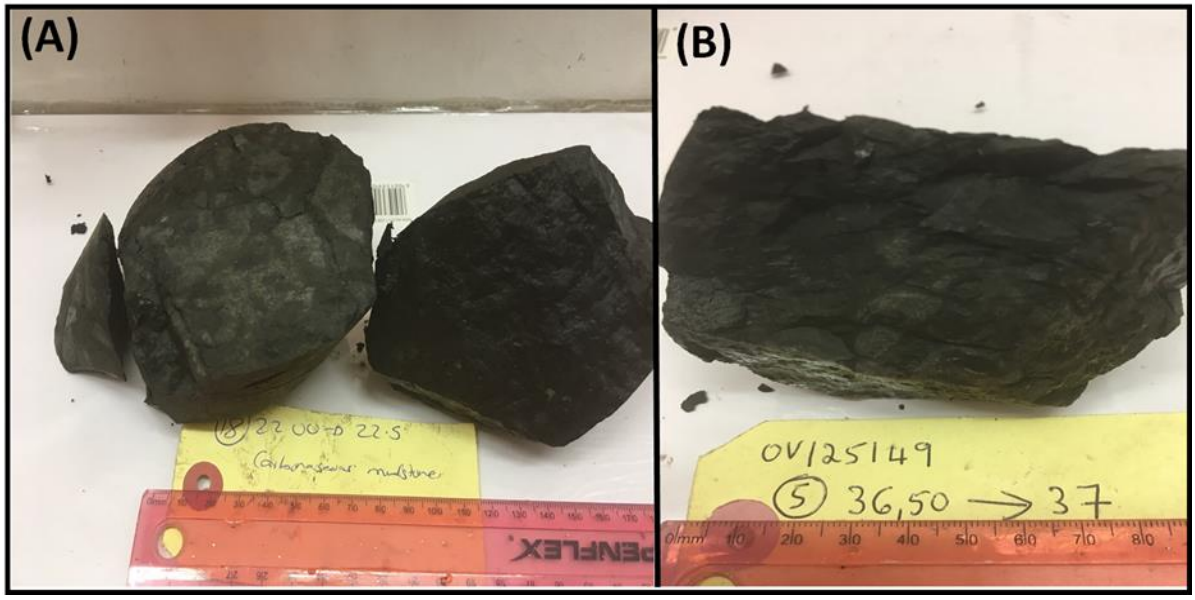

Figure 6.1: Photograph of Fc facies showing laminated carbonaceous shale.

6.2.1.1 Interpretation

FA 1 is made up of Fc and Fmb facies, and it is interpreted as suspension sedimentation in a low-energy, floodplain environments with a slight variation of hydrodynamic energy. The occurrence of blackish thick-bedded mudstone in association with coal perhaps points to deposition by vertical accretion in backswamps or flood plain environments (Walker and Cant, 1984). Moderate growth of vegetation in and around the coalfield is indicated by the presence of carbonaceous mudstone and it is assumed to denote flood basin pond and swamp deposits, based on the abundance of conserved organic material (Bordy, 2000). Thus, FA 1 represents flood plain and backswamps deposits.

6.2.2 Black coal and shaly coal (FA 2)

FA 2 comprises of the C and Cs facies, and it is mostly existing in the middle part of the Madzaringwe Formation. The C facies is commonly interlayered with Cs facies. The C facies is made up of different types of coal. There is an occurrence of vitrinite coal which is 1–7 cm thick and 2–3 m long. The Colour of coal is black with the type of vitrinite coal that varies from, dull heavy coal, bright coal and combination of bright and heavy coal, with the occurrence of pyrite and sometimes calcite nodules. The coal distribution in FA 2 is shown in Figure 6.2, with different coal marked as B1, B2, B3, B4 and B5 on core log tray. B1 and B2 represent dull and heavy vitrinite coal, B3, B4 and B5 represent bright coal with a combination of both bright and dull colour. On the other hand, the Cs facies consist of dark grey to black shaly coal (immature coal). The formation of Cs facies starts to be visible at the beginning of each of the logged boreholes, mostly at the Top Upper and Top Middle seam. Coal interlayered with thin bands of carbonaceous shale and shale is referred to as shaley coal. (Figure 6.3). The lithofacies usually overlies the alternated sequences of sandstone, siltstone and mudstone. The coal is dull black to shiny black in colour and vitreous to sub-vitreous, classified as sub-bituminous to bituminous. A few instances, the coal grades into shaly coal to carbonaceous shale.

Figure 6.2: Photograph of borehole OV125156 showing coal (C) that varies from dull heavy coal, bright coal and combination of bright and heavy coal of the Madzaringwe Formation.

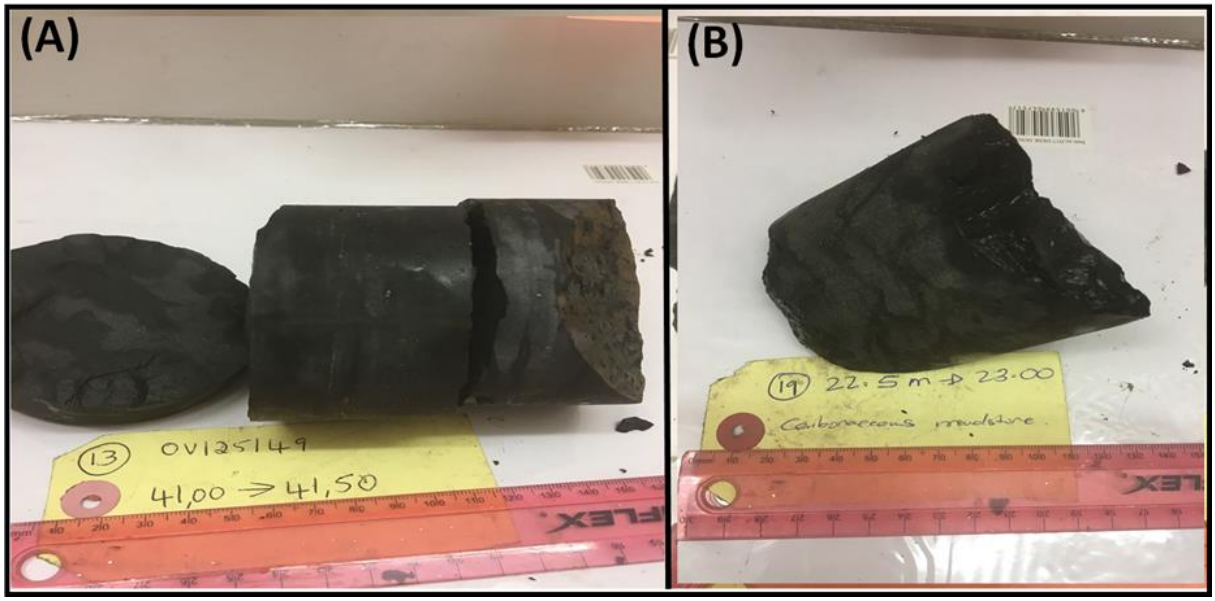

Figure 6.3: Photograph of core samples recovered from borehole OV125149 , showing immature coal referred to as shaley coal (Cs facies).

6.2.2.1 Interpretation

The shaly coal facies (Cs) is understood to signify flood basin pond and swamp deposits, based on the higher amount of preserved organic matter. Carbonaceous shale is frequently seen as part of the Cs facies gradually capping many floodplain pond successions. The dull and dark grey colours and aquatic faunas in the Madzaringwe Formation are the results of the high carbon content. The carbonaceous shales are presumed to have been transpired within a well-vegetated. Wet palaeoenvironment. The occurrence of the thick coal seam (C) of about 3-7 m, perhaps indicates a long persistent, gradually subsiding, moderately drained and heavily vegetated back swamp or flood plain (Diessel, 2007). The thin coal seams in Madzaringwe Formation contain a lot of splits of carbonaceous mudstone that is pointing to short-lived flooding events during the period when they were formed. The thick coal seams are considered to have to resulted from the combined interaction of numerous factors, such as localised aggradation of channels. This also signifies slow and steady subsidence of the Tuli basin area, higher rainfall to grow luxuriant vegetation, abundant supply of paleoflora, moderately higher water table and a long period of time of water merge (Suárez-ruiz et al., 2012). FA 2 is interpreted to represent thickly vegetated backswamps.

6.2.3 Dark grey shale and mudstone with subordinate siltstones (FA 3)

The lower part of the Madzaringwe Formation largely comprises of dark-grey shale and mudstone with subordinate siltstones (FA 3). FA 3 is made up of Fls, Fm, Fc, Fms, and Fmb facies. The Fc facies consist of black laminated shale and massive mudstones (Figure 6.4). The shale and mudstone facies of FA 3 are sometimes

enriched or occurs as ferruginous shale/mudstone, pyritic shale/mudstone, and micaceous shale. The carbon materials in the carbonaceous shales gave room for the dark grey colour to form. The shales are weakly graded in some places and split along bedding planes. Some of the shales comprise brownish weathered calcareous concretions and small worm burrows. In a few places, the mudstones are medium to thick-bedded. Lenticular siltstone beds are intercalated within the mudstone. The contacts between the siltstone and mudstone in the Fls facies are gradational.

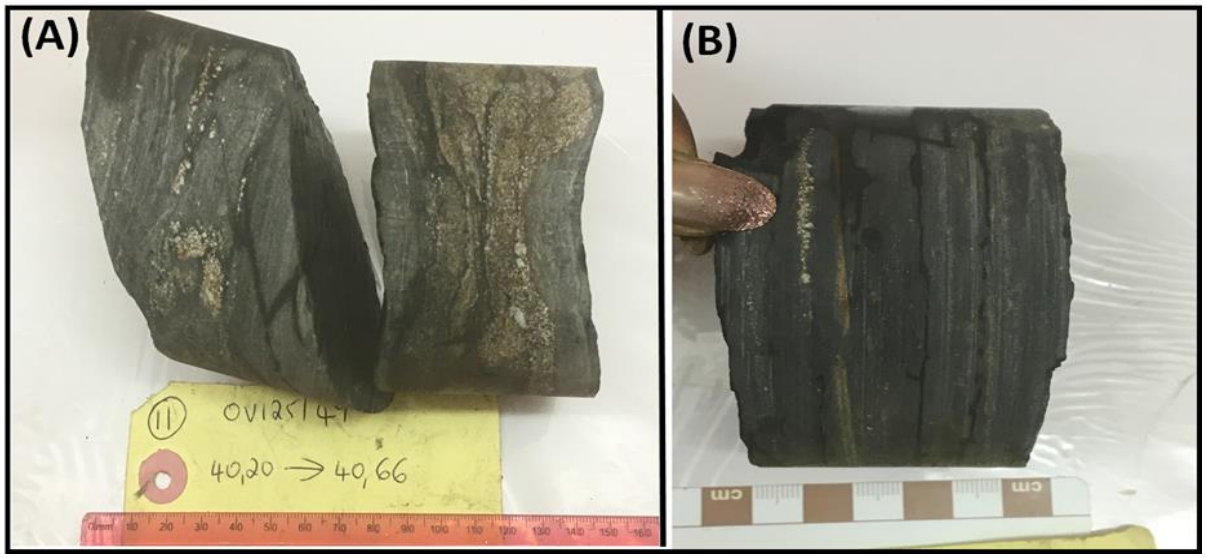

Figure 6.4: (A) Photograph of massive to faintly laminated mudstone intercalated with siltstone and shale; (B) Photograph showing soft –deformation (slump) or bioturbided structure.

6.2.3.1 Interpretation

The moderate growth of vegetation in the depositional environment is marked by the occurrence of carbonaceous mudstone. Shallow waters in the depositional basin is perhaps indicated by the trace fossils/burrows, consequently allowing plants (vegetation) to flourish in the presence of sunlight. Accumulation of the organic carbon-

rich shales and mudstones occurred in the swamps that formed on the flood plains. The parallel horizontal laminated shale suggests deposition by suspension in a floodplain environment with a regular fluctuation in the hydrodynamic energy. FA 3 represents low energy periodic sedimentation in a floodplain environment.

6.2.4 Siltstone intercalated with fine and coarse grained sandstones (FA 4)

FA 4 comprises of the Fms, Fss, and Sm facies, making up the basal part of the Madzaringwe Formation (Figures 6.5 and 6.6). FA 4 shows coarsening upward sequence with Fms facies making up the basal part, followed by the Fss facies, while the upper part encompasses of the Sm facies. The contact between Fms or Fss and Sm facies is sharp. Just like the FA 4 Facies, the shale and mudstone facies of FA 4 are sometimes enriched or occurs as ferruginous shale/mudstone, pyritic shale/mudstone, and micaceous shale. FA 4 attains a maximum thickness of about 20 m in the open pit, with an average thickness of approximately 14 m in the boreholes.

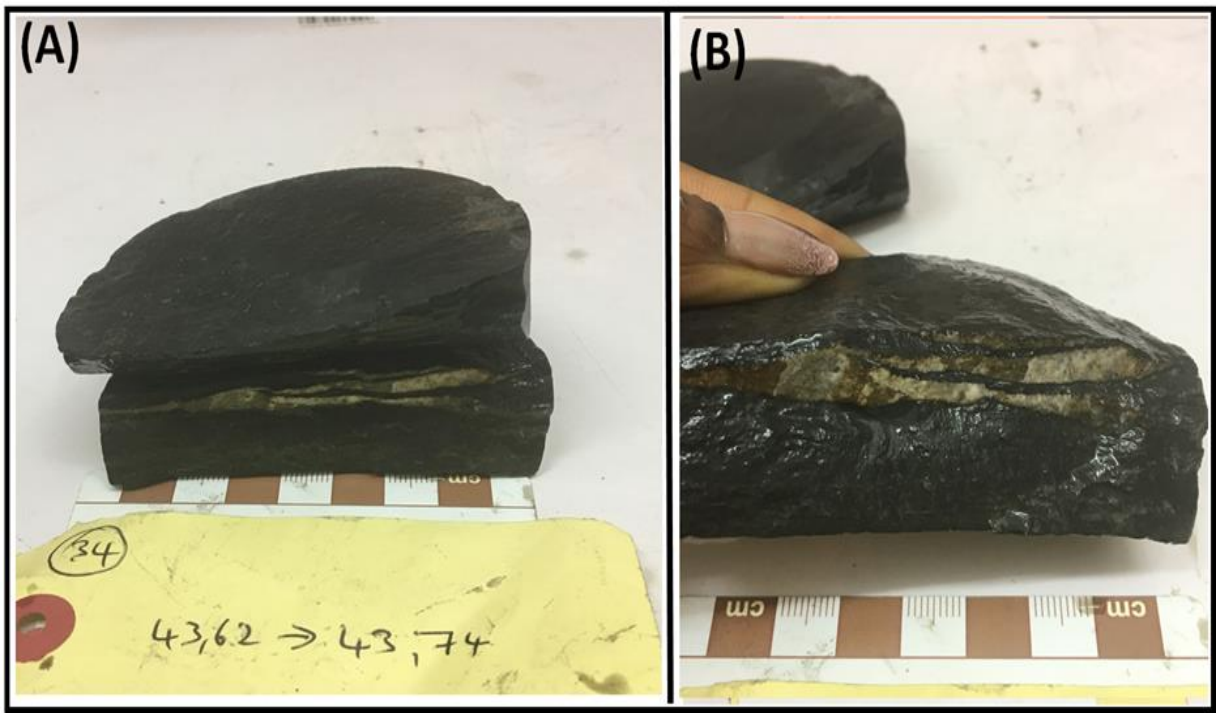

Figure 6.5: Photograph of carbonaceous shales with lenticular sandstone (lenses) facies.

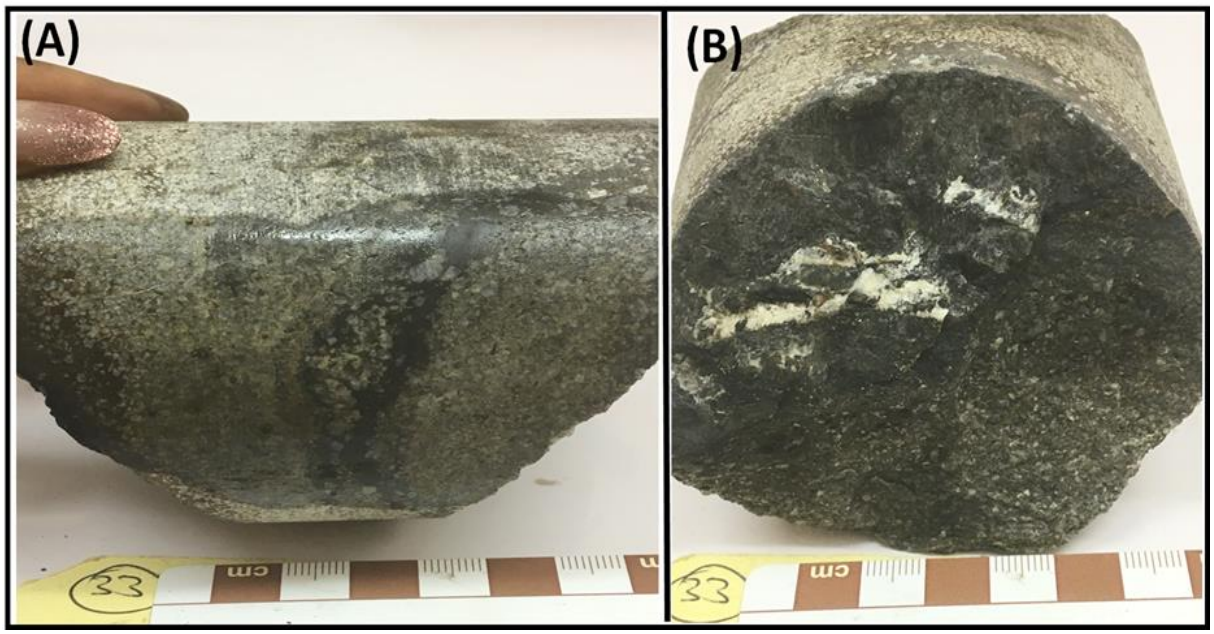

Figure 6.6: Photograph of dark-grey, coarse grained massive sandstones in interbedded with shale and siltstone. The deposit is cravasse splay or abanded channels deposits; or increase hydrodynamic energy during flooding.

6.2.4.1 Interpretation

The parallel laminated shale in FA 4 suggests that sediments were deposited in floodplain environments with consistent fluctuation in the hydrodynamic energy. The occurrence of thin-bedded mudstone at the top of the channel sandstones conceivably designates deposition from suspension load during channel abandonment (Malaza et al., 2013). The dark-grey thick-bedded mudstone that co-existed with the C facies (coal) point to deposition by vertical accretion in a back swamp or flood basin environments. During periodic floods, thin layers of sandstone and siltstone are introduced or deposited within the FA 4. FA 4 is generally interpreted as floodplain deposits.

CHAPTER 7

MUDROCK AND SANDSTONE PETROGRAPHY

7.1 Introduction

Petrography study is a part of petrology, which gives detailed descriptions of the composition and textural relationship of the rocks. Mudrocks (i.e. shale, mudstone and siltstone) which are referred to as argillites, are fine-grained sedimentary rocks composed of mostly silt and clay size fragments. Owing to their small grain size, mudrocks are difficult to study, even with the petrographic microscope. To date, mudrocks are the least understood, and one of the most understudied sedimentary rock. Nonetheless, they are vital rocks because they are the most abundant sedimentary rocks on earth, contributing more than 65% of all sedimentary rocks. Thus, they are about twice as abundant as sandstones and conglomerates combined. Furthermore, the mudrocks are the protoliths (precursor rock) for aluminous metamorphic rocks, mostly referred to as pelitic metamorphic rocks. On the other hand, Sandstones are clastic sedimentary rocks consisting mostly of sand-sized (0.0625 to 2 mm) mineral particles or rock fragments. It also composed of cementing materials that bind the sand grains together as well as a matrix of silt- or clay-size particles that occupy the spaces between the sand grains.

In this study, petrographic study of the mudrocks and sandstones from the Madzaringwe Formation in the Vele Colliery were carried to provide information about their texture, mineral composition, matrix and cement types.

7.2 Texture

Most of the rocks in the three existing boreholes within the Vele Colliery are mostly argillaceous (i.e. shale, mudstone and siltstone), with minor or few occurrences of arenaceous rocks (i.e. sandstone). The lamination or fissility texture of Madzaringwe shales allows the rocks to break along laminae planes (Figure 7.1 (A-B)). In cases, where lamination on the mudrock was not preserved, thin and massive bedded mudstones were observed (Figure 7.1(C-D)). Coarser silts tend to accumulate in silt laminae and bands, whereas finer silt is dispersed among clays. The sandstones are very fine to coarse grained and mostly poorly sorted (Figure 7.2). Thin sandstone layers are observed within the mudrocks (Figure 7.3). Grain morphology for the sandstones range from subangular to angular and are cemented by clay minerals and in few cases are grain supported. Typically, detritus clay and silt size particles with some chemically precipitated cement and organic materials make up the argillaceous rocks.

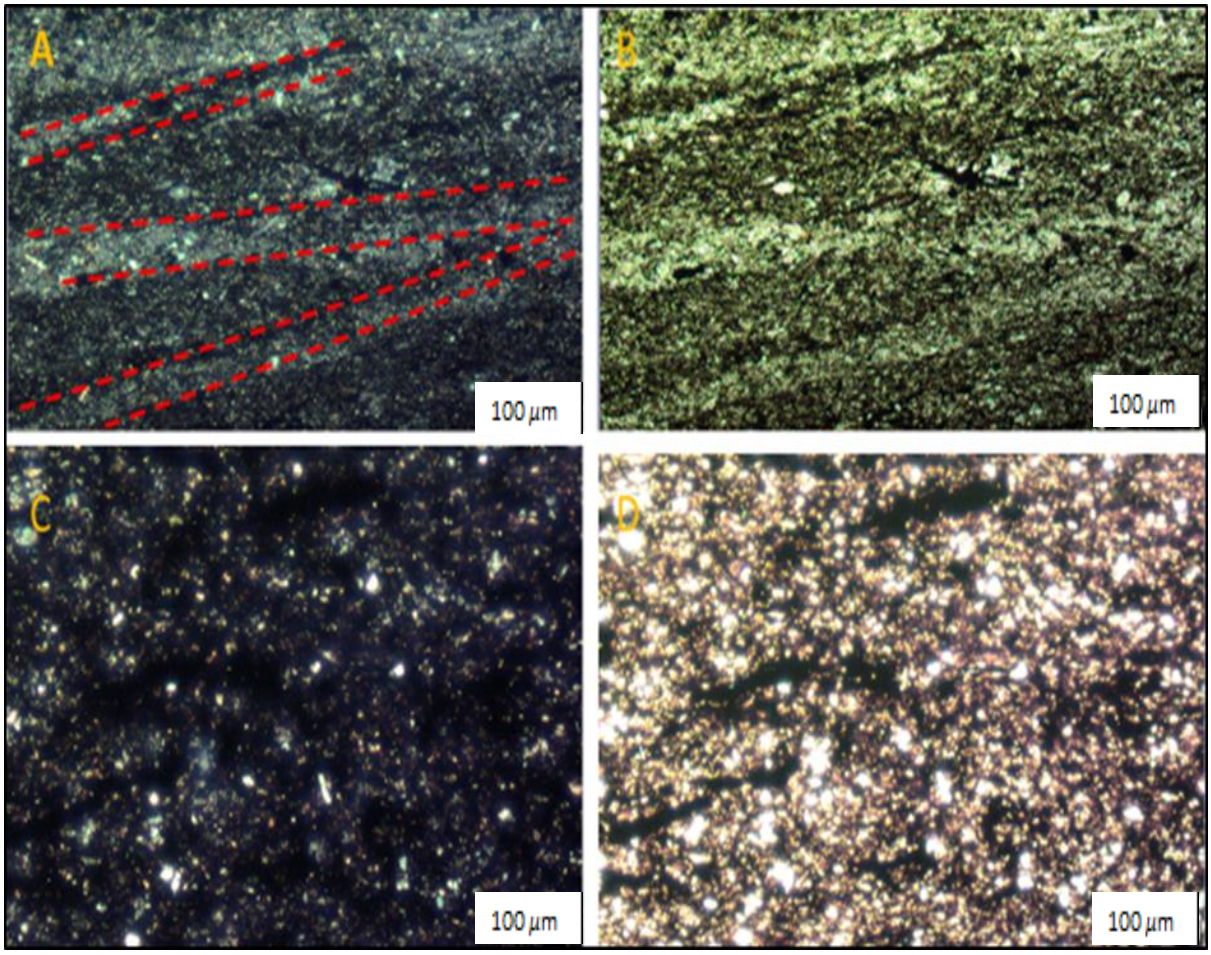

Figure 7.1: (A-B) Thin section photomicrographs showing: finely laminated shale with the bright silt laminae under XPL and PPL (siltstone is shown by the red dotted lines under XPL); (C-D) siltstone under XPL and PPL.

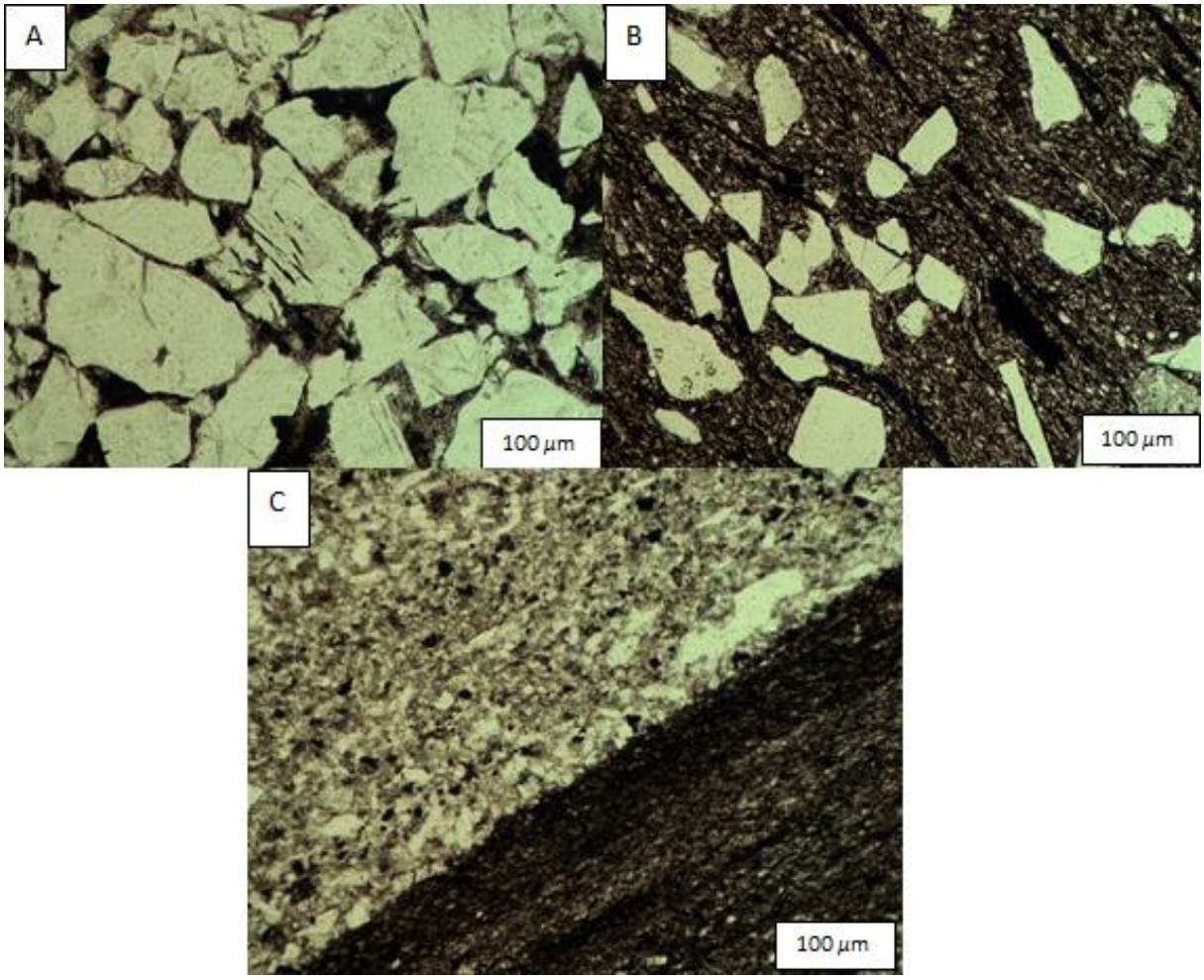

Figure 7.2: Thin section photomicrograph showing: (A) Sandstone with sub-angular to angular grains; (B) Sandstone with poorly sorted sub-angular grains; (C) Alignment of the mineral and contact between the carbonaceous clay matrix and silty grain particles (cross-light).

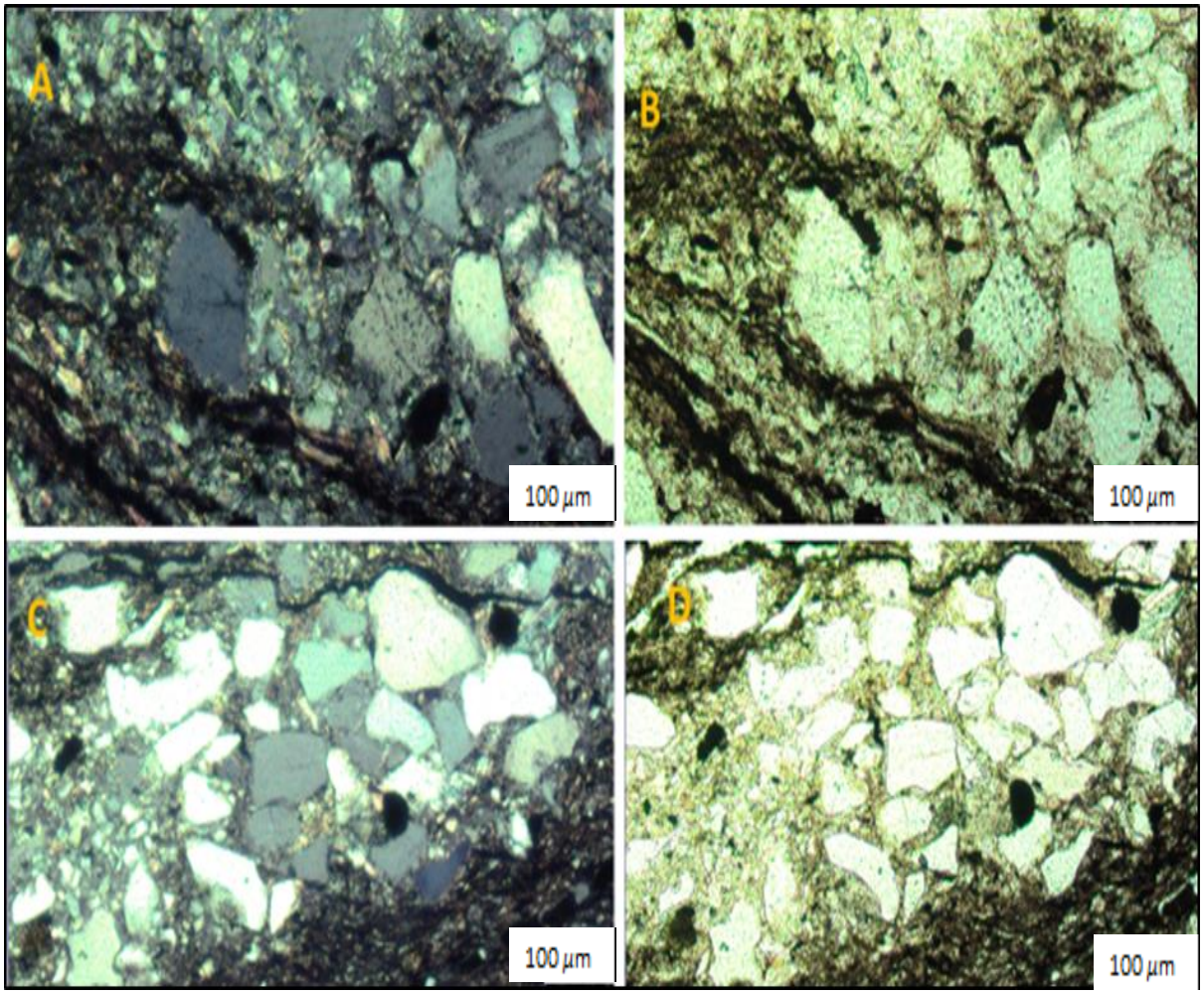

Figure 7.3: (A-D) Thin section photomicrograph showing sand-size particles within a mud or clay matrix.

7.3 Mineral composition

7.3.1 Quartz

The most dominant mineral in the sandstone samples is quartz. The shape of the quartz grains is mostly sub-angular to sub-rounded. The quartz minerals occur as monocrystalline and polycrystalline grains. The monocrystalline quartz consists of single-crystalline quartz, whereas the polycrystalline quartz has more than one crystalline grain. A large percentage of the monocrystalline exhibit undulatory

extinction, whereas only a small fraction of the polycrystalline quartz grains shows undulatory extinction. Similarly, limited number of the monocrystalline quartz have uniform extinction and show overgrowth. In rare cases, the quartz grains comprise muscovite, rutile needle and zircon inclusions within the grains. As reported by Blatt and Christie (1963), quartz grains with non-undulatory extinction were possibly sourced from igneous and sedimentary rocks, while quartz with undulatory extinction was derived from a metamorphic rock source. However, Pettijohn et al. (1987) alleged that there are occurrences of high percentage of undulatory quartz in volcanic rocks. Hence, the metamorphic origin cannot be ascertained for the rocks based on the proportion of undulatory to non-undulatory quartz. In fact, it appears that most of the studied quartz grains could be the recycled quartz which is regarded as being deposited more than one time.

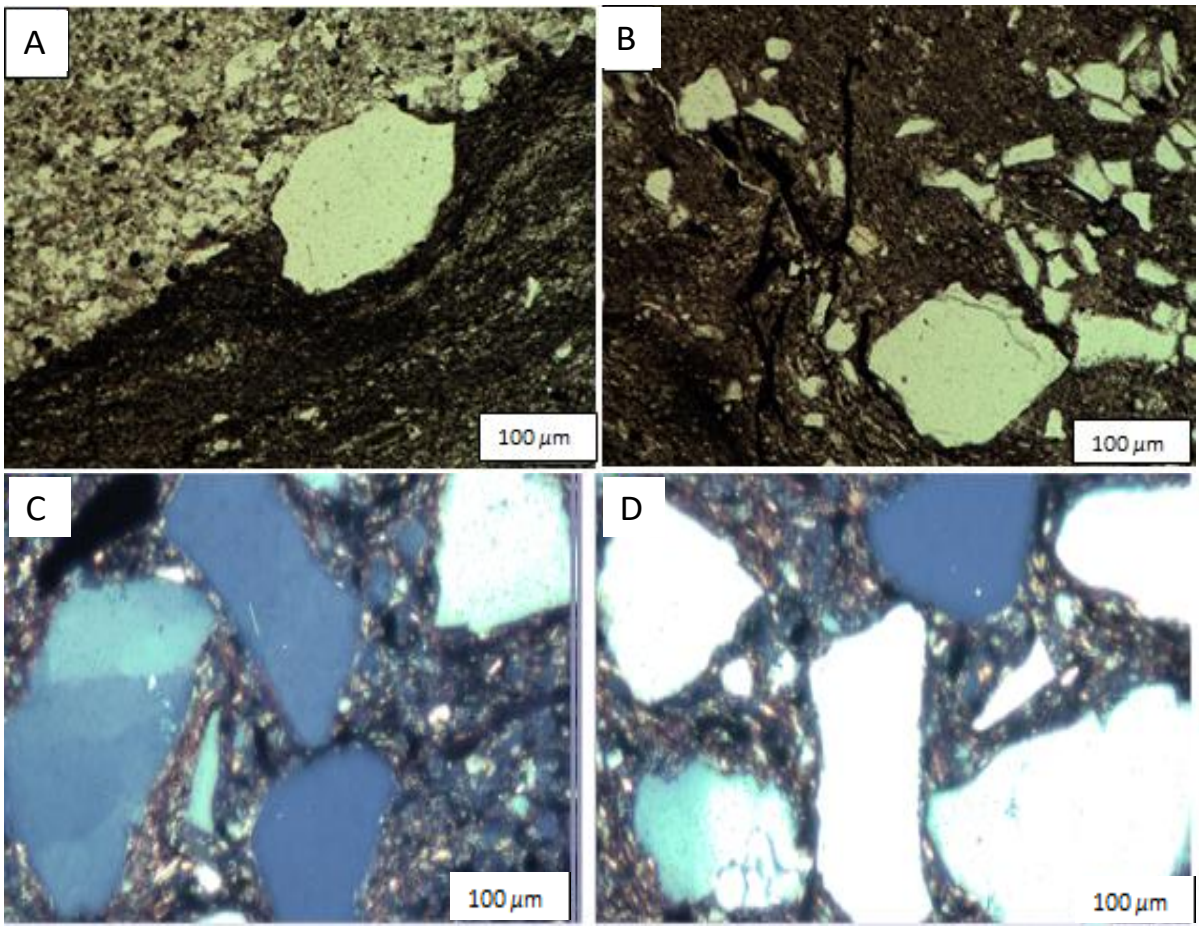

Figure 7.4: Photomicrograph of sub-angular to sub-rounded poorly sorted sandstone showing: (A-B) Monocrystalline quartz grains; (C-D) Quartz grains.

7.3.2 Feldspar

Feldspar is one of the dominant minerals in the sandstone samples. The shape of the feldspar grains is frequently sub-angular to sub-rounded. The feldspar minerals occur as monocrystalline grains and polycrystalline grains. The monocrystalline feldspar comprises of single-crystalline feldspar, whereas the polycrystalline feldspar contains of more than one crystalline grain. The grains are poorly sorted, and they are both surrounded by the clay minerals. The clay minerals are slowly covering the feldspar minerals. Feldspar grains show that the minerals have been under a lot of pressure due to the display of the cracks on the grains and they were inherited from protolith

(source rocks); they were not formed in situ (Figure 7.5). The large grains are scattered hence poorly sorted.

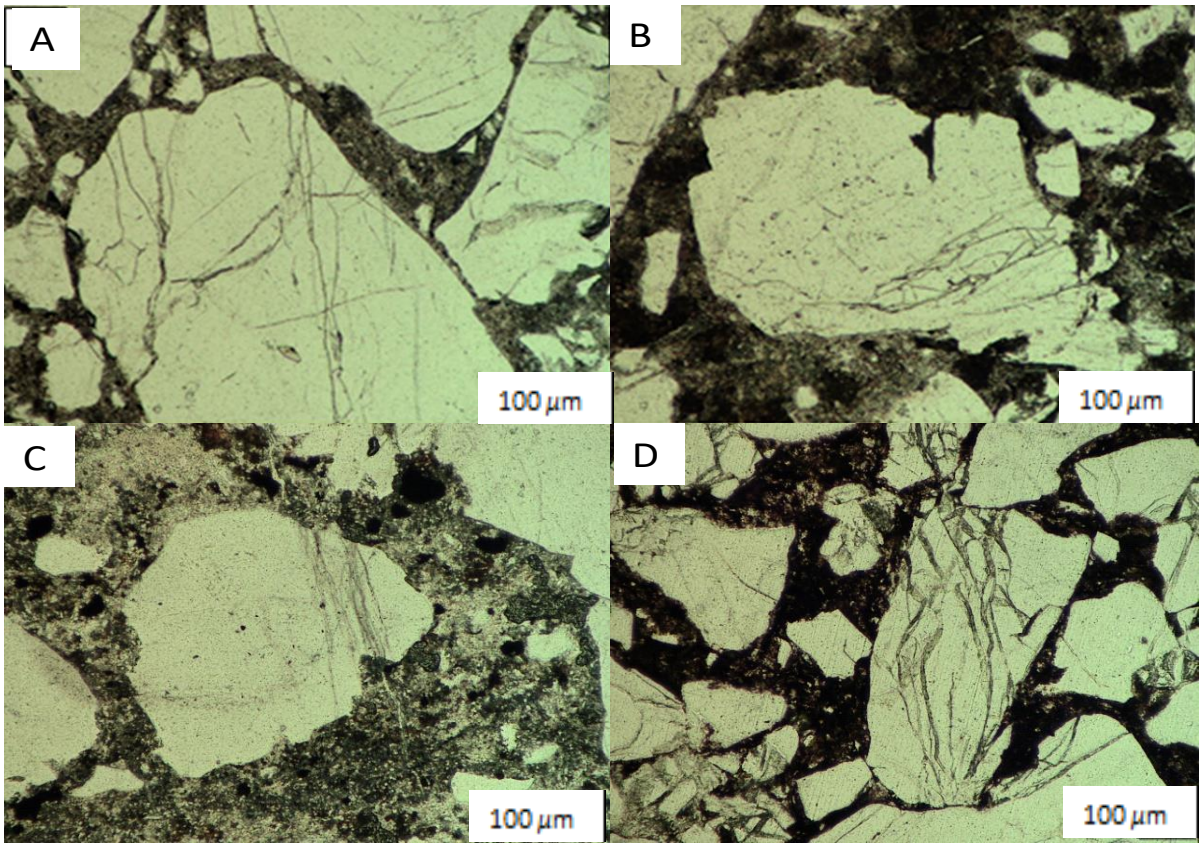

Figure 7.5: Thin section photomicrograph of poorly sorted sandstone showing fractured feldspar grains.

7.3.3 Lithic fragment

Rock or lithic fragments recognized in the mudrocks and sandstones include igneous and sedimentary lithics (Figure 7.6) and are frequently sub-angular to sub-rounded. The observed lithics give clues of igneous and sedimentary origin.

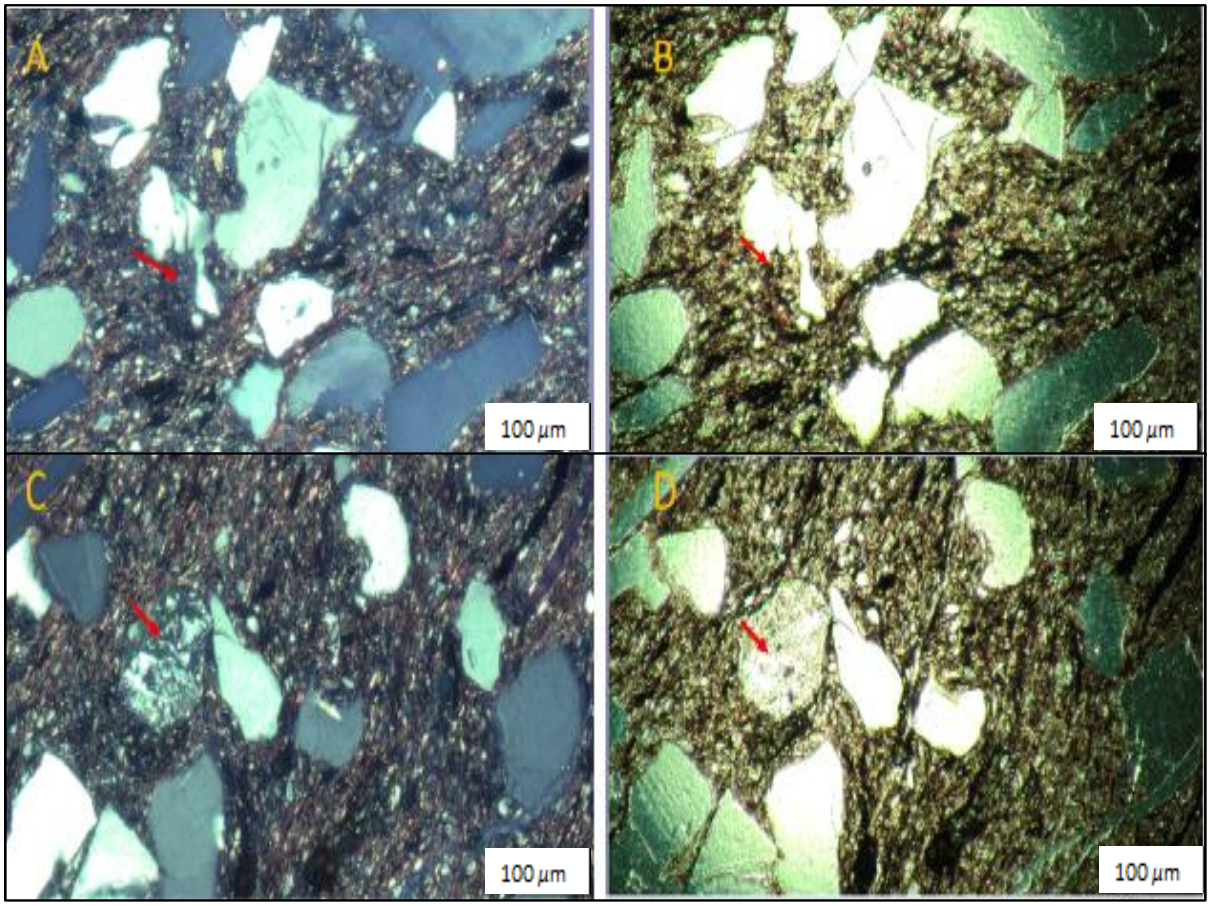

Figure 7.6: Thin section photomicrograph of poorly sorted sandstone showing: (A-B) mudstone-siltstone lithic (red arrow) under XPL and PPL; (C-D) more likely an igneous or metamorhic lithic(quartzite) (red arrow) under XPL and PPL.

7.3.4 Matrix and cement

the framework grains are bound together by both cement and matrix. Minerals like clay, quartz, pyrite, hematite, and feldspar are common cementing materials. The matrix is commonly clay minerals (Figure 7.7) and they are either detrital or diagenetic in form. Quartz cement occurs in the form of quartz overgrowths. This overgrowth is observed as syntaxial overgrowth, growing outwardly from detrital quartz grain surface (Figure 7.8). The overgrowths have similar optical properties as the original detrital quartz grains.

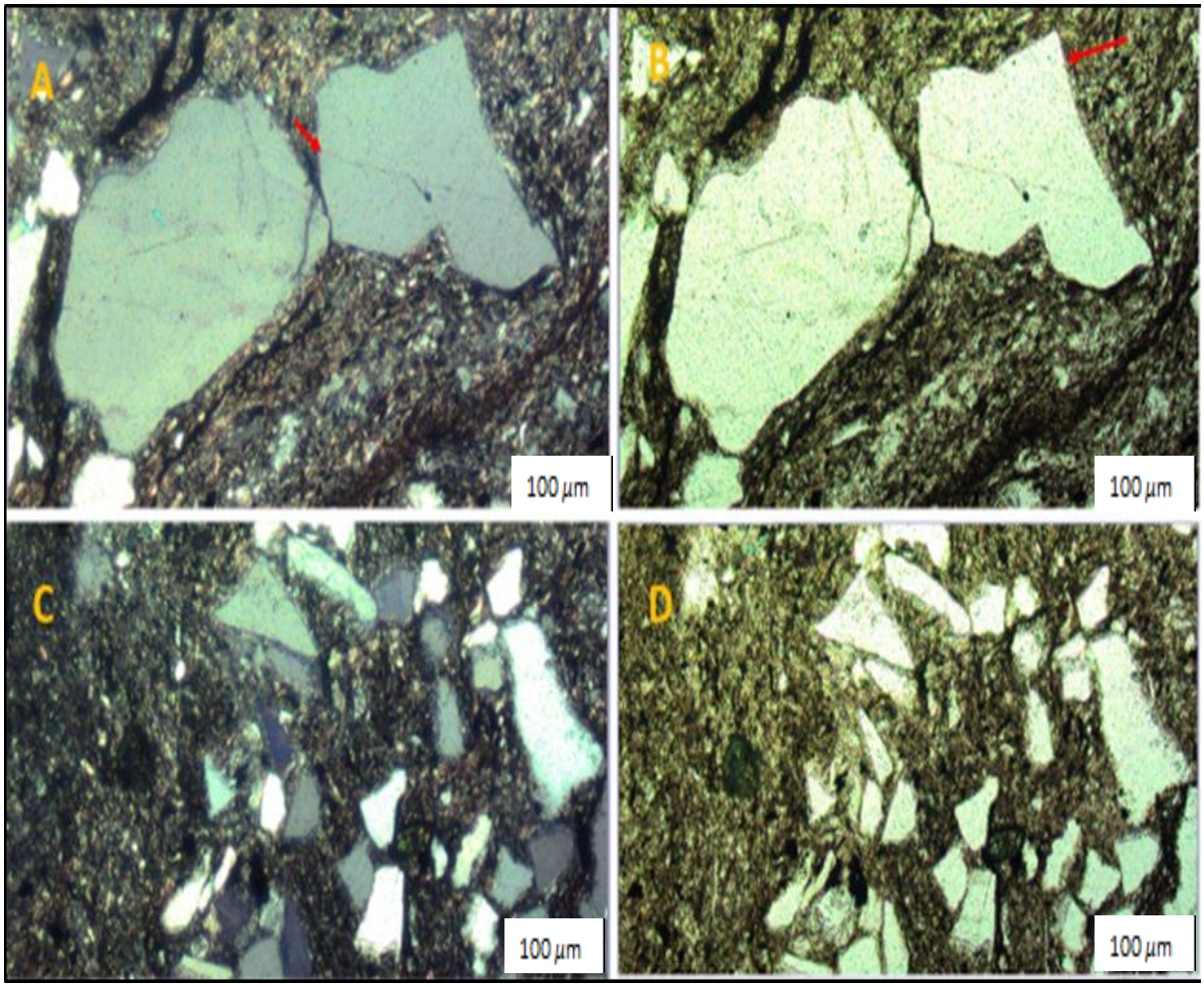

Figure 7.7: (A-D) Thin section photomicrograph of poorly sorted sandstone showing quartz grains in the clay matrix.

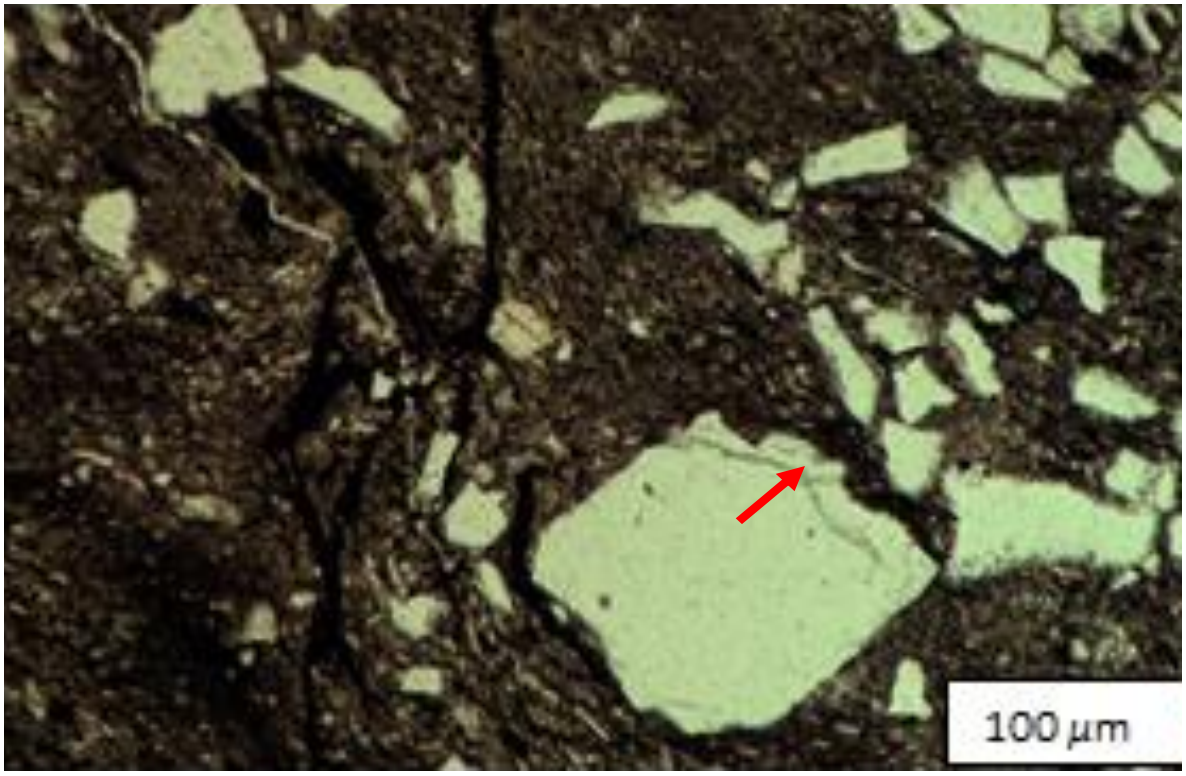

Figure 7.8: Thin section photomicrograph of poorly sorted sandstone showing quartz overgrowth(red arrow). The quartz overgrowth is inherited from protolith not formed insitu.

7.3.4.1 Pyrite

Pyrite is present in the Madzaringwe shale and the pyrites are the most common mineral preserved in the analyzed shale samples. Pyrite in Madzaringwe shales appears as authigenic mineral or diagenic nodular forms and are also usually distributed in the form of thin strips along the bedding surface. The pyrite also fills the pore spaces between grains and coat or surround the grains. The presence of pyrite in the sandstones signifies reducing conditions, perhaps indicating a deoxygenated environment of deposition. Pyrite forms in an anoxic organic-rich environment, where decaying organic materials consume oxygen and releases sulphur. In this scenario,

pyrite may have replaced plant debris and shells to create pyrite nodules in the shale. Figures 7.9 and 7.10 shows the occurrence of pyrite in the studied carbonaceous shale and mudstones under plane-polarized and crossed polarized.

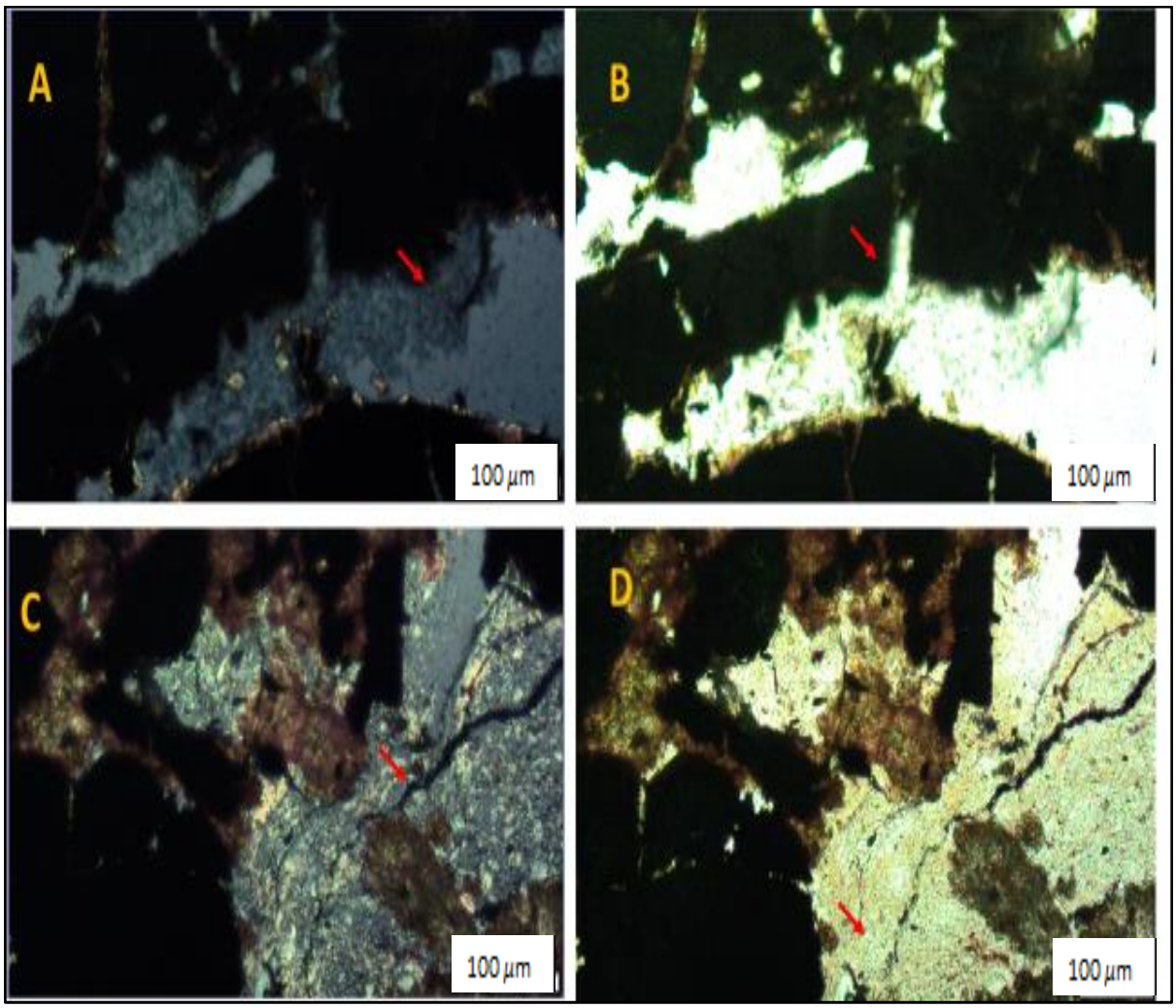

Figure 7.9: Thin section photomicrograph of carbonaceous shale showing nodular pyrite: (A and C) under XPL; (B and D) under PPL.

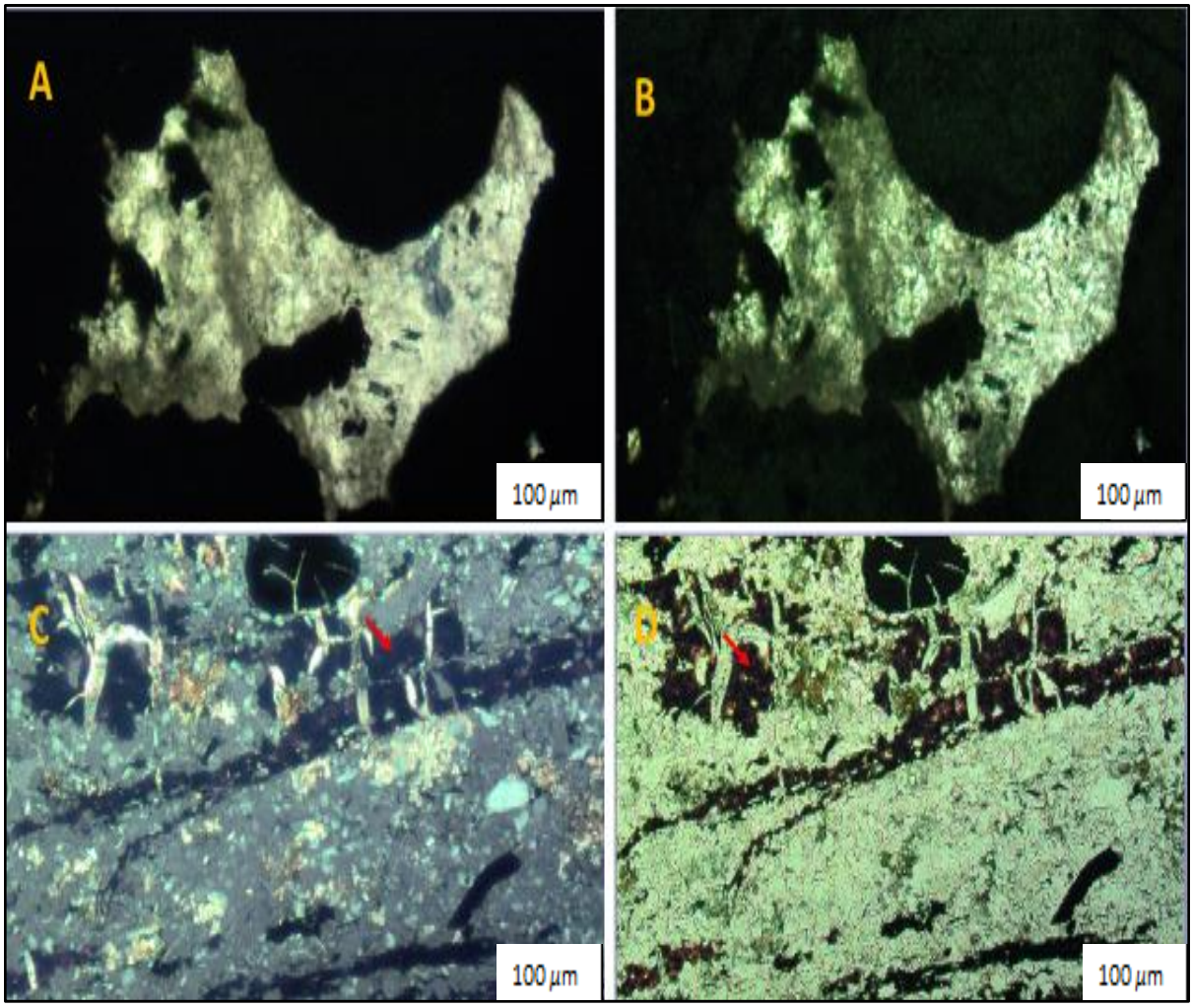

Figure 7.10: Thin section photomicrograph of carbonaceous mudstone showing the distribution of pyrite (A and C) under XPL; (B and D) under PPL. Figure 7.10 (C and D) also shows that some clay muscovite minerals filled the cracks.

7.3.4.2 Hematite

Hematite cement is another common cementing agent in mudrocks and sandstones. Under the microscope, hematite has brownish-reddish colour and is observed as grain-coating and pores filling cement (Figure 7.11).

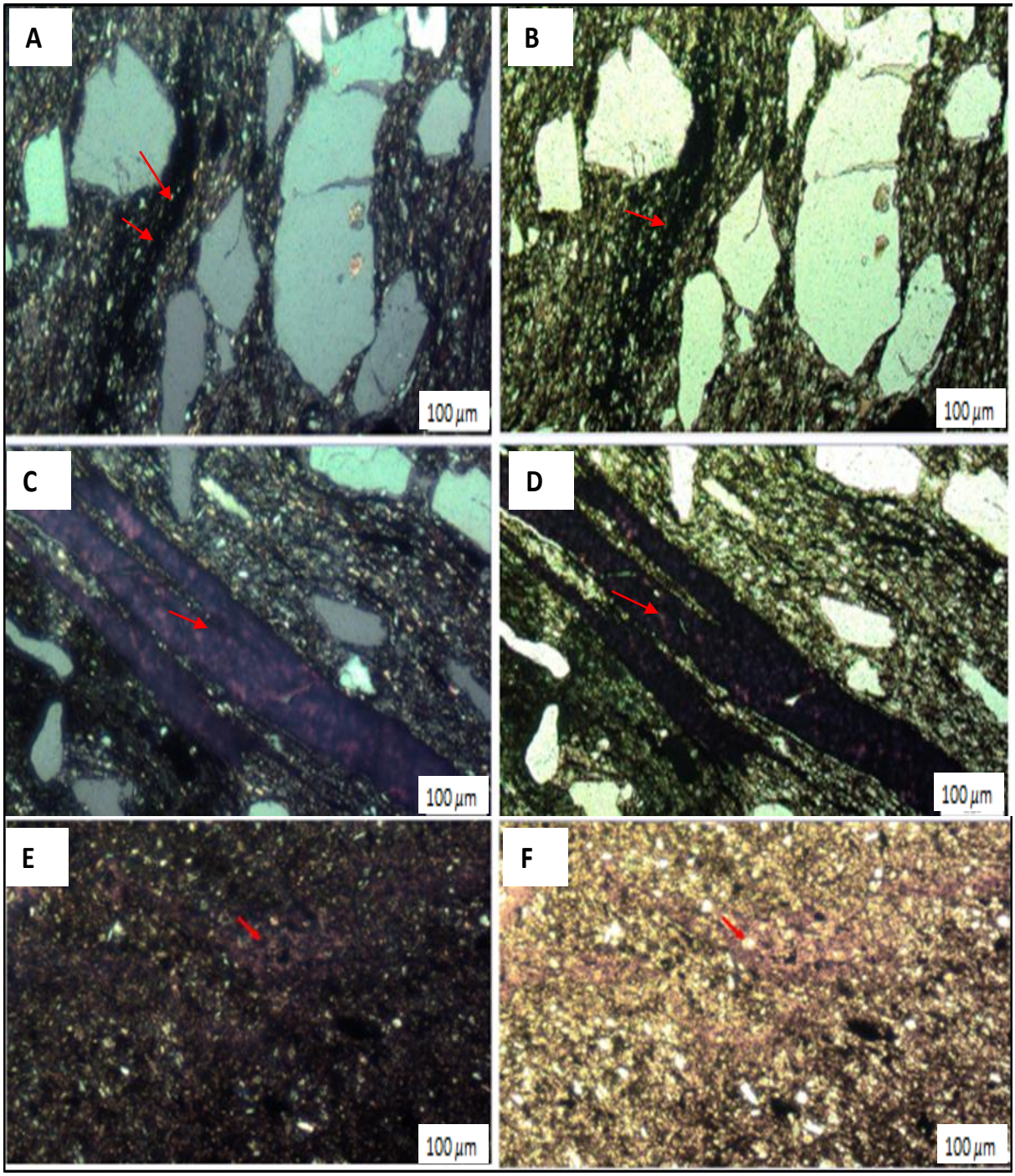

Figure 7.11: Thin section photomicrograph of carbonaceous mudstone showing grain coating, pore-filling hematite along cracks and hematite staining: (A, C and E) under XPL; and (Figure B, D and F) under PPL. Figure 7.11D also shows that some clay/muscovite minerals had filled cracks.

7.3.5 Mica and accessory minerals

Muscovite and biotite are the mica in the sandstones, with muscovite occurring more regularly than biotite. This could be because muscovite is chemically more stable than biotite in the depositional environment. Observed mica is often seen as inclusion within quartz grains (Figure 7.11(A-B)). Detrital garnet, rutile and zircon are the observed accessory mineral in the rocks (Figure 7.11(C-D)).

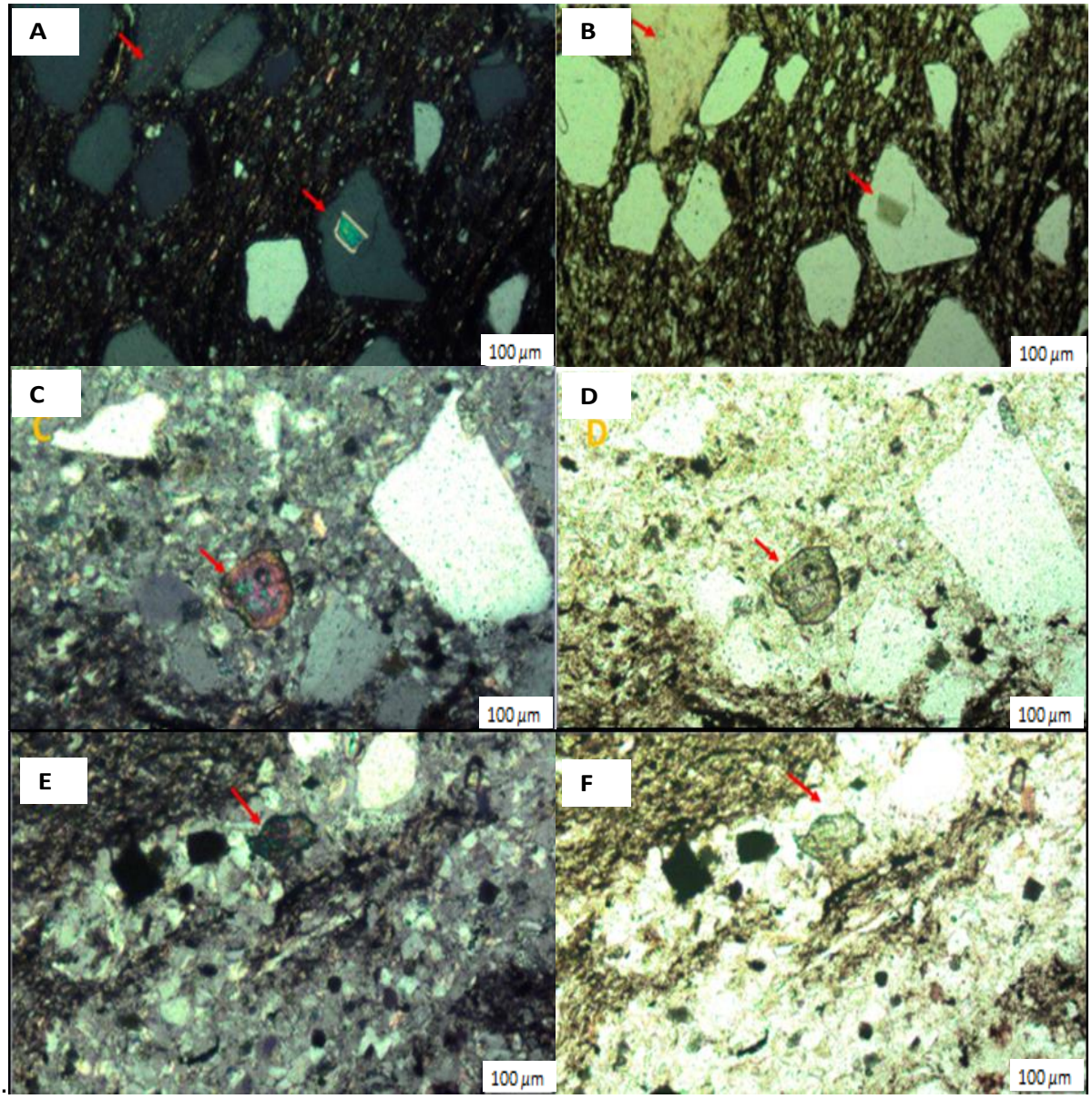

Figure 7.12: Thin section photomicrograph showing grain coating, pore-filling hematite along cracks and hematite staining under XPL (Figure 7.12 A, C and E) and PPL (Figure 7.12 B, D and F), respectively shown by red arrows.

Mica and accessory minerals constitute less than 1% of the total grains in the samples and their grains are mostly sub-rounded. Their presence in the rocks indicates the mudrocks and sandstones of the Madzaringwe Formation came from igneous and sedimentary rock sources.

CHAPTER 8

GEOCHEMISTRY OF THE MUDROCKS AND SANDSTONES

8.1 Introduction

The geochemistry of clastic sedimentary rocks is a vital tool used in the study of provenance, paleoweathering conditions and tectonic setting (Nesbitt and Young, 1982; Raza et al., 2010). The mineralogical and chemical compositions of clastic sedimentary rocks are the products of numerous variables that include provenance, weathering conditions, transport, diagenesis, climate and tectonism (Taylor and McLennan, 1985). In geochemical studies, some selected major oxides especially TiO_2 and trace elements like La, Y, Sc, Cr, Th, Zr, Hf, and Nb are sensitive indicators of the source rocks, provenance, paleoweathering, and tectonic setting (Bhatia and Crook, 1986). This is as a result of their relatively low mobility and insolubility during sedimentary processes (McLennan et al., 1993). Also, the comparative distribution of the immobile trace elements with changing concentration in felsic and basic rocks has been employed to deduce the relative contribution of felsic and basic sources in clastic sedimentary rocks from different tectonic environments (Wronkiewicz and Condie, 1990). This chapter is intended to investigate the geochemistry of the mudrocks and sandstones from the Madzaringwe Formation to provide information on the provenance, paleoweathering and tectonic setting of the Madzaringwe Formation.

8.2 Major elements

The major oxides concentrations in the selected coal, shale and sandstones are presented in Table 8.1. The major elements found in the collected samples include SiO_2, TiO_2, Al_2O_3, Fe_2O_3, MnO, MgO, CaO, Na_2O, K_2O, P_2O_5, and Cr_2O_3. In the coal samples, the concentration of SiO_2 TiO_2, Al_2O_3, CaO, Fe_2O_3, MnO, MgO, Na_2O, K_2O and P_2O_5 ranges from 9.64 – 24.13%, 0.14 – 0.23%, 2.17 – 7.20%, 0.87 – 2.20%, 0.48 – 2.17%, 0.01 – 0.02%, 0.03 – 0.08%, 0.32 – 0.08%, 0.23 – 0.08%, and 0.03 – 0.05%, respectively. The SiO_2, TiO_2, Al_2O_3, Fe_2O_3, MnO, MgO, CaO, Na_2O, K_2O, P_2O_5, and Cr_2O_3 contents in the shale and sandstones range from 58.52 to 79.45%, 0.20 to 0.89%, 3.32 to 20.73%, 0.26 to 3.55%, 1.23 to 29.33%, 0.20 to 0.89%, 0.01 to 0.06%, 0.05 to 0.84%, 0.74 to 2.90%, and 0.01 to 0.29%, respectively. The concentration of SiO_2, Al_2O_3, CaO and Fe_2O_3 in the shales are higher than those in the coal samples. There is an outlier sample (shale) from Borehole 125 160, in which all major elements diagrams has a lower concentration of SiO_2. Generally, the composition of the studied samples is variable but comparable with the average shales (Table 8.2) documented by Pettijohn (1957), Turekan and Wedephol (1961) and Gromet et al. (1984).

Table 8.1: Results of oxides (wt%) analysed by X-ray fluorescence spectrometry.

Sample	SiO_2	TiO_2	Al_2O_3	Fe_2O_3(t)	MnO	MgO	CaO	Na_2O	K_2O	P_2O_5	Cr_2O_3	LOI	Total
Coal S1676	24,13	0,30	7,20	2,17	0,02	0,47	2,20	0,08	0,82	0,029	0,005	62,35	99,77
Coal S1677	17,83	0,23	5,51	1,19	0,02	0,33	2,15	0,05	0,68	0,036	0,005	71,59	99,62
Coal S1678	9,64	0,14	3,17	0,42	0,02	0,50	1,93	0,03	0,32	0,035	0,005	83,41	99,62
Coal S1679	11,18	0,15	3,69	0,63	0,01	0,25	1,32	0,03	0,42	0,042	0,005	81,96	99,69
Coal S1680	12,82	0,17	4,30	0,48	0,01	0,27	0,87	0,03	0,49	0,047	0,005	80,52	100,01
Coal S1681	11,96	0,18	4,45	0,73	0,01	0,17	0,49	0,03	0,43	0,053	0,003	81,41	99,91
OVI125 -156 S25	65,16	0,82	18,69	3,53	0,01	1,06	0,73	0,60	2,88	0,050	0,017	6,62	100,17

OVI125 -156 S26	67,26	0,77	18,73	2,66	0,01	0,81	0,43	0,51	2,83	0,053	0,015	6,00	100,08
OVI125 -156 S27	67,03	0,83	19,16	2,87	0,01	0,84	0,46	0,35	2,92	0,043	0,012	5,67	100,20
OVI125 -156 S28	65,63	0,84	19,98	3,03	0,01	0,81	0,44	0,29	2,76	0,047	0,013	6,18	100,03
OVI125 -156 S30	67,36	0,82	16,86	1,68	0,01	0,49	0,32	0,84	2,15	0,121	0,014	9,49	100,15
OVI125 -156 S31	67,54	0,81	16,93	1,67	0,01	0,50	0,32	0,51	2,09	0,123	0,012	9,52	100,04
OVI125 -156 S32	60,99	0,82	17,93	1,23	0,01	0,50	0,26	0,26	2,16	0,060	0,015	15,88	100,11
OVI125 -156 S33	79,45	0,31	5,69	5,93	0,04	0,99	0,86	0,12	0,74	0,093	0,031	5,73	99,98
OVI125 -156 S34	66,60	0,81	17,24	2,41	0,02	0,84	1,25	0,24	2,51	0,286	0,023	7,77	100,00
OVI125 -156 S35	39,99	0,20	3,32	29,33	0,01	0,16	3,55	0,05	0,36	0,029	0,035	22,96	99,98
OVI125 -156 S36	61,22	0,88	20,63	2,67	0,01	0,82	0,44	0,25	2,80	0,132	0,021	10,11	99,99
OVI125 149 S1	69,56	0,75	17,42	2,07	0,01	0,78	0,49	0,56	2,32	0,056	0,012	6,08	100,11
OVI125 149 S2	66,25	0,76	18,00	2,83	0,01	0,91	0,50	0,60	2,69	0,057	0,012	7,45	100,07
OVI125 149 S3	67,10	0,74	17,82	2,42	0,01	0,85	0,50	0,56	2,79	0,060	0,012	7,12	99,98
OVI125 149 S4	68,01	0,79	18,68	1,76	0,01	0,72	0,42	0,47	2,55	0,062	0,016	6,70	100,18
OVI125 149 S5	64,85	0,77	18,39	4,29	0,02	1,00	0,62	0,37	2,28	0,051	0,015	7,36	100,01
OVI125 149 S6	65,50	0,87	20,48	2,13	0,01	0,75	0,44	0,36	2,62	0,057	0,016	6,97	100,20
OVI125 149 S7	62,93	0,79	18,51	2,87	0,01	0,90	0,47	0,32	2,35	0,059	0,012	10,74	99,96
OVI125 149 S8	69,48	0,77	16,45	1,67	0,01	0,52	0,34	0,83	2,38	0,125	0,017	7,53	100,12
OVI125 149 S9	62,52	0,79	17,13	1,06	0,01	0,43	0,26	0,26	2,15	0,056	0,023	15,36	100,04
OVI125 149 S10	71,90	0,79	15,82	1,87	0,01	0,43	0,31	0,54	2,38	0,149	0,030	5,87	100,10
OVI125 149 S11	62,17	0,88	19,32	2,81	0,02	0,82	1,48	0,35	2,90	0,336	0,016	8,90	100,00
OVI125 149 S12	61,23	0,85	20,00	3,35	0,02	0,92	0,51	0,30	2,76	0,107	0,015	10,11	100,17
OVI125 149 S13	58,52	0,87	21,73	2,10	0,01	0,78	0,40	0,26	2,91	0,074	0,014	12,34	100,01
OVI125 149 S14	59,97	0,83	19,80	3,90	0,06	0,86	0,49	0,31	2,63	0,119	0,019	11,01	100,00
OVI125 160 S16	66,92	0,71	17,21	2,57	0,01	0,97	0,32	0,45	2,80	0,053	0,014	8,05	100,08
OVI125 160 S17	64,74	0,76	17,73	3,15	0,02	1,16	0,76	0,40	2,71	0,055	0,012	8,61	100,10
OVI125 160 S18	65,94	0,79	18,58	2,15	0,01	0,98	0,32	0,29	2,69	0,059	0,012	8,23	100,05
OVI125 160 S19	64,33	0,79	19,51	3,63	0,02	1,19	0,54	0,20	2,52	0,053	0,011	7,38	100,17
OVI125 160 S20	64,04	0,77	18,31	1,65	0,01	0,81	0,33	0,20	2,34	0,060	0,010	11,48	100,01
OVI125 160 S22	72,13	0,55	11,41	2,89	0,04	0,91	2,13	0,28	1,38	0,072	0,014	8,19	99,99

Table 8.2: Comparing the average chemical composition of the shales and coal from Madzaringwe Formation in the Tuli basin with published average shales.

Oxides	This study (Average)		Average shale (Pettijohn, 1957)	Turekan and Wedephol (1961)	UCC	PAAS	NASC (Gromet et al., 1984)
	Shale	Coal					
SiO_2 (%)	64.92	14.59	58.10	58.50	66.60	62.40	64.82
TiO_2 (%)	0,76	0.20	0.60	0.77	0.64	0.99	0.80
Al_2O_3 (%)	17.43	4.72	15.40	15.00	15.40	18.78	17.05
Fe_2O_3 (%)	3.49	0.94	6.90	4.72	5.04	7.18	5.70
MnO (%)	0,01	0.01	Trace	-	0.10	0.11	-
MgO (%)	0.79	0.33	2.40	2.50	2.48	2.19	2.83
CaO (%)	0.67	1.49	3.10	3.10	3.59	1.29	3.51
Na_2O (%)	0.38	0.04	1.30	1.30	3.27	1.19	1.13
K_2O (%)	2.41	0.53	3.20	3.10	2.80	3.68	3.97
P_2O_5 (%)	0.10	0.04	0.20	0.16	0.12	0.16	0.15

The abundance of Al_2O_3 was also used as a normalization factor to make contrasts among the different lithologies due to their immobile nature throughout weathering, diagenesis, and metamorphism. Major oxides of the studied shale and coal samples were plotted against Al_2O_3 and as shown in Figure 8.1. Also, the average UCC (Upper continental Crust) and PAAS (Post–Archean Australian Shale) and NASC (North American Shale Composite) values were also included in the plot for comparison purpose. In the shale and coal samples, major oxides like SiO_2, TiO_2, and K_2O, shows a positive correlation with Al_2O_3, whereas MnO, CaO, Na_2O and P_2O_5 show no particular trend (Figure 8.1). The strong positive correlation of the of these major oxides with Al_2O_3 indicates that they are associated with micaceous/clay minerals

(Baiyegunhi et al., 2017). As Aluminium (Al) concentration is reasonably thought to be a good measure of detrital flux excellent positive correlations of SiO_2, TiO_2, and K_2O.

Relative to UCC, NASC and PAAS, the concentrations of most major elements in the shale samples are generally similar, except for MgO, CaO and Na_2O, which consistently yields much lower average relative concentration values. The depletion of Na_2O (<1%) in the Madzaringwe coals and shales can be attributed to a relatively smaller amount of Na-rich plagioclase in them, which is consistent with the petrographic data. The ratio of K_2O/Na_2O also shows that K-feldspars dominate over plagioclase (albite) feldspar. K_2O and Na_2O contents and their ratios ($K_2O/Na_2O > 1$) are also consistent with the petrographic interpretations. In contrast with UCC, NASC, and PAAS, the shales are low in MgO, CaO, Na_2O. On average, the shales have a similar concentration of SiO_2 with that of NASC.

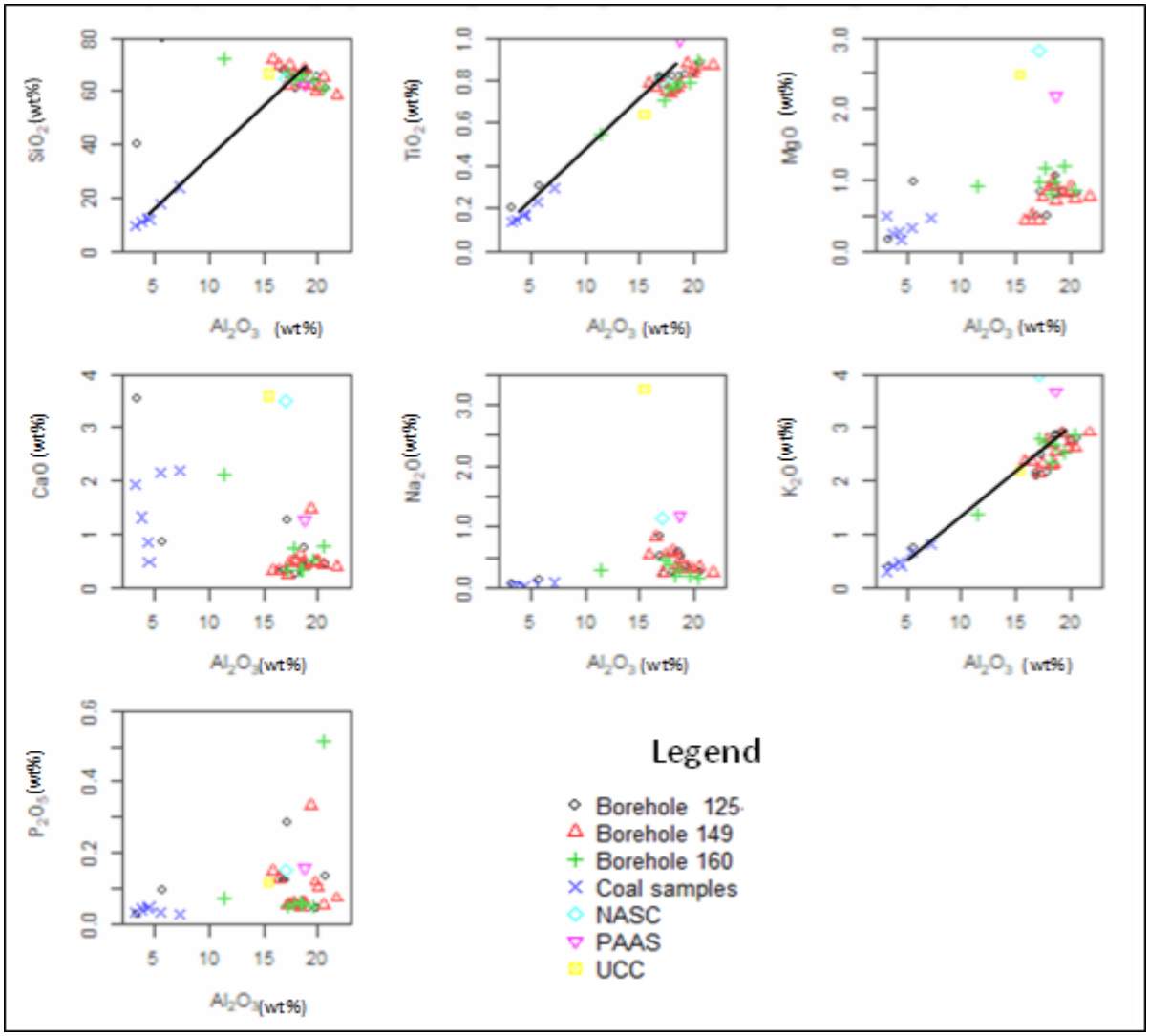

Figure 8.1: Bivariate plot of major oxides against Al_2O_3 showing the distribution of shale and coal samples from the Madzaringwe Formation. Average data of UCC, NASC, and PAAS are plotted for comparison.

8.3 Trace elements

The trace element concentrations in the analysed coal, shale and sandstones are presented in Table 8.3. Trace elements which are found in the samples include Ag, As, Ba, Bi, Br, Cd, Ce, Co, Cr, Cu, Ga, Ge, Hf, La, Mo, Nb, Ni, Pd, Rb, Sb, Sc, Se, Sn, Sr, Ta, Th, Ti, U, V, W, Y, YB, Zn and Zr. The trace element compositions are divided

into large ion lithophile elements (LILE), high field strength elements (HFSE) and transition trace elements (TTE). The contents of LILE such as Rb, Ba, Th and Sr range from 17 to 173 ppm, 99 to 340 ppm, 2.2 to 20 ppm and 44 to 211 ppm, respectively. The contents of HFSE such as Zr, Y and Nb vary from 50 to 432 ppm, 11 to 55 ppm and 2.9 to 24 ppm, respectively. Likewise, TTE like Sc, V, Cr, Ni and Zn vary from 4.2 to 17 ppm, 22 to 108 ppm, 15 to 340 ppm, 5.2 to 101 ppm and 2.7 to 215 ppm respectively. Generally, the studied samples have a high concentration of Ba, Zn, Zr, Rb and Ce. The concentration (in ppm) of these elements are fairly variable but still similar with those average concentrations reported by Turekan and Wedephol (1961), Vine and Tourtelot (1970), Levinson (1974), and Gromet et al. (1984) (Table 8.4).

Table 8.3: XRF data for trace element distribution in the rock samples of the Madzaringwe Formation.

Sample	Coal Samples 1676	Coal Samples 1677	Coal Samples 1678	Coal samples 1679	Coal samples 1680	Coal samples 1681	OVI125 - 156 Sample 25	OVI125 - 156 Sample 26	OVI125 - 156 Sample 27	OVI125 - 156 Sample 28	OVI125 - 156 Sample 30	OVI125 - 156 Sample 31	OVI125 - 156 Sample 32	OVI125 - 156 Sample 33	OVI125 - 156 Sample 34	OVI125 - 156 Sample 35	OVI125 - 156 Sample 36	OVI125 149 Sample 1	OVI125 149 Sample 2
Ag	<2	<2	<2	<2	<2	<2	<2	<2	<2	<2	<2	<2	<2	<2	<2	<2	<2	<2	<2
As	7,9	6,2	<3	3	<3	4,3	5,1	5,7	<3	12	22	4,7	3,6	6	6,8	133	3,6	5	6,6
Ba	117	147	99	122	114	106	319	310	302	294	277	299	373	185	761	3340	378	321	260
Bi	<5	<5	<5	<5	<5	<5	<5	<5	<5	<5	<5	<5	<5	<5	<5	<5	<5	<5	<5
Br	<3	<3	<3	<3	<3	<3	<3	<3	<3	<3	<3	<3	<3	<3	<3	<3	<3	<3	<3
Cd	<4	<4	<4	<4	<4	<4	<4	<4	<4	<4	<4	<4	<4	<4	<4	<4	<4	<4	<4
Ce	46	33	23	37	36	28	87	85	35	46	73	164	81	46	134	51	142	91	95
Co	8,5	9,1	10	11	12	13	11	5,4	5,1	13	7,7	18	5,9	5,9	20	21	31	2,9	10
Cr	28	18	15	20	20	19	63	62	60	57	56	98	114	253	94	340	84	50	54
Cu	7,1	<2	<2	3,9	3,7	6,7	26	20	21	21	8,1	16	27	9,3	34	9,6	37	41	20
Ga	12	11	8,2	11	11	11	26	27	27	26	25	18	25	6,6	24	3,9	30	23	24
Ge	12	<2	2,2	3,2	3,1	2,3	<2	<2	<2	<2	<2	<2	<2	<2	<2	<2	<2	<2	<2
Hf	5,3	5	<5	5,7	<5	<5	7,5	6,3	6,8	6,4	7,2	12	8,9	<5	9,5	<5	5,3	5,3	7,7
La	27	16	13	15	20	14	43	45	20	22	34	80	39	21	64	18	68	47	50
Mo	6,5	2,2	<2	<2	<2	<2	2,2	2,6	2,6	3	4,2	3,1	2,6	2,7	2,6	7,3	2,3	2,6	3,4
Nb	13	7,9	5,2	11	9,5	6,7	21	22	22	22	20	18	22	7,5	22	2,9	24	21	20
Nd	21	17	13	20	19	15	39	37	18	20	30	72	35	24	62	20	63	50	41
Ni	5,6	6,4	5,2	6,5	6,9	9	50	15	15	42	16	16	13	16	33	101	48	9,3	27
Pb	9,8	8,3	4,2	4,4	4,6	6,6	33	29	26	38	38	21	27	12	29	60	35	17	30
Rb	43	35	17	25	29	26	159	173	161	147	126	95	129	37	141	19	163	131	140
Sb	<3	<3	<3	<3	<3	<3	<3	<3	<3	<3	<3	<3	<3	<3	<3	14	<3	<3	<3
Sc	6	5,7	4,9	6,4	7,1	7,6	11	13	10	9,8	9,1	8,2	12	7	17	5,6	16	9	12
Se	<2	<2	<2	<2	<2	<2	<2	<2	<2	<2	<2	<2	<2	<2	<2	<2	<2	<2	<2
Sn	<3	<3	<3	<3	<3	<3	5	3,5	5,5	3,1	3,7	<3	3,8	<3	<3	9,6	4,2	3,6	3,3
Sr	64	78	73	69	59	44	208	211	188	183	177	140	95	60	209	90	160	125	144
Ta	<2	<2	<2	<2	<2	<2	<2	<2	<2	<2	<2	<2	<2	<2	<2	5,6	<2	<2	<2
Th	4,7	5,6	4,7	4,4	4,7	7,2	16	20	16	16	14	13	18	4,5	18	<2	19	14	17
Tl	<2	<2	<2	<2	<2	<2	<2	<2	<2	<2	<2	<2	<2	<2	<2	13	<2	<2	<2
U	2,5	2,2	<2	2,3	<2	2,4	5,7	5	4,4	4,7	5,2	6,1	5,6	3,1	7,6	3,8	7,7	4,6	4,8
V	59	33	24	56	49	32	77	83	77	76	78	57	89	34	87	78	99	66	84
W	<5	<5	<5	<5	<5	<5	<5	<5	<5	<5	<5	<5	<5	11	<5	16	<5	<5	<5
Y	32	24	21	21	22	21	35	32	22	21	24	45	30	18	55	18	51	39	38
Yb	4,8	<4	<4	<4	<4	<4	<4	<4	<4	<4	<4	<4	<4	<4	6,1	<4	4,4	<4	<4
Zn	215	41	4,6	6,7	4,7	2,7	39	37	33	36	62	107	96	38	90	22	115	58	75
Zr	187	78	50	97	94	65	243	242	227	215	204	427	268	119	287	139	258	210	219

Sample	OVI125 149 Sample 3	OVI125 149 Sample 4	OVI125 149 Sample 5	OVI125 149 Sample 6	OVI125 149 Sample 7	OVI125 149 Sample 8	OVI125 149 Sample 9	OVI125 149 Sample 10	OVI125 149 Sample 11	OVI125 149 Sample 12	OVI125 149 Sample 13	OVI125 149 Sample 14	OVI125 160 Sample 16	OVI125 160 Sample 17	OVI125 160 Sample 18	OVI125 160 Sample 19	OVI125 160 Sample 20	OVI125 160 Sample 22	OVI125 160 Sample 23
Ag	<2	<2	<2	<2	<2	<2	<2	<2	<2	<2	<2	<2	<2	<2	<2	<2	<2	<2	<2
As	4,7	3,4	8,7	7,2	5,7	8,3	11	5,6	7,1	3,7	<3	3,3	<3	3,2	4,1	6,8	<3	3,4	<3
Ba	1453	324	274	325	311	276	322	129	555	377	310	329	367	513	311	280	352	273	290
Bi	<5	<5	<5	<5	<5	<5	<5	<5	<5	<5	<5	<5	<5	<5	<5	<5	<5	<5	<5
Br	<3	<3	<3	<3	<3	<3	<3	<3	<3	<3	<3	<3	<3	<3	<3	<3	<3	<3	<3
Cd	<4	<4	<4	<4	<4	<4	<4	<4	<4	<4	<4	<4	<4	<4	<4	<4	<4	<4	<4
Ce	117	120	72	126	105	128	162	40	135	129	106	121	82	95	119	71	100	73	104
Co	6,3	4,4	4,2	14	8,8	13	13	2,5	44	5,1	13	14	3,9	5,9	5,3	21	2,9	5,8	14
Cr	60	53	64	73	54	108	102	243	105	70	69	73	53	52	55	55	46	75	102
Cu	25	21	19	31	10	11	13	<2	40	31	29	32	32	17	13	21	6,1	13	25
Ga	24	26	27	27	26	17	16	5	28	27	29	26	26	25	25	26	26	18	19
Ge	<2	<2	<2	<2	<2	<2	<2	<2	<2	<2	<2	<2	<2	<2	<2	<2	<2	2	<2
Hf	6,5	5,6	<5	8,3	6,8	12	14	<5	8,7	6,9	6,3	8,3	7,1	8,2	6,6	5,3	<5	9,2	5,3
La	61	66	35	56	53	59	77	20	65	64	50	55	44	47	55	38	51	34	52
Mo	2,8	2,9	3,4	<2	3,3	3,3	2,9	<2	3,8	<2	2,3	<2	3,2	2,8	2,3	2,9	3,5	<2	<2
Nb	20	20	22	24	21	15	15	3,9	24	20	23	23	22	20	21	19	22	16	17
Nd	57	51	33	50	39	58	70	16	57	61	43	51	36	40	58	31	40	32	42
Ni	13	10	13	26	12	14	15	6,5	70	16	26	24	11	11	10	21	6,5	9,2	26
Pb	28	32	29	33	24	22	26	4,8	34	32	30	30	31	26	28	29	22	17	21
Rb	146	141	131	156	134	93	77	24	157	143	159	150	154	152	151	135	136	97	104
Sb	<3	<3	<3	<3	<3	<3	<3	<3	<3	<3	<3	<3	<3	<3	<3	<3	<3	<3	<3
Sc	14	13	11	15	10	8,8	10	4,2	17	15	14	13	12	13	12	13	11	9,3	13
Se	<2	<2	<2	<2	<2	<2	<2	<2	<2	<2	<2	<2	<2	<2	<2	<2	<2	<2	<2
Sn	<3	5,4	3,9	3,8	3,5	3,5	<3	<3	3,7	3,8	5,1	3,4	3,2	<3	<3	4,5	4,6	<3	<3
Sr	201	157	157	153	152	201	182	131	210	157	138	147	98	111	106	92	103	112	158
Ta	<2	<2	2	<2	<2	<2	<2	<2	<2	<2	<2	<2	<2	<2	<2	<2	<2	<2	<2
Th	17	20	19	19	16	10	13	2,2	20	19	19	20	15	15	15	18	15	14	12
Tl	<2	<2	<2	2,2	2,5	<2	2,3	3,9	<2	<2	<2	<2	<2	<2	<2	<2	<2	<2	<2
U	4,9	6,8	6,5	8,2	6,2	5,9	6,7	<2	7,7	7,1	5,3	7	6,7	5	6,1	9,6	11	4,5	5,6
V	82	75	79	84	75	45	63	22	108	86	87	82	77	81	82	77	74	53	68
W	<5	<5	<5	<5	<5	<5	<5	7,2	<5	<5	<5	<5	<5	<5	<5	<5	<5	<5	<5
Y	49	38	28	49	31	40	42	11	50	50	42	46	34	39	43	23	29	29	38
Yb	<4	<4	<4	7	<4	4,3	4,7	<4	5,2	<4	4,1	<4	<4	<4	4,8	<4	<4	<4	4,7
Zn	88	49	51	104	57	65	132	15	108	59	76	103	43	80	105	137	74	72	82
Zr	237	208	217	253	212	407	432	63	290	217	226	243	214	234	246	199	208	290	209

Table 8.4: Comparison of the average concentration of trace elements in the studied samples with published values.

Trace element	This study		Levinson (1974)	Vine and Tourtelot (1970)	Turekan and Wedephol (1961)	UCC	PAAS	NASC (Gromet et al., 1984)
	Coal	Shale						
Ba	117.50	462.19	300.00	700.00	580.00	628.00	650.00	636.00
Co	10.60	11.19	10.00	20.00	-	17.30	23.00	n.a.
Cr	20.00	90.53	-	-	-	92.00	110.00	-
Cu	4.23	21.28	70.00	50.00	45.00	28.00	50.00	n.a.
Ga	10.70	22.77	-	-	-	17.50	20.00	n.a.
Hf	5.17	7.19	-	-	-	5.30	5.00	n.a.
Nb	8.88	19.13	20.00	20.00	n.a.	12.00	19.00	-
Ni	6.60	23.17	50.00	70.00	-	47.00	55.00	58.00
Pb	6.32	27.93	20.00	n.a.	n.a.	17.00	20.00	
Rb	29.17	126.91	140.00	n.a.	n.a.	84.00	160.00	n.a.
Sc	6.28	11.50	-	-	-	14.00	16.00	n.a.
Sr	64.50	148.63	200.00	300.00	300.00	320.00	200.00	142.00
Th	5.22	15.18	12.00	n.a.	n.a.	10.50	14.60	n.a.
U	2.28	5.97	4.00	n.a.	n.a.	2.70	3.10	n.a.
V	42.17	74.53	150.00	150.00	130.00	97.00	150.00	130.00
Y	23.58	35.59	30.00	25.00	-	21.00	27.00	n.a.
Zn	45.78	72.13	300.00	100.00	95.00	67.00	85.00	n.a.
Zr	95.17	239.47	70.00	160.00	160.00	193.00	210.00	200.00

NB. UCC- Upper Continental Crust; PAAS- Post-Archean Australian Shale; NASC- North-American Shale Composite

8.4 Sandstone classification

The concentrations of silica, aluminium, potassium, sodium and iron oxides have been used to classify sandstones (Pettijohn et al., 1987; Herron, 1988). The classification of the studied sandstones is based on the geochemical classification diagrams of Pettijohn et al. (1987) and Herron (1988). The geochemical classification of Madzaringwe Formation sandstones was investigated using the log ratios of Na_2O/K_2O plotted against the log ratios of Fe_2O_3/K_2O plotted against the log ratios of SiO_2/Al_2O_3 (Herron, 1988) and the log ratios of SiO_2/Al_2O_3 (Pettijohn et al., 1987). The SiO_2 content and SiO_2/Al_2O_3 ratio are the most commonly used geochemical criteria for classifying clastic sedimentary rock. Herron's classification diagram revealed that the sandstones could be classified as subarkose and sub-lithic arenite (Figure 8.2). Similarly, the geochemical classification diagram of Pettijohn et al. (1987) shows that the sandstones could be classified as subarkose and lithic arenite (Figure 8.3).

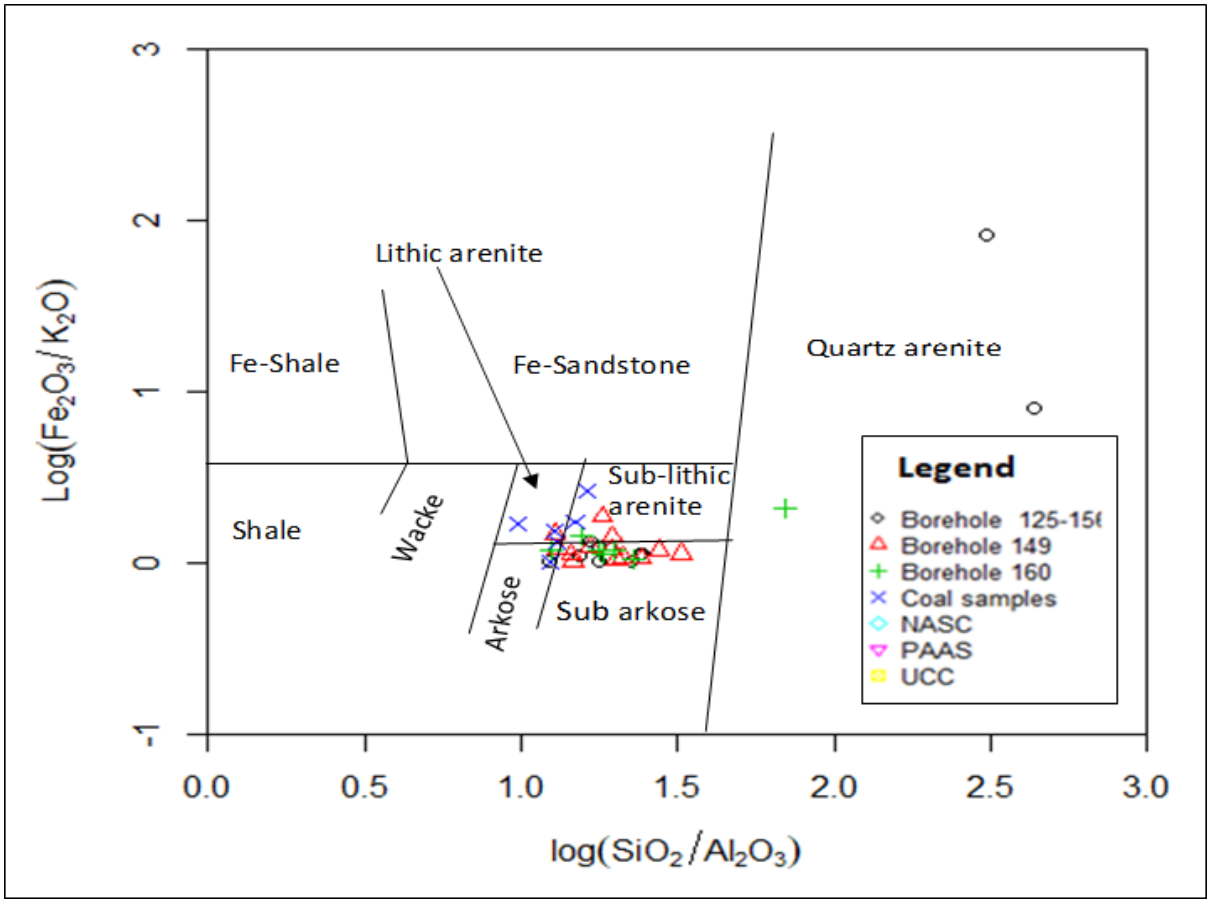

Figure 8.2: Bivariate plot of log (Fe_2O_3/K_2O) versus log (SiO_2/Al_2O_3) showing geochemical classification of the studied sandstones (after Herron, 1988).

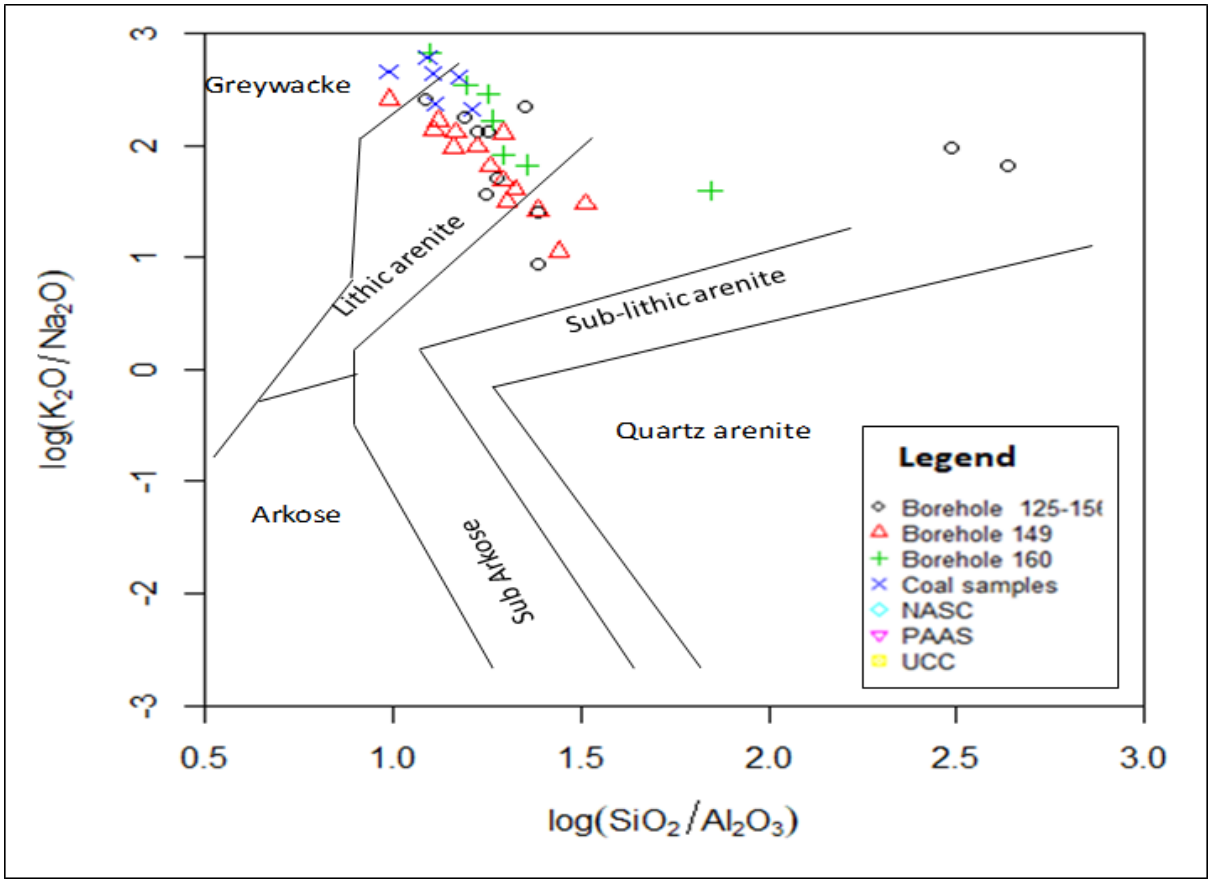

Figure 8.3: Binary plot of log (Na_2O/K_2O) versus log (SiO_2/Al_2O_3) showing geochemical classification of the studied sandstones (after Pettijohn et al., 1987).

8.5 Provenance

Using major oxides as variables, Roser and Korsch (1988) established major element discriminant functions (plot of discriminant 1 versus discriminant 2) to differentiate four major provenance fields, namely mafic, intermediate, felsic and quartzose recycled. Likewise, the binary plots of TiO_2 vs Zr, and La/Sr vs Th/Co have been successfully used to infer provenance of clastic sedimentary rocks (Taylor and McLennan, 1985; Bhatia and Crook, 1986; McLennan et al., 1993; Armstrong-Altrin et al., 2004; Baiyegunhi et al., 2017). The bivariate plot of discriminant 1 against discriminant 2 of Roser and Korsch (1988) background diagram shows that most of the shale samples

fall under the felsic igneous provenance field, only one shale sample from borehole OV125156 plotted in the intermediate igneous provenance. The coal samples plotted in the mafic igneous provenance field (Figure 8.4). Also, the binary diagram of the TiO_2 versus Zr (Figure 8.5) and La/Sr against Th/Co (Figure 7.6) shows that the studied rocks are from silicic or felsic igneous rocks.

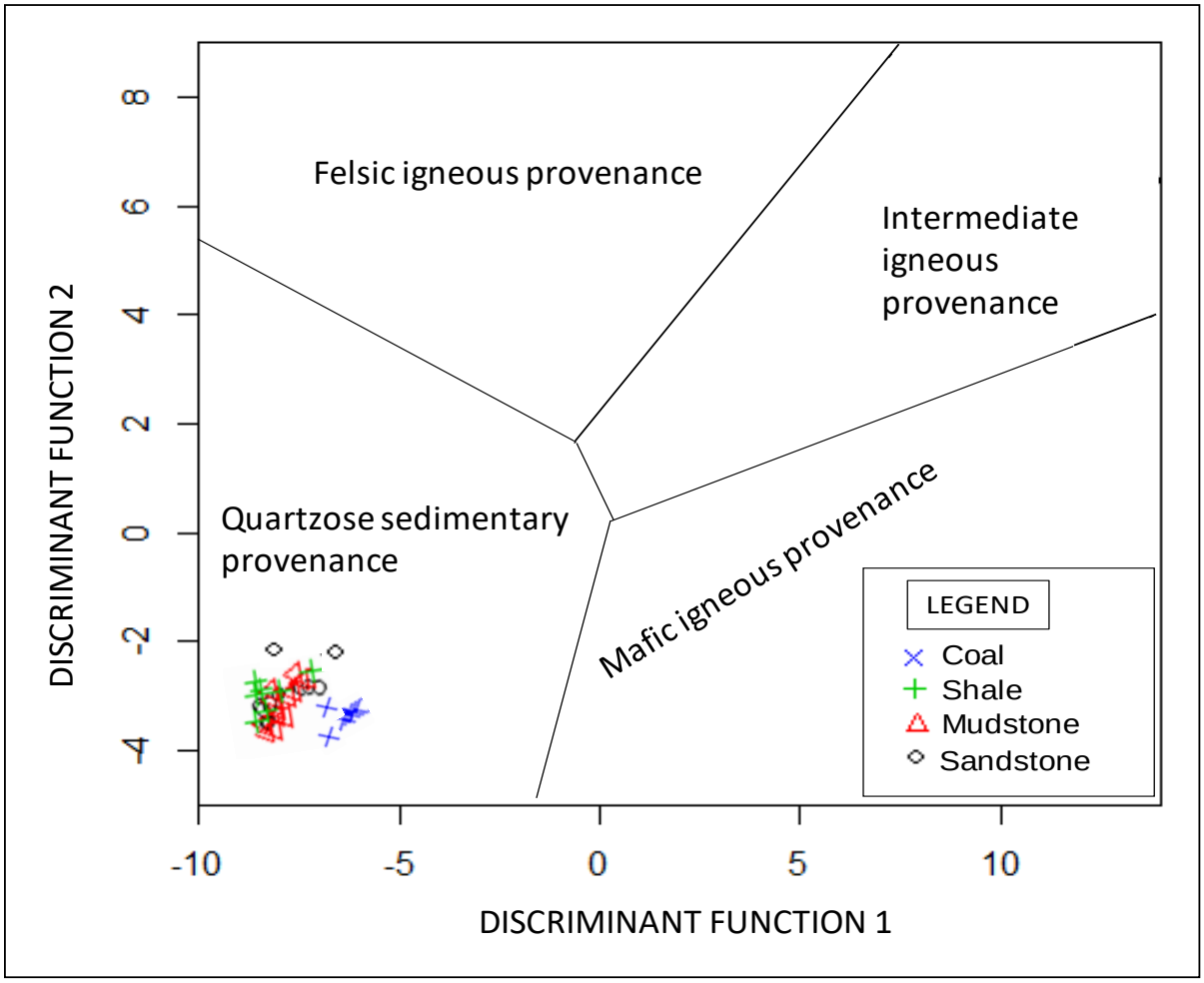

Figure 8.4: Major element Discriminant Function diagram for sedimentary provenance (shale, and coal samples (after Roser and Korsch,1988). The discriminant functions are: Discriminant Function 1 = (−1.773 TiO_2) + (0.607 Al_2O_3) + (0.760 Fe_2O_3) + (−1.500MgO) + (0.616CaO) + (0.509 Na_2O) + (−1.224 K_2O) +(−9.090); Discriminant Function 2 = (0.445 TiO_2) + (0.070 Al_2O_3) + (-0.250 Fe_2O_3) + (-1.142 MgO) + (0.438 CaO) + (1.475 Na_2O) + (-1.426 K_2O) + (6.861).

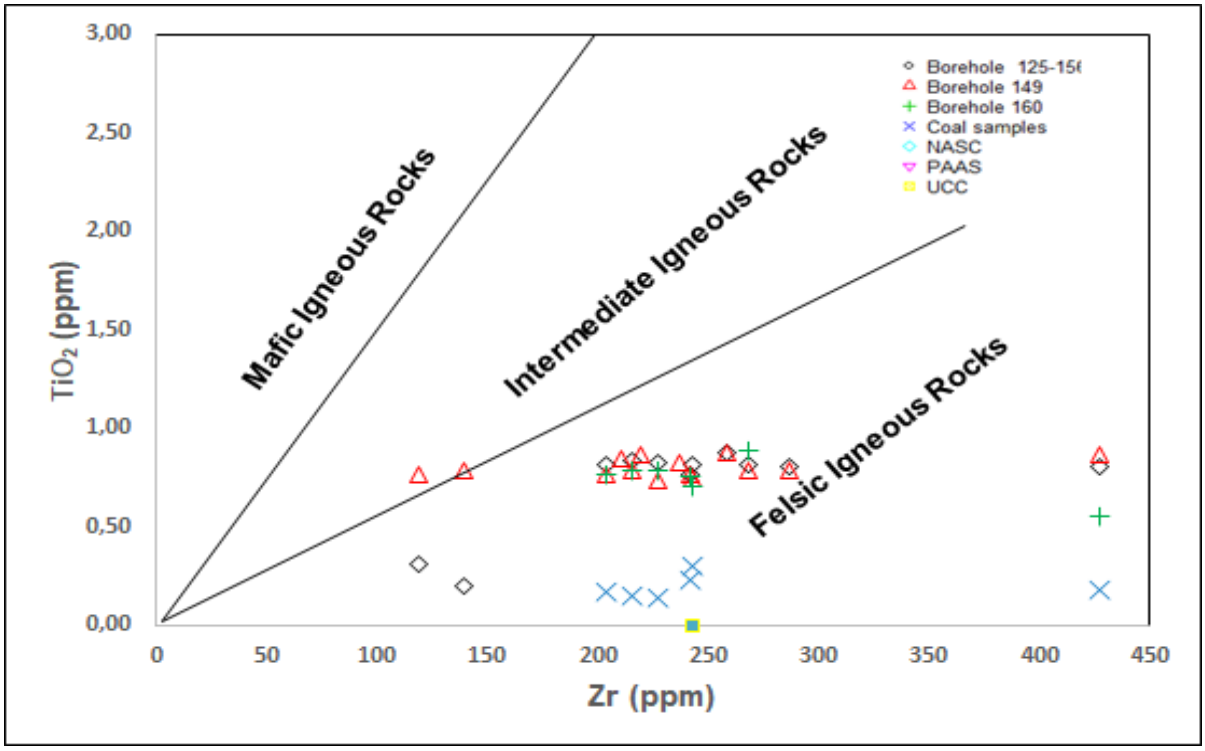

Figure 8.5: Binary plot of TiO_2 against Zr for the studied samples showing provenance (after Bracciali et al., 2007).

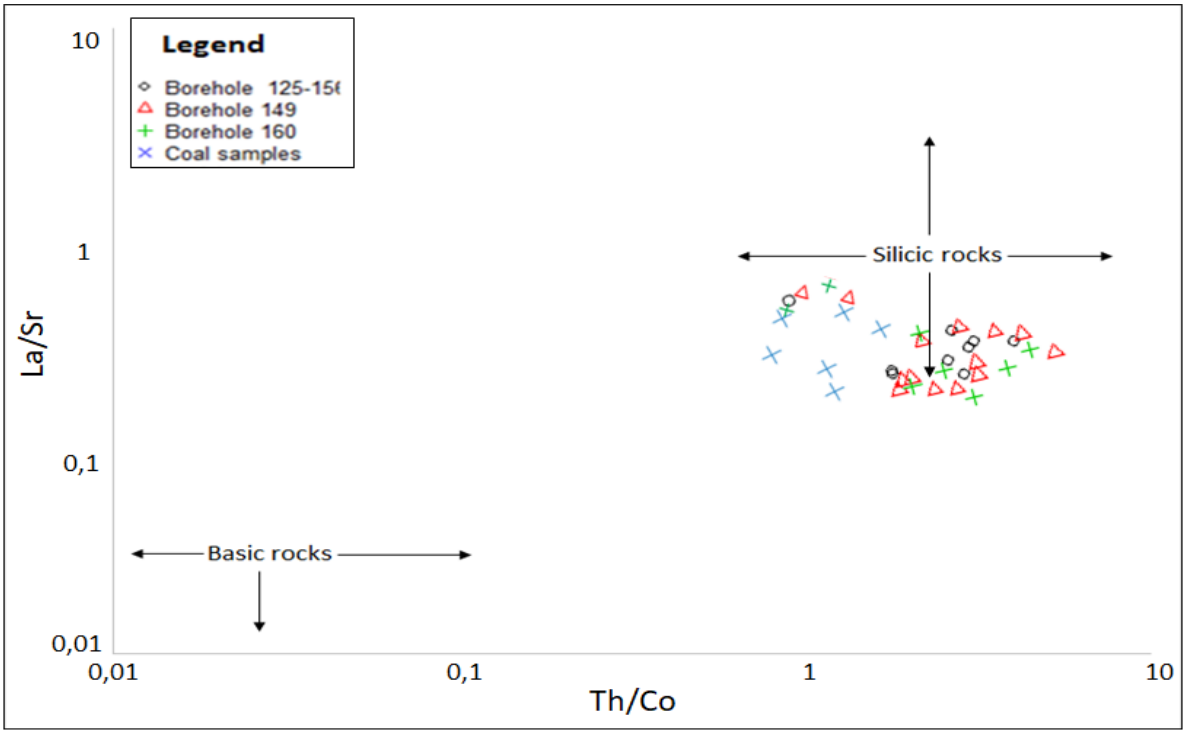

Figure 8.6: Binary plot of La/Sr versus Th/Co for the studied samples showing provenance (Background field after Roser and Korsch, 1986).

8.6 Tectonic setting

Several researchers including Bhatia (1983), Bhatia and Crook (1986) and Roser and Korsch (1986) have envisaged that tectonic settings control or influence the chemical compositions of clastic sedimentary rocks, indicating that variety of tectonic settings have terrain-specific signatures. Different tectonic setting discrimination diagrams have been used to separate between different tectonic settings, and they all provide consistent results for siliciclastic rocks that have not been strongly affected by post-depositional weathering and metamorphism (Bhatia, 1983; Bhatia and Crook, 1986; and Roser and Korsch, 1986). The bivariate and ternary plots of major and trace element geochemistry has been widely used by numerous academics to determine the tectonic setting of shales (Baiyegunhi et al., 2017). The most used discrimination diagrams are major element-based discrimination diagrams of (Bhatia 1983 and Bhatia and Crook, 1986). The geochemical data of the studied samples were plotted on binary plots of TiO_2 versus (Fe_2O_3 + MgO) and SiO_2 against K_2O/Na_2O, and ternary plots of Na_2O–CaO–K_2O and Th–Sc–Zr/10.

The binary plots of TiO_2 versus (Fe_2O_3 + MgO) and SiO_2 against K_2O/Na_2O show that the studied samples are mostly related to active continental setting, with little contribution from passive continental margin setting (Figures 8.7 and 8.8). On the contrary, the ternary plots of Na_2O–CaO–K_2O and Th–Sc–Zr/10 revealed that the studied samples are mainly of passive continental setting, with little contribution from active continental margin setting (Figures 8.9 and 8.10). The active continental margins are subduction-related basins, continental basins and pull-apart basins associated with strike-slip fault zones.

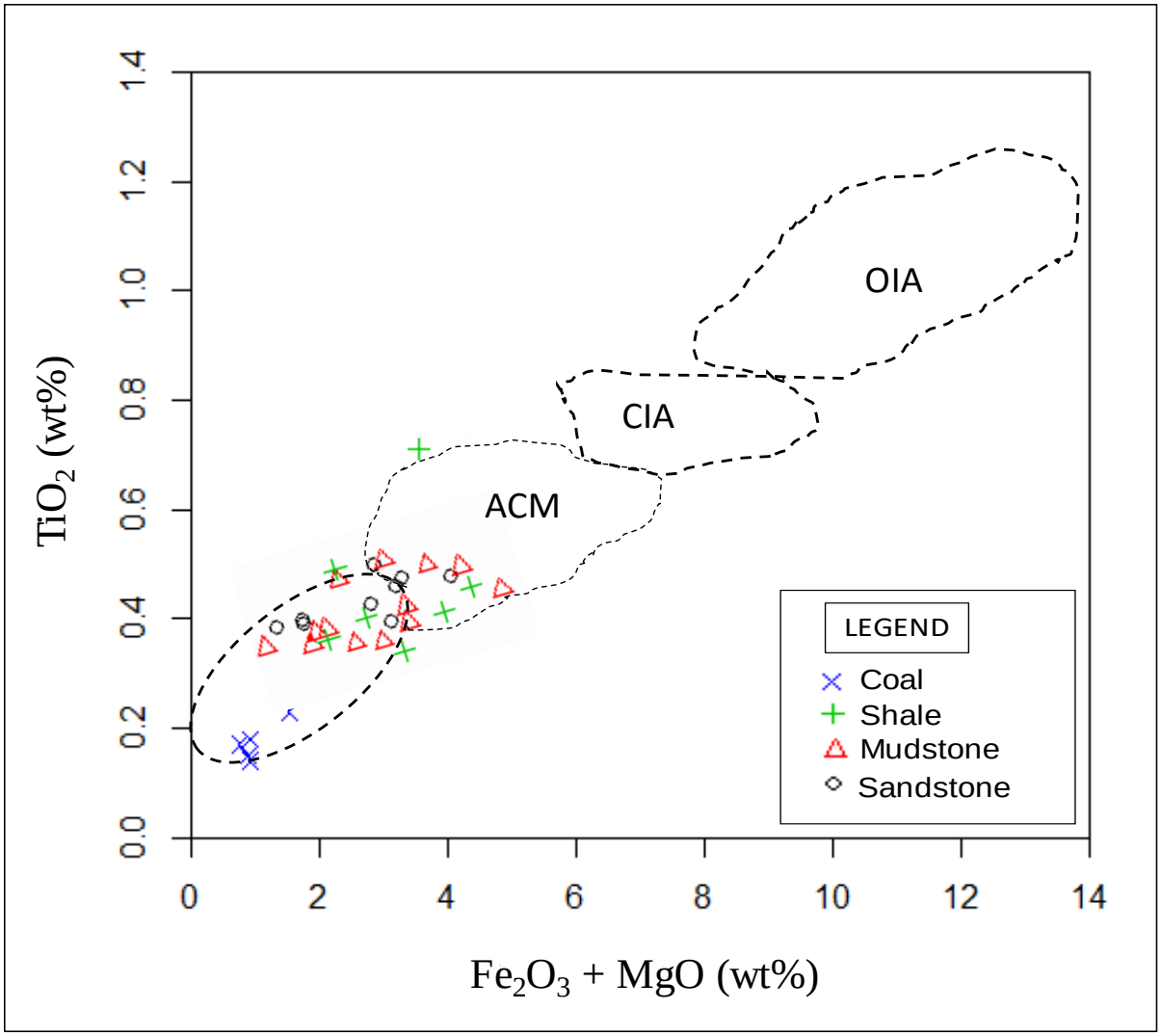

Figure 8.7: Bivariate plot of TiO_2 (wt.%) versus (Fe_2O_3 +MgO) (wt.%) for the studied samples showing tectonic setting (Background field after Bhatia, 1986). Note: PM, ACM, CIA and OIA represent Passive Margin, Active Continental Margin, Continental Island Arc, and Oceanic Island Arc, respectively.

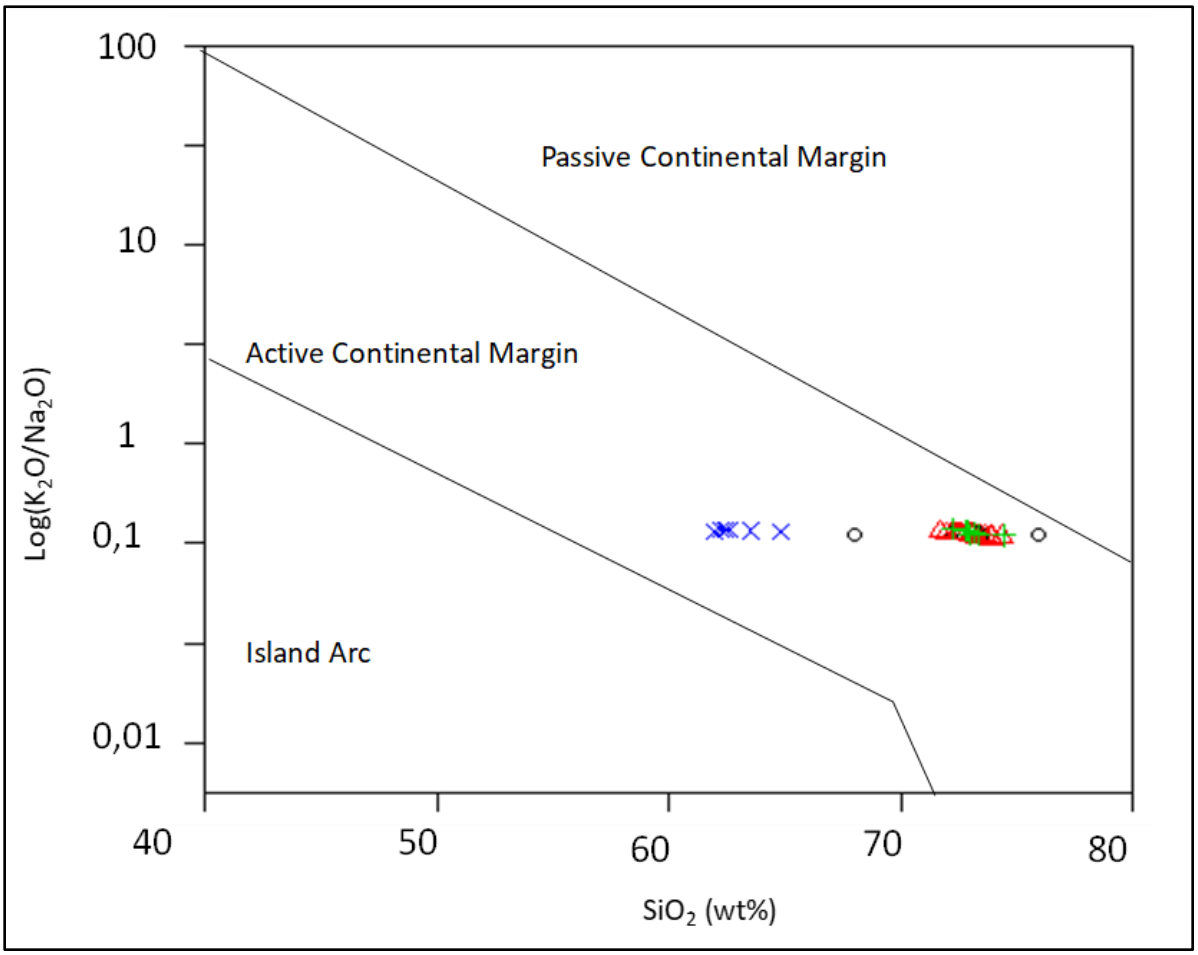

Figure 8.8: Bivariate plot of SiO_2 versus K_2O/Na_2O for the studied samples showing tectonic setting (Background field after Roser and Korsch, 1986). Note: PM, ACM, CIA and OIA represent Passive Margin, Active Continental Margin, Continental Island Arc, and Oceanic Island Arc, respectively.

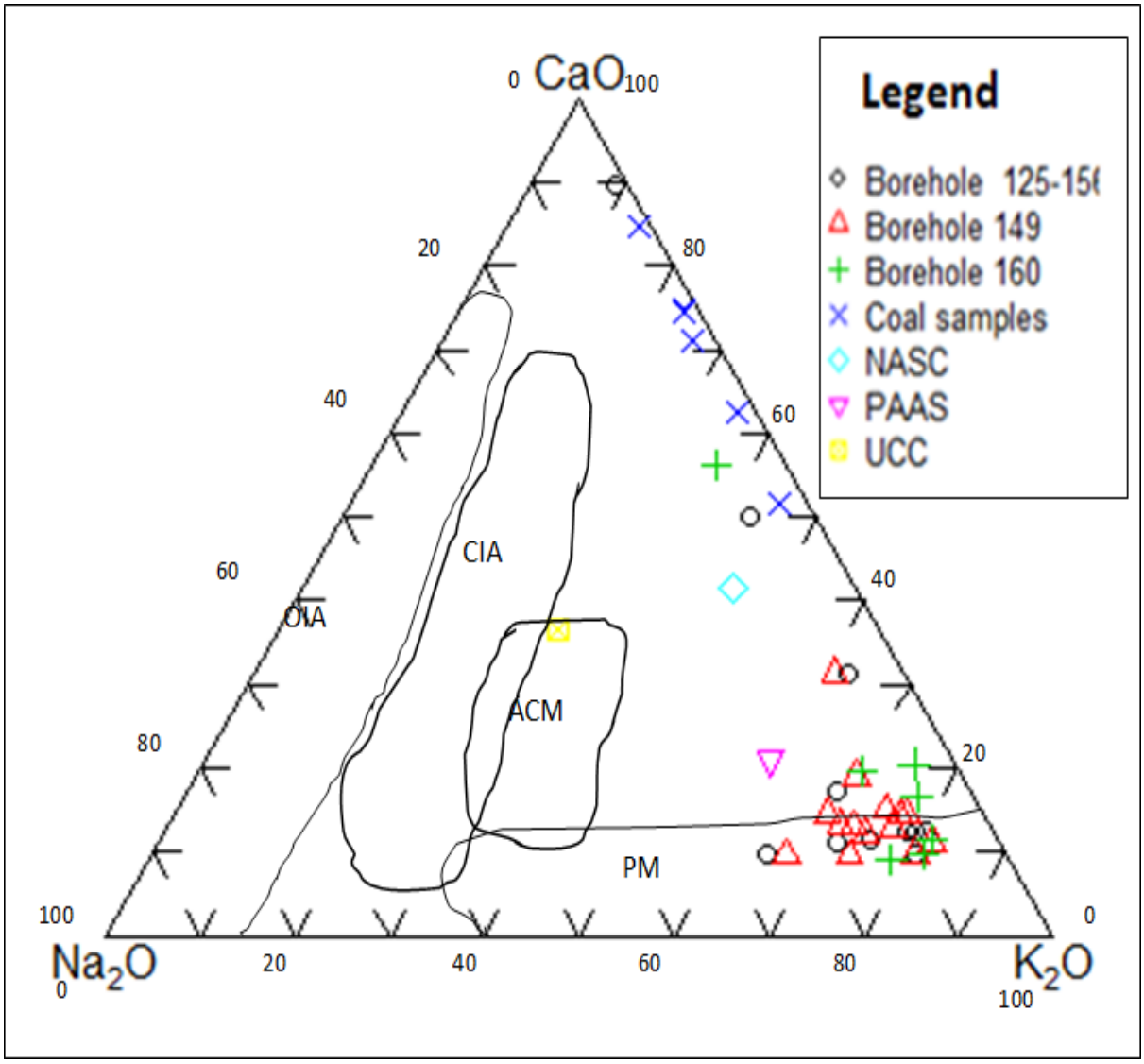

Figure 8.9: Na_2O- CaO-K_2O ternary plot for the studied samples showing tectonic setting (Background field after Toulkeridis et al., 1999). Note: PM, ACM, CIA and OIA represent Passive Margin, Active Continental Margin, Continental Island Arc, and Oceanic Island Arc, respectively.

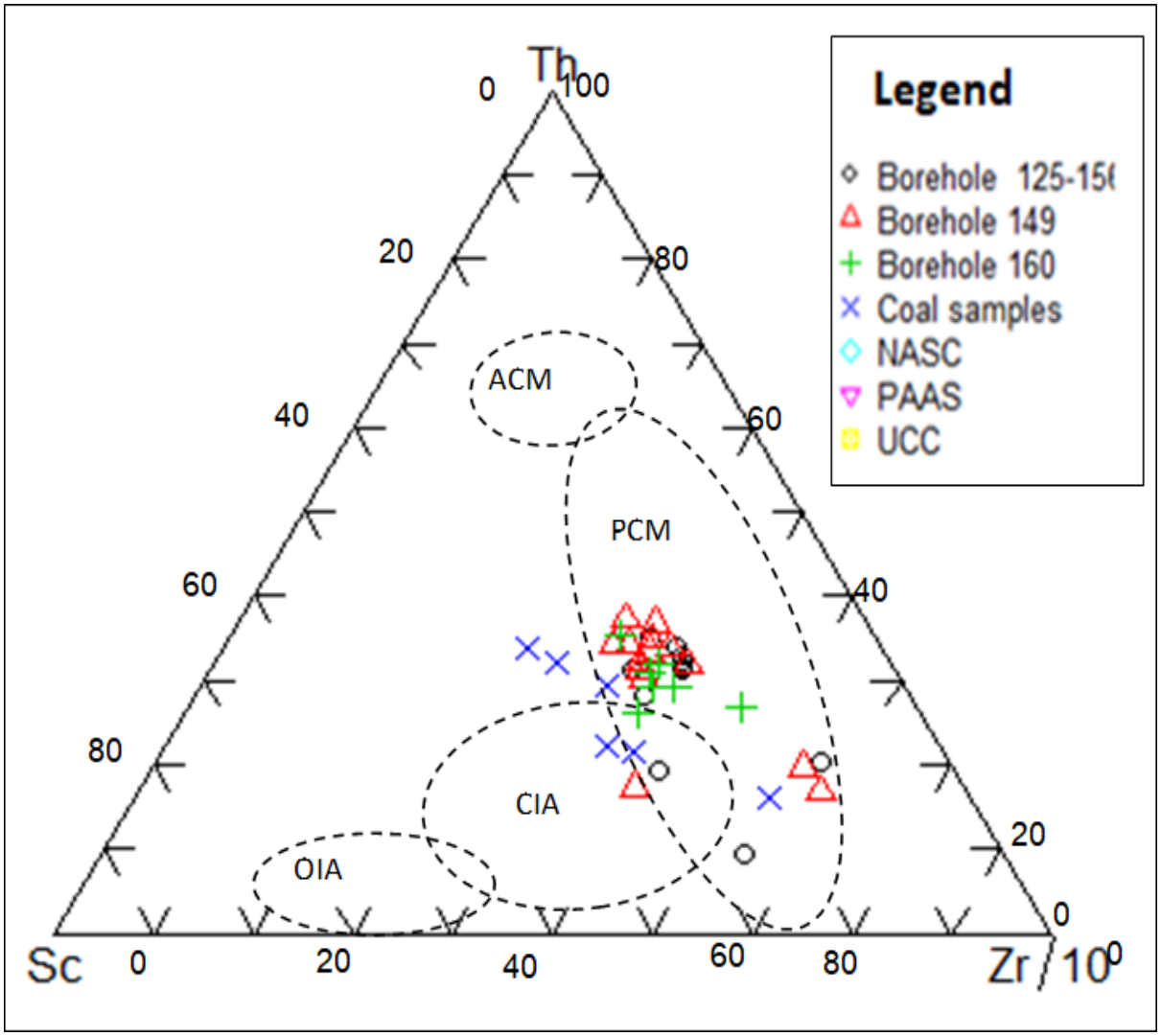

Figure 8.10: Th- Sc-Zr/10 ternary plot for the studied samples showing tectonic setting (Background field after Toulkeridis et al., 1999). Note: PM, ACM, CIA and OIA represent Passive Margin, Active Continental Margin, Continental Island Arc, and Oceanic Island Arc, respectively.

8.7 Paleoweathering conditions

Chemical weathering intensity of source rocks is mostly controlled by the composition of the source rock, period of weathering, climatic conditions and rates of tectonic uplift of the source region (Wronkiewicz and Codie, 1987). Calcium (Ca), sodium (Na), and

potassium (K) are largely removed from source rocks during chemical weathering and the amount of these elements remaining in the sediments derived from the rocks aided as an indicator of the intensity of chemical weathering (Cullers, 2000). If siliciclastic sedimentary rocks are free from alkali related post-depositional modifications, their alkali contents (K_2O + Na_2O) and K_2O/Na_2O ratios should be considered as reliable indicators of the intensity of the source material weathering (Pe-Piper et al., 2008).

A few indices of weathering have been proposed based on the molecular proportions of mobile and immobile element oxides (Na_2O, CaO, K_2O, and Al_2O_3) to determine the degree of source rock weathering. Therefore, chemical compositions of weathering products in a sedimentary basin are anticipated to disclose the mobility of various elements during weathering. The indices of weathering/alteration include chemical index alteration (CIA), chemical index weathering (CIW) and plagioclase index weathering (PIA). To determine the paleoweathering conditions for the studied samples, the formula for the weathering indices were used as follows:

$$\mathrm{CIA} = [\mathrm{Al_2O_3}/(\mathrm{Al_2O_3} + \mathrm{CaO^*} + \mathrm{Na_2O} + \mathrm{K_2O})] \times 100$$

$$\mathrm{CIW} = [\mathrm{Al_2O_3}/(\mathrm{Al_2O_3} + \mathrm{CaO^*} + \mathrm{Na_2O})] \times 100$$

$$\mathrm{PIA} = [(\mathrm{Al_2O_3} - \mathrm{K_2O})/(\mathrm{Al_2O_3} + \mathrm{CaO^*} + \mathrm{Na_2O} - \mathrm{K_2O})] \times 10$$

Where $\mathrm{CaO^*}$ is the content of CaO incorporated in silicate fraction.

The calculated values for the chemical index alteration (CIA), chemical index weathering (CIW) and plagioclase index weathering (PIA) are presented in Table 8.5. The CIA is simply the ratio of primary minerals to secondary products (i.e. clay

minerals). CIA values usually range from about 50 for unweathered rocks up to 100 in highly weathered rocks. The CIA values for the studied samples range from 45,64 to 87,00% (averaging 80,44%) (Figure 8.13). The high CIA values (70 to 90%) implies moderate to high weathering conditions. Fewer samples plot within the weak weathering portion (between 0 and 70%), whereas the majority of the samples plotted in the intensive weathering region (75 to 100%). The high CIA values suggest the presence of clay minerals and absence of detrital feldspar in the sediments. Also, the weathering of feldspars to clay minerals can be monitored using the Plagioclase Index of Alteration (PIA) (Fedo et al.,1995). The PIA values of the studied samples range from 45.16 to 96.81% (averaging 88.58%). The PIA values indicate moderate-intense destruction of feldspars during transport, sedimentation and diagenesis.

Table 8.5: Indices of weathering (CIA, CIW and PIA) calculated from the major elements.

Borehole	Depth (m)	Lithology	CIA	CIW	ICV	PIA
Coal Sample 1676	32.00	Vitrinite coal	69.90	75.95	0.80	73.67
Coal Sample 1678	32.00	Vitrinite coal	58.17	61.79	1.02	59.25
Coal Sample 1679	33.00	Vitrinite coal	67.58	73.21	0.72	70.78
Coal Sample 1680	38.00	Vitrinite coal	75.57	82.69	0.50	80.89
Coal Sample 1681	37.00	Vitrinite coal	82.41	89.54	0.42	88.55
Coal Sample 1677	24.00	Vitrinite coal	65.67	71.47	0.80	68.71
OVI125 149 Sample 1	34.50	Black mudstone	83.79	94.32	0.36	93.50
OVI125 149 Sample 2	35.50	Black mudstone	82.63	94.26	0.42	93.32
OVI125 149 Sample 3	36.00	Black mudstone	82.23	94.39	0.40	93.41
OVI125 149 Sample 4	36.50	Black mudstone	84.45	95.45	0.32	94.77
OVI125 149 Sample 5	36.50	Black mudstone	84.90	94.89	0.47	94.21
OVI125 149 Sample 6	37.40	Black mudstone	85.69	96.24	0.31	95.71
OVI125 149 Sample 7	37.80	Black mudstone	85.50	95.91	0.37	95.34
OVI125 149 Sample 8	39.10	Black shale	82.25	93.36	0.35	92.32

OVI125 149 Sample 9	39.70	Black mudstone	86.52	97.05	0.24	96.65
OVI125 149 Sample 10	39.85	Greyish sandstone	83.04	94.90	0.35	94.05
OVI125 149 Sample 11	40.66	Greyish sandstone	80.33	91.35	0.43	89.97
OVI125 149 Sample 12	41.66	Greyish sandstone	84.85	96.11	0.39	95.51
OVI125 149 Sample 13	41.50	Black shale	85.89	97.05	0.30	96.61
OVI125 149 Sample 14	42.00	Black shale	85.23	96.12	0.42	95.55
OVI125 160 Sample 16	21.25	Black shale	82.82	95.72	0.41	94.93
OVI125 160 Sample 17	21.50	Black shale	82.08	93.86	0.46	92.83
OVI125 160 Sample 18	22.99	Black shale	84.92	96.82	0.35	96.30
OVI125 160 Sample 19	22.60	Black shale	85.68	96.35	0.41	95.83
OVI125 160 Sample 20	23.66	Coal	86.45	97.19	0.29	96.79
OVI125 160 Sample 22	25.10	Greyish sandstone	75.07	82.56	0.67	80.63
OVI125 160 Sample 23	25.55	Black mudstone	84.30	95.56	0.33	94.88
OVI125 -156 Sample 25	39.58	Black shale	81.62	93.36	0.47	92.24
OVI125 -156 Sample 26	40.25	Black shale	83.24	95.22	0.39	94.42
OVI125 -156 Sample 27	41.00	Black shale	83.70	95.94	0.39	95.25
OVI125 -156 Sample 28	41.65	Black shale	85.13	96.48	0.37	95.93
OVI125 -156 Sample 30	43.80	Black shale	83.60	93.58	0.33	92.71
OVI125 -156 Sample 31	43.05	Black shale	85.29	95.33	0.30	94.70
OVI125 -156 Sample 32	43.15	Black shale	87.00	97.18	0.25	96.81
OVI125 -156 Sample 33	43.38	Black shale	76.79	85.31	1.53	83.47
OVI125 -156 Sample 34	43.62	Black shale	81.17	92.04	0.42	90.81
OVI125 -156 Sample 35	43.74	Black shale	45.64	47.99	10.07	45.16
OVI125 -156 Sample 36	43.87	Black shale	85.53	96.76	0.34	96.27
PAAS	-	-	75.30	88.33	0.83	85.89
UCC	-	-	61.45	69.18	1.12	64.75

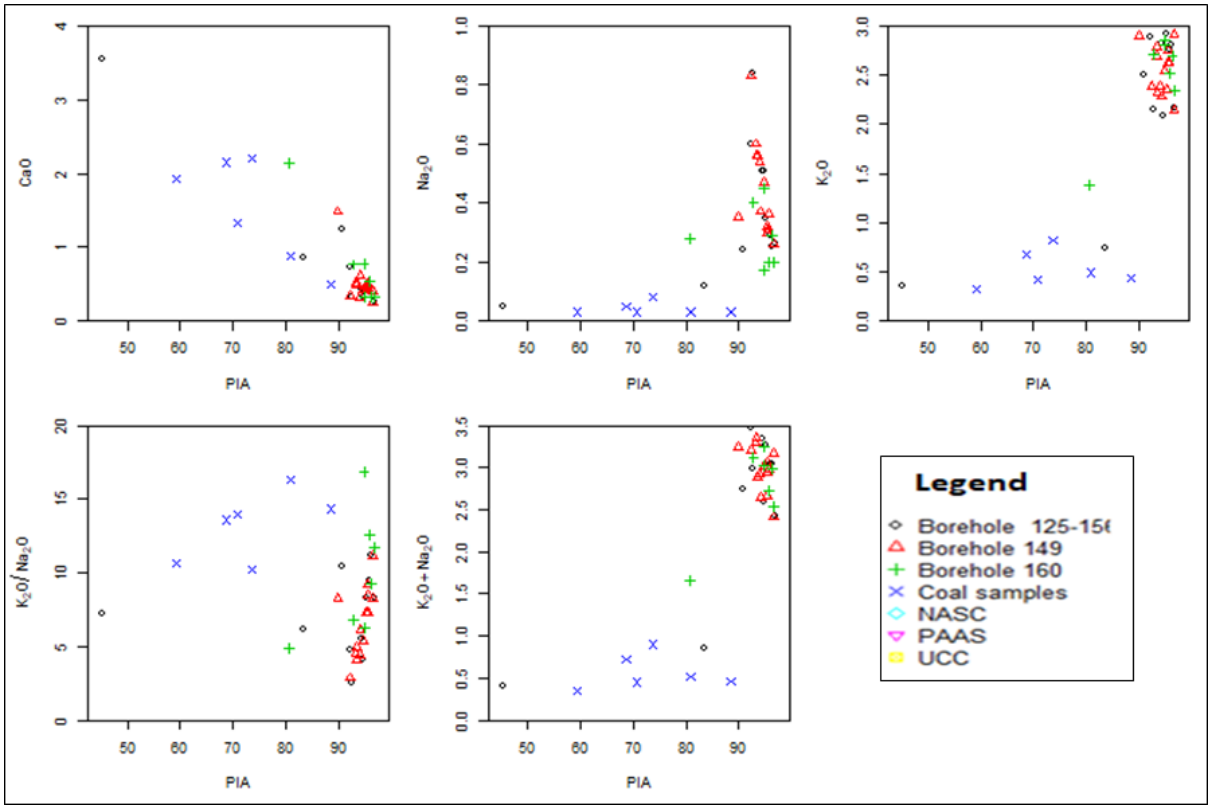

Figure 8.11: Bivariate diagrams depicting mobility of elements during weathering of feldspars in the shale ad coal samples of Madzaringwe Formation; (a) (K_2O/Na_2O) wt.% versus PIA; (b) Na_2O wt.% versus PIA; (c) K_2O wt.% Versus PIA; (d) (K_2O/Na_2O) wt.% versus PIA; (e) ($K_2O + Na_2O$) wt.% versus PIA.

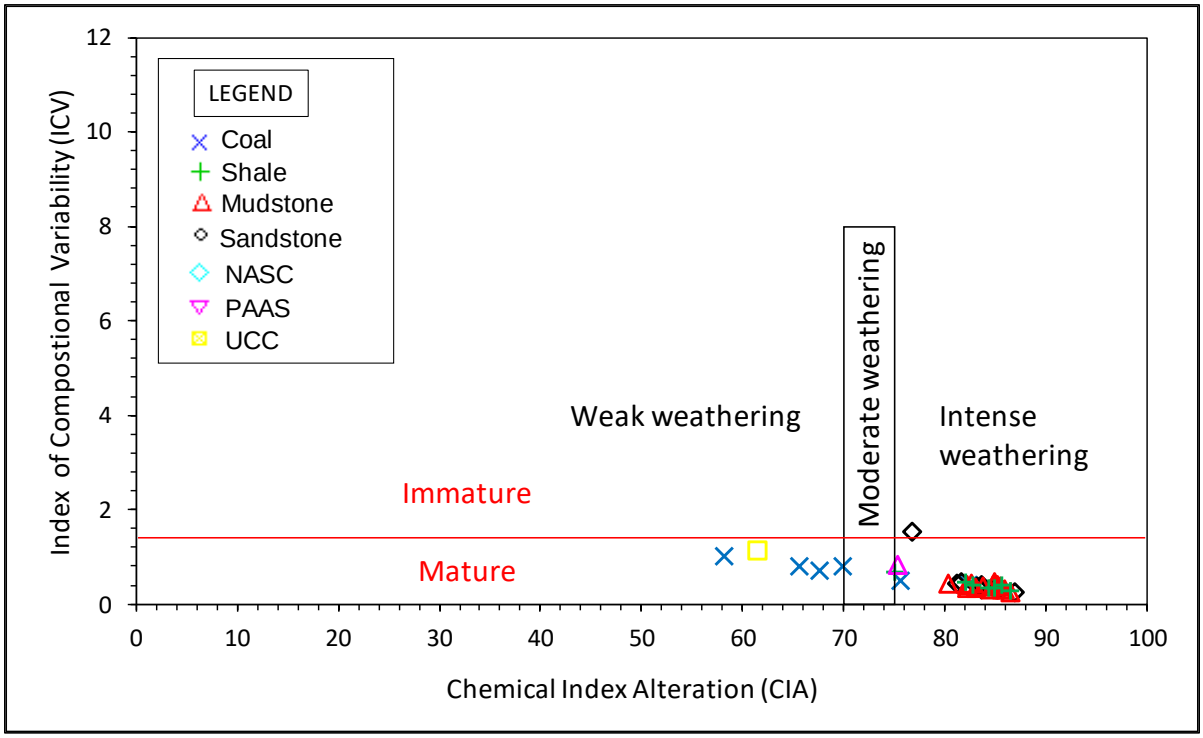

Figure 8.12: Binary plot of CIA against ICV for the Madzaringwe Formation samples.

The ternary plot of A–CN–K proposed by Nesbitt and young (1982) is another way of evaluating the composition of the source rock as well as the mobility of elements during the process of chemical weathering of source materials and post-depositional chemical modification. The ternary plot of Al_2O_3–($CaO+Na_2O$)–K_2O (exemplified as A–CN–K) shows that the studied samples plotted above the line joining plagioclase and K-feldspar (Figure 8.13). The weathering trendline of the samples tends towards the A–K boundary, suggesting the silicates (i.e. feldspar) have experienced moderate to high weathering causing the leaching of calcium (Ca) and sodium (Na) out of plagioclase. Furthermore, the trendline (arrows in Figure 8.13) parallels with the A–CN boundary and slightly extend towards the illite, signifying leaching of potassium (K) and enrichment of aluminium (Al) resulting in the decomposition of K-bearing

minerals (biotite, kaolinite and potassium feldspar). Thus, illite dominates the secondary clay minerals. On the other hand, the weathering trendline of the samples is relatively closer to the A–CN boundary, indicating that plagioclase is the first to be weathered, out of which Ca and Na leached rapidly, whereas K-feldspar is relatively stable. In the sandstones, illite is the main weathering products.

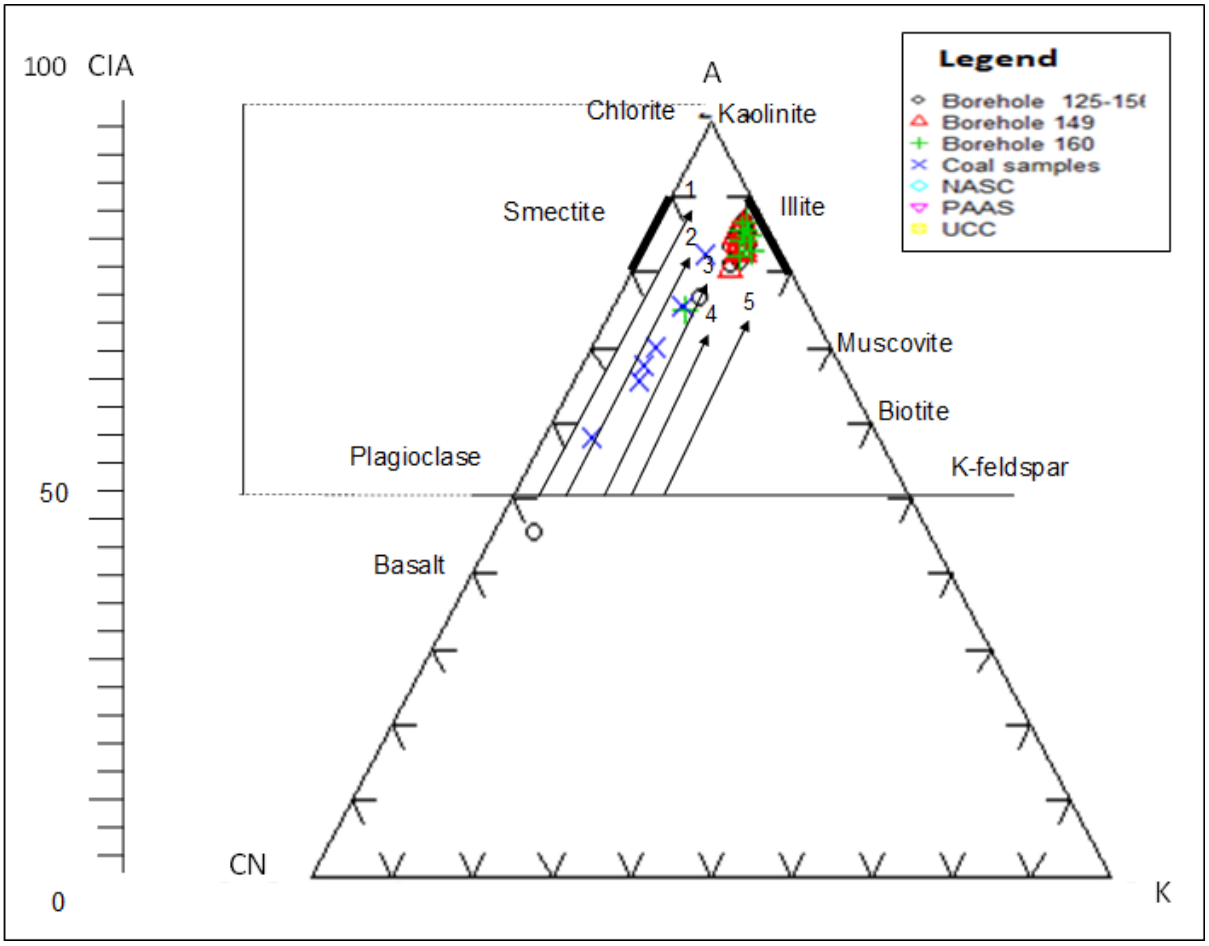

Figure 8.13: A-CN-K ternary diagram of molecular proportions of Al_2O_3-($CaO+Na_2O$)-K_2O for Bredasdorp mudrocks (Background field after Nesbitt and Young, 1984). The CIA scale shown at the left side is for comparison.

CHAPTER 9

DISCUSSION, CONCLUSIONS AND RECOMMENDATION

9.1. Discussion

Previous published data gives an overview of the stratigraphy of the Madzaringwe Formation in the Tuli coalfield, to date, little is known of the petrographic characteristics, lithofacies and geochemistry of the Madzaringwe Formation. Hence, this research work is undertaken to better define the lithological characteristics, provenance and tectonic setting of the Madzaringwe Formation. The study is mainly focused on the stratigraphy, sedimentary facies, petrography and geochemistry of the Madzaringwe Formation in the Vele Colliery, Limpopo Province, South Africa.

In the Vele colliery, diamictite is contained in the Tshidzi Formation that is developed at the base of the Karoo sequence. The diamictite has a maximum thickness of about 10 m and it comprises of angular and subrounded clasts. The Tshidzi Formation is possibly related to the glacial Dwyka tillite/diamictite in the main Karoo Basin. The Madzaringwe Formation overlies the Tshidzi Formation and it consists of shale, mudstone and sandstones with subordinate siltstones and coal seams. In the open pit, the Madzaringwe Formation consists of a lower grit layer with conglomerate lenses and can be up to 5 m thick in places. These, in turn, are overlain by a thick shale succession with a distinctive coal-bearing zone in the middle of up to 10 m in thickness. On the other hand, in the three boreholes, three coal horizons are interbedded with shale and mudstone units with varying coal quantities and qualities.

The Madzaringwe Formation in the Vele Colliery has a thickness of about 61 m, 60 m and 42 m in boreholes OV125149, OV125156 and OV125160, respectively. The rocks of the Madzaringwe Formation are dominated by mudstones and carbonaceous shales with thin layers of coal seams and sandstones. The coal zones can be subdivided into four coal sections or composite seams. There is no consistency in the development of coal seams throughout the stratigraphy in the three boreholes. In the boreholes, the Top Seam is 0 – 7.66 m thick and contains 55% to 65% coal. The Middle Seam is 0 – 2.19 m thick and it is made up of 20% to 45% coal, while the Bottom Upper Seam is 0 – 5.48 m thick and comprises of 65% to 80% coal. The Bottom Lower Seam is 0 – 7.87 m thick and it is composed of 65% to 80% coal. The top upper and Top middle coal seam contains immature non-economical coal, whereas the top-bottom seam is made up of matured mixed bright coal which is of economic value, due to its maturity. The middle seam and bottom seam comprises mixed bright and dull coal. The sedimentary rocks partings within the coal seams show some induration or alteration along with the minerals such as iron oxides, calcite veins, calcium carbonates, and siderite and pyrite nodules. Some of the coal seams and partings are highly fractured, they sometimes exhibit slickensides. Succeeding the Madzaringwe Formation in the open pit is the Mikambeni Formation, and it is made up of black carbonaceous shale, mudstone and sandstones with minor coal and sandy shale layers.

Sedimentary facies study of the Madzaringwe Formation in the Vele Colliery was performed to infer the depositional environment. A total of ten lithofacies were identified and grouped into four distinct facies associations (FAs), which are FA 1:

Carbonaceous and pyritic shale and mudstones (Fls + Fss), FA 2: Black coal and shaly coal (C + Cs), FA 3: Dark grey micaceous and calcareous shale and mudstone, with subordinate siltstones (Fls + Fm, Fc + Fms + Fmb), and FA 4: Siltstone intercalated with fine to coarse-grained sandstones (Fms + Fss + Sm + D). Based on the lithofacies analyses, it can be concluded that FA 1) represents floodplain and backswamps deposits, FA 2 represents thickly vegetated backswamps, while FA 3 and FA4 represent shallow lake or floodplain deposits and floodplain deposits, respectively.

The coal petrographic characterization revealed that vitrinite is the dominant maceral group in the coals, making up to 80 – 92% of the total sample (excl. mm). Collotelinite is the dominant vitrinite maceral, followed by corpogelinite. All the analysed samples have pseudovitrinite, which is a major concern in terms of exploitation. Pseudovitrinite is known to affect the swelling properties of the coal, despite the very high vitrinite content. Also, the studied coals show the occurrence of epigenetic carbonate minerals with pyrites shattering vitrinite and other sulphide minerals. The inertinite content is very low in the samples, ranging from 4 – 16 vol.%, and is dominated by fusinite, most commonly in the form of small fragments possibly indicative of a fire origin that is some fusinite, particularly that in laterally extensive fusain horizons, is derived from wildfires which resulted in the formation of fossil charcoal (pyrofusinite). The liptinite content ranges from extremely low in the top samples (i.e. 0.5vol % mmf. in Sample 1675), to high in the bottom samples (i.e. 12 vol.% mmf in sample 1681). Sample 1681 is dominated by cutinite. The occurrence of cutinite in contrast to the very low proportion of liptinite in the top samples indicates different depositional and preservation

environments through the sequence. The observed mineral matter ranges from 21 – 26 vol.% in the top samples and 4 – 8 vol.% in the middle and bottom coal seams. The top coal seam generally has a high amount of epigenetic carbonate minerals which appear to have shattered the vitrinites. The pyrite content is also high in the top coal seam (about 5.4 vol.%), which is in contrast to the middle and bottom coal seams, where the pyrite content is below 1 vol.% or completely absent. The dominance of collotellinite in the analysed coal samples gives a clear indication that the coals are derived from the parenchymatous and woody tissues of roots, stems and leaves. The mean random vitrinite reflectance values range between 0.75 and 0.76%, placing the coals in the medium rank category (also known as the high volatile bituminous coal) based on the UN-ECE coal classification scheme. The standard deviation values are low, indicating a single population, with no blending or heat affect determined. In general, the high amount of inertinite, especially fusinite with empty cells and semifusinite in the coals will pose a threat to coal mining because it aids the formation of dust during mining.

Petrographic studies of the mudrocks and sandstones show that the mudrocks are mostly composed of silt and clay size minerals, whereas the sandstones are made up of quartz, feldspar, lithic fragments, mica, clay matrix and heavy minerals. The observed cements are clay minerals, pyrite, hematite and quartz. Clay minerals are the most common cementing materials in the sandstones. The quartz and feldspar grains in the sandstones are both polycrystalline and monocrystalline, indicating that they were not fully separated by long transportation, which is consistent with the immature nature of the rocks. Grain morphology for the sandstones range from sub-

angular and sub-rounded and are mostly poorly sorted, pointing to the fact that the sediments might have travelled over a relatively short distance from the source area. From the observed lithics and heavy minerals and the nature of quartz and feldspar minerals, it can be inferred that the sediments came from igneous and sedimentary rock sources, rarely from metamorphic rock source.

Geochemical compositions of the mudrocks and sandstones were analysed to identify provenance, paleoweathering conditions and tectonic setting of the Madzaringwe Formation. The geochemical data of major and trace elements show that the studied mudrocks and sandstones have the same source. The geochemical classification diagrams show that the sandstones could be classified as subarkose and lithic arenite. The binary diagram of the TiO_2 versus Zr and La/Sr against Th/Co as well as the discriminant function plots revealed that the mudrocks (shale and mudstone) and sandstones are mostly of silicic or felsic igneous provenance.These source areas might have been from adjacent areas which include the Limpopo Belt (igneous and sedimentary rocks), and basement uplifted rocks of the Beit-Bridge Complex, consisting of the granite, granite-gneisses and schists near Tuli coalfield. The A–CN–K ternary diagram and indices of weathering revealed that the source rocks underwent a moderate to a high degree of chemical weathering. The binary plots of TiO_2 versus (Fe_2O_3 + MgO) and SiO_2 against K_2O/Na_2O, and ternary plots of Na_2O–CaO–K_2O and Th–Sc–Zr/10 revealed that the studied samples are of passive-active continental margin settings. The indices of weathering/alteration and the binary plot of the index of compositional variability (ICV) against the chemical index of alteration shows that the studied samples have been subjected to moderate to intensive weathering.

9.2 Conclusions

Based on the results presented in this study, the following conclusions are made:

- The rocks of the Madzaringwe Formation are dominated by mudstones and carbonaceous shales with thin layers of coal seams and occasional sandstones.
- The aforementioned studied rocks are floodplain and backswamps deposits.
- The mean random vitrinite reflectance values of the analysed coal samples range between 0.75 and 0.76%, placing the coals in the medium rank category.
- The sandstones could be classified as subarkose and lithic arenite.
- The shale, mudstone and sandstones are derived from silicic or felsic igneous provenance, while the coal samples are of mafic igneous provenance.
- The Madzaringwe Formation supports the passive-active continental margin settings.
- The source rocks underwent a moderate to a high degree of chemical weathering.

9.3 Reccomendations

This project could perhaps serve as a basis for future study on the nature and rank of coal in the Madzaringwe Formation. Since the thin coal seams in the Vele colliery are of medium rank under complex geological setting, it is recommended that further and detailed coal characterization study be carried out in the Madzaringwe Formation as well as the neighbouring formations because the area could posses or holds a better opportunities for potentially exploitable coal deposits. It is also strongly recommended

that detailed diagenetic study of coal (biochemical coalification) be carried on the Madzaringwe coal so as to determine the degree of the coalification. Considering the fact the different rank parameters of coal change with the degree of coalification or the character or rank of coal in any deposit is a function of the combined influence of the processes that formed it.

REFERENCES

Alexander, N., Golab A., Adrian C., and Hutton, D. H., (2007). 'The impact of igneous intrusions on coal, cleat carbonate, and groundwater composition.', *International journal of Coal Geology*, pp 1-9.

Armstrong-Altrin, J.S., Lee, Y.I., Verma, S.P. and Ramasamy, S., (2004). Geochemistry of sandstones from the Upper Miocene Kudankulam Formation, southern India: implications for provenance, weathering, and tectonic setting. *Journal of Sedimentary Research*, *74*(2), pp.285-297.

Baiyegunhi, C., Liu, K. and Gwavava, O., (2017) 'Geochemistry of sandstones and shales from the Ecca Group, Karoo Supergroup, in the Eastern Cape Province of South Africa : Implications for provenance, weathering and tectonic setting', Geoscience 9(1) pp. 340–360.

Barton, J. M. and Key, R. M., (1981). 'Chapter 8 The Tectonic Development of the Limpopo Mobile belt and the Evolution of the Archaean Cratons of Southern Africa', *Developments in Precambrian Geology*. Elsevier, 4, pp. 185–212.

Bhatia, M.R., (1983). Plate tectonics and geochemical composition of sandstones. *The Journal of Geology*, *91*(6), pp.611-627.

Bhatia, M.R. and Crook, K.A.W., (1986). 'Mineralogy and Trace element characteristics of graywackes and tectonic setting discrimination of sedimentary basins', Contribution to Mineralogy and Petrology 92(2) pp. 181–193.

Bibler, C.J., Marshall, J.S. and Pilcher, R.C., (1998). Status of worldwide coal mine methane emissions and use. *International Journal of Coal Geology*, *35*(1-4),

pp.283-310.

Blatt, H. and Christie, J.M., (1963). Undulatory extinction in quartz of igneous and metamorphic rocks and its significance in provenance studies of sedimentary rocks. *Journal of Sedimentary Research*, *33*(3), pp.559-579.

Bordy, E.M., 2000. *Sedimentology of the Karoo Supergroup in the Tuli Basin.* Doctoral dissertation, Rhodes University, 614pp.

Bordy, E.M. and Catuneanu, O., (2002). 'Sedimentology and palaeontology of upper Karoo aeolian strata (Early Jurassic) in the Tuli Basin, South Africa', *Journal of African Earth Sciences*, 35(2), pp. 301–314.

Bordy, E.M. and Catuneanu, O., (2002). 'Sedimentology of the Beaufort-Molteno Karoo fluvial strata in the Tuli Basin, South Africa', *South African Journal of Geology*, 105(1), pp. 51–66.

Bordy, E.M., Hancox, P.J., and Rubidge B.S., (2005). "The contact of the Molteno and Elliot formations through the main Karoo Basin, South Africa: a second-order sequence boundary." *South African Journal of Geology* 108, 3: 351-364.

Bracciali, L., Marroni, M., Pandolfi, L., Rocchi, S., Arribas, J., Critelli, S. and Johnsson, M.J., (2007). Geochemistry and petrography of Western Tethys Cretaceous sedimentary covers (Corsica and Northern Apennines): from source areas to configuration of margins. *Special Papers-Geological Society Of America*, *420*, p.73.

Brandl, G. and McCourt, S., (1980). A lithostratigraphic subdivision of the Karoo Sequence in the north-eastern Transvaal. *Annals Geological Survey of South Africa*, *14*, pp.51-56.

Burke, K. and Dewey, J.F., (1973). Plume-generated triple junctions: key indicators in applying plate tectonics to old rocks. *The Journal of Geology*, *81*(4), pp.406-433.

Chevallier, L. and Woodford, A., (1999). Morpho-tectonics and mechanism of emplacement of the dolerite rings and sills of the western Karoo, South Africa. *South African Journal of Geology*, *102*(1), pp.43-54.

Chidley, CM., (1985). 'The geology of the Country around Evangelina and Pontdrift (1: 50 000 sheets 2228BD and 2229A,)', in *The geology of the Country around Evangelina and Pontdrift (1: 50 000 sheets 2228BD and 2229A,)*. Unpublished South African Published Report.

Catuneanu, O., (2006). *Principles of sequence stratigraphy*. Elsevier.

Catuneanu, O., Wopfner, H., Eriksson, P.G., Cairncross, B., Rubidge, B.S., Smith, R.M.H. and Hancox, P.J., (2005). The Karoo basins of south-central Africa. *Journal of African Earth Sciences*, *43*(1-3), pp.211-253.

Diessel, C.F.K., (2007). 'Utility of coal petrology for sequence-stratigraphic analysis. International Journal of Coal Geology 3(34).', *International Journal of Coal Geology*, pp. 70.

Gomet, L.P., Haskin, L.A., Korotev, R.L. and Dymek, R.F., (1984). The "North American shale composite": its compilation, major and trace element characteristics. *Geochimica et Cosmochimica Acta*, *48*(12), pp.2469-2482.

Gressly, A., (1838). *Observations géologiques sur le Jura Soleurois*. auf Kosten der Gesellschaft.

Hackely, P.C. and Kolak, J.J., (2008). 'Petrographic and vitrinite reflectance analyses

of a suite of high volatile bituminous coal samples from the United States and Venezuela U. S. Department of the Interior', *U S Geological Survey*, Open-File report, pp.1-36.

Hancox, P. J. and Götz, A. E., (2014). 'South Africa's coalfields — A 2014 perspective', *International Journal of Coal Geology*. Elsevier, 132(1), pp. 170–254.

Herron, M.M., (1988). Geochemical classification of terrigenous sands and shales from core or log data. *Journal of Sedimentary Research*, *58*(5), pp.820-829.

Hower, J. C., Wagner N.J, Jennifer, M.K., Drew, J.W.,Stacker J.D. and Richardson, A.R., (2012). 'International Journal of Coal Geology Maceral types in some Permian southern African coals', *International Journal of Coal Geology*. Elsevier. 100, pp. 93–107.

International Committee for Coal and Organic Petrology (ICCP) (2001) 'The new inertinite classification (ICCP System 1994)', 82 (4), pp. 459–471.

Johnson, M.R., Van Vuuren, C.J., Hegenberger, W.F., Key, R. and Show, U., (1996). Stratigraphy of the Karoo Supergroup in southern Africa: an overview. *Journal of African Earth Sciences*, *23*(1), pp.3-15.

Johnson, M.R., (1994). Lexicon of South African Stratigraphy.

Luyt, J.P., (2017). *The tectono-sedimentary history of the coal-bearing Tshipise Karoo basin* (Doctoral dissertation, University of Pretoria).

Malaza, N., (2013). Basin Analysis of the Soutpansberg and Tuli Coalfields, Limpopo Province of South Africa. Unpublished PhD Thesis, University of Fort Hare, 270pp.

Malaza, N., Liu, K. and Zhao, B., (2013). 'Facies Analysis and Depositional Environments of the Late Palaeozoic Coal-Bearing Madzaringwe Formation in the Tshipise-Pafuri Basin, South Africa', *International Scholarly Research Notices- Geology*, 2013, pp. 1–11.

Malaza, N., Liu, K. and Zhao, B., (2016). Subsidence Analysis and Burial History of the Late Carboniferous to Early Jurassic Soutpansberg Basin, Limpopo Province, South Africa. *Acta Geologica Sinica-English Edition*, *90*(6), pp.2000-2007.

McLennan, S. M., Hemming, S., McDaniel, D.K., and Hanson, G.N., (1993). 'Geochemical approaches to sedimentation, provenance, and tectonics', Geological Society of America (special paper) 284 pp. 21–40.

McLennan, S. M., Taylor, S. R. and Eriksson, K. A., (1983). 'Geochemistry of Archean shales from the Pilbara Supergroup, Western Australia', *Geochimica et Cosmochimica Acta*. Pergamon, 47(7), pp. 1211–1222.

Miall, A.D., (1978). Lithofacies types and vertical profile models in braided river deposits: a summary. In: A.D. Miall (Editor), Fluvial Sedimentology. Canadian Society of Petroleum Geologists Memoir, 5, 597-604.

Miall, A.D., (1995). Description and interpretation of fluvial deposits: a critical perspective. *Sedimentology*, *42*(2), pp.379-379.

Mial, A.D., (1996). The geology of fluvial deposits. Springer-Verlag, New York Inc, 616 pp. 400

Miall, A.D., (2000). Principles of Sedimentary Basin Analysis. 3rd edition, Springer-

Verlag, New York Inc, 616pp.

Middleton, G.V., (1978). Subaqueous sediment transport and deposition by sediment gravity flows. *Marine sediment transport and environmental management*.

Misiak, J., (2006). 'Petrography and depositional environment of the No. 308 coal seam (Upper Silesian Coal Basin, Poland)—a new approach to maceral quantification and facies analysis', *International Journal of Coal Geology*. Elsevier, 68(1–2), pp. 117–126.

Moore, R.C., (1949). Meaning of facies. *Geol. Soc. America Mem*, *39*, pp.1-34.

Mtimkulu, M. N., (2009). 'A provisional basinal study of the Waterberg-Karoo , South Africa by Mtimkulu Nhlanhla Mtimkulu A thesis submitted in fulfilment of the requirements for the degree of masters in science in geology in the faculty of natural and agricultural sciences of the', (July).

Nesbitt, H. W. and Young, G. M., (1982). 'Early Proterozoic climates and plate motions inferred from major element chemistry of lutites', *Nature*, 299(5885), pp. 715–717.

Pettijohn, F.J., (1957). Paleocurrents of Lake Superior Precambrian quartzites. *Geological Society of America Bulletin*, *68*(4), pp.469-480.

Pettijohn, F.J., Potter, P.E. and Siever, R., (1987). Sand and sandstone, 2nd edition. SpringerVerlag, 533 pp.

Raza, M., Dayal, A.M., Khan, A., Bhardwaj, V.R. and Rais, S., (2010). Geochemistry of lower Vindhyan clastic sedimentary rocks of Northwestern Indian shield: Implications for composition and weathering history of Proterozoic continental

crust. *Journal of Asian Earth Sciences*, *39*(1-2), pp.51-61.

Roser, B.P. and Korsch, R.J., (1986). Determination of tectonic setting of sandstone-mudstone suites using SiO2 content and K2O/Na2O ratio. *The Journal of Geology*, *94*(5), pp.635-650.

Roser, B.P. and Korsch, R.J., (1988). Provenance signatures of sandstone-mudstone suites determined using discriminant function analysis of major-element data. *Chemical geology*, *67*(1-2), pp.119-139.

Reading, H.G. and Reading, H.G., (1978). *Sedimentary environments and facies,* Vol. 60, Oxford: Blackwell.

Rutherford, M.C., Mucina, L. and Powrie, L.W., (2006). Biomes and bioregions of southern Africa. *The vegetation of South Africa, Lesotho and Swaziland*, *19*, pp.30-51.

Smith, G.C. and Cook, A.C., (1980). Coalification paths of exinite, vitrinite and inertite. *Fuel*, *59*(9), pp.641-646.

Steno, N., (1973). Tag Archives: Nicolaus Steno three principles.

Steyn, J.G.D. and Smith, W.H., (1977). Coal petrography in the evaluation of SA coals. *Coal, Gold and Base Minerals*, pp.107-117.

Snyman, C.P., (1989). The role of coal petrography in understanding the properties of South African coal. *International Journal of coal geology*, *14*(1-2), pp.83-101.

Stach, E., Mackowsky, M.T., Teichmüller, M., Taylor, G.H., Chandra, D. and Teichmüller, R., (1982). Coal petrology. *Gebrüder Borntraeger, Berlin*, pp.1-535.

Suárez-Ruiz, I., Flores, D., Mendonça Filho, J.G. and Hackley, P.C., (2012). Review and update of the applications of organic petrology: Part 1, geological applications. *International Journal of Coal Geology*, *99*, pp.54-112.

Sýkorová, I., Pickel, W., Christanis, K., Wolf, M., Taylor, G.H. and Flores, D., (2005). Classification of huminite—ICCP System 1994. *International Journal of Coal Geology*, *62*(1-2), pp.85-106.

Toulkeridis, T., Clauer, N., Kröner, A., Reimer, T. and Todt, W., (1999). Characterization, provenance, and tectonic setting of Fig Tree greywackes from the Archaean Barberton greenstone belt, South Africa. *Sedimentary Geology*, *124*(1-4), pp.113-129.

Turekian, K.K. and Wedepohl, K.H., (1961). Distribution of the elements in major unit of the earth crust. *Geological Society of America Bulletin*, *72*, pp.172-192.

Tyson, R.V., (1995). Abundance of organic matter in sediments: TOC, hydrodynamic equivalence, dilution and flux effects. In *Sedimentary organic matter* (pp. 81-118). Springer, Dordrecht.

Vail, J.R. and Dodson, M.H., (1969). Geochronology of Rhodesia. *South African Journal of Geology*, *72*(3), pp.79-113.

van der Merwe, W.C., Flint, S.S. and Hodgson, D.M., (2010). Sequence stratigraphy of an argillaceous, deepwater basin-plain succession: Vischkuil Formation (Permian), Karoo Basin, South Africa. *Marine and Petroleum Geology*, *27*(2), pp.321-333.

Suárez-Ruiz, I. and Ward, C.R., (2008). Basic factors controlling coal quality and

technological behavior of coal. In *Applied Coal Petrology* (pp. 19-59).

Ward, C.R., (2016). Analysis, origin and significance of mineral matter in coal: An updated review. *International Journal of Coal Geology*, *165*, pp.1-27.

Watkeys, M.K. and MK, W., (1979). Explanation of the geological map of the country west of Beitbridge.

Wronkiewicz, D.J. and Condie, K.C., (1990). Geochemistry and mineralogy of sediments from the Ventersdorp and Transvaal Supergroups, South Africa: cratonic evolution during the early Proterozoic. *Geochimica et Cosmochimica Acta*, *54*(2), pp.343-354.